MITIGATION OF SYNCHRONOUS MACHINE BASED DISTRIBUTED GENERATION INFLUENCES ON FUSE-RECLOSER PROTECTION SYSTEMS IN RADIAL DISTRIBUTION NETWORKS USING SUPERCONDUCTING FAULT CURRENT LIMITERS

A Thesis

Submitted to the College of Graduate Studies and Research

In Partial Fulfillment of the Requirements

For the Degree of Master of Science

In the Department of Electrical and Computer Engineering

University of Saskatchewan

Saskatoon, Saskatchewan

By

Keaton A. Wheeler

PERMISSION TO USE

I agree that the Library, University of Saskatchewan, may make this thesis freely available for inspection. I further agree that permission for copying of this thesis for scholarly purpose may be granted by the professor or professors who supervised the thesis work recorded herein or, in their absence, by the Head of the Department or the Dean of the College in which the thesis work was done. It is understood that due recognition will be given to me and to the University of Saskatchewan in any use of the material in this thesis. Copying or publication or any other use of this thesis for financial gain without approval by the University of Saskatchewan and my written permission is prohibited.

Request for permission to copy or to make any other use of the material in this thesis in whole or part should be addressed to:

Head of the Department of Electrical and Computer Engineering

University of Saskatchewan

57 Campus Drive

Saskatoon, Saskatchewan S7N 5A9

Canada

ABSTRACT

Distributed generation (DG) is increasingly employed in modern utility grids to address the growing complexity and size of consumer energy demands. The obstacles associated with DG integration are related to the additive effect the DG has on the short circuit current characteristics of power systems during short circuit conditions.

This thesis proposes a novel mitigation technique for synchronous machine based DG integration effects on existing radial fuse-recloser protection infrastructure. The mitigation method provides a comparative analysis of the utilization of resistive (R), inductive (L) and resonant (LC) type superconducting fault current limiters (FCLs) for prevention of excessive fault current contribution from DG sources. Within the frame of reference of this thesis is an interrogation into the effects of synchronous machine based DG sources, in conjunction with mitigation capabilities of FCL integration in the context of fuse-recloser coordination, recloser sensitivity and recloser directionality behavior during radial distribution short circuit conditions. For validation purposes, the proposed methods are demonstrated on a suburban test benchmark using the PSCAD/EMTDC program.

ACKNOWLEDGEMENTS

Foremost, I would like to express my sincere gratitude to my supervisor Dr. Sherif O. Faired. This thesis would not have been possible without your continuous support, enthusiasm and guidance and it has helped me develop a passion and motivation for problem solving.

I would also like to thank Dr. Mohamed Elsamahy for his constant encouragement and support throughout the duration of this research. Your advice and guidance has been invaluable in my academic and professional journey.

I would also like to express my appreciation to my parents, sister and friends for their encouragement and support. Special thanks go to my mother, Colleen Wheeler, for helping me with the editing of this thesis.

TABLE OF CONTENTS

LIST OF TABLES

LIST OF FIGURES

LIST OF SYMBOLS

i_s, i_r	steady-state DFIG stator and rotor current
i_g	grid current
A	amperes
t(I)	time (seconds)
D, B, *u*	TCC curve constants
M	input current over pick up current ratio
TDS	time dial setting
p.f.	power factor
S_{load}	load complex power
V_{LL}	line to line voltage
Ω	ohm
Z	impedance
Y	admittance
P_{load}	real load power
Q_{load}	reactive load power
V_0	initial voltage
r_1, r_2	stator and rotor resistance
L_1, L_2	stator and rotor inductance
L_m	magnetizing inductance
ω_r	rotor angular frequency
d	direct axis
q	quadrature axis
i_{1d}, i_{2d}	d-axis damper winding currents
i_{1q}, i_{2q}	q-axis damper winding currents
v_{1d}, v_{2d}	d-axis damper winding voltages

v_{1q}, v_{2q}	q-axis damper winding voltages
X`	transient reactance
X_1, X_2	stator and rotor reactance
X_m	magnetizing reactance
i_{sc}	short circuit current
i_{ac}, i_{dc}	ac and dc short circuit current
E	prefault voltage
t	time
T`	short circuit transient time constant
T_{dc}	DC decay time constant
ω	angular velocity
ω_r	rotor angular frequency
e_d, e_q	d- and q- axis components of the stator voltage
e_{fd}	filed voltage
i_d, i_q	d- and q- axis components of the stator current
i_{fd}	field winding current
i_{sd}, i_{sq}	d- and q- axis components of the stator current
L_d, L_q	d- and q- axis components of the stator inductance
L_{ad}	d-axis magnetizing inductance
L_{aq}	q-axis magnetizing inductance
L_{ffd}	self-inductance of the field winding
L_{11d}	self-inductance of the d-axis damper winding
L_{11q}, L_{22q}	self-inductances of the q-axis damper winding
R_a	armature resistance
R_L	resistance of the series capacitor compensated transmission line
R_{fd}	field winding resistance

R_{1d}	d-axis damper winding resistance
R_{1q}, R_{2q}	q-axis damper winding resistances
T_e	electromagnetic torque
Ψ_d, Ψ_q	d- and q- axis components of the stator flux linkages
Ψ_{fd}	field winding flux linkage
Ψ_{1d}	d-axis damper winding flux linkage
Ψ_{1q}, Ψ_{2q}	q-axis damper winding flux linkages
ω_0 (f_0)	synchronous frequency (337 rad/sec)
R_p	parallel resistance
R_{FCL}	resistive state FCL resistance
L_{TC}	FCL trigger coil inductance
L_{FCL}	FCL limiting coil inductance
f_c	resonant frequency
L_f	resonant frequency inductance
C_f	resonant frequency capacitance
I_{fault}	fault current
I_{feeder}	feeder head end recloser current

LIST OF ABBREVIATIONS

DG	distributed generation
FCL	fault current limiter
R	resistive
L	inductive
AC	alternating current
DC	direct current
A	amperes
TCC	time current characteristic
MMT	minimum melt time
TCT	total clearing time
CT	current transformer
VA	volt ampere
V	volt
MOV	metal oxide varistor
VAR	volt ampere reactive
RMS	root mean square

1. INTRODUCTION

1.1 Distributed Generation

Due to the growing complexity of modern utility grids and increasing consumer energy demand, power utilities worldwide are seeking methods yielding increased generating capacity. One low capital method of increasing this capacity is through the inclusion of small generators on the distribution side of the grid to meet local power demands. This form of capacity increase is known as distributed generation (DG) [1]. Although DG inclusion has undeniable advantages such as voltage profile improvement, increased grid capacity and increased power delivery reliability, it also has drawbacks in relation to existing system design and operation [1-9].

A key drawback in the utilization of DG sources is the effect they can have on power system protection [1-9]. Most modern utility distribution networks are set up in a radial configuration such that power flows in a unidirectional manner from the utility to the consumer. DG integration into such grids potentially causes this radial behavior of the network to be lost [10, 11], and may cause magnitudinal (and possibly directional) changes in system short circuit levels. This can cause possible failure or limit existing protection setting adequacy under fault conditions. The extent of such influences is determined by DG size, location and interconnection methods [3, 5, 9].

DG sources come in a variety of types including traditional (such as gas and diesel generators) and non-traditional (renewables). Traditional sources include low speed turbines, diesel engines and micro-turbines. Micro turbines in particular are being used fairly frequently due to their efficiency, and their capacity to operate using resources such as natural gas and propane. These types of turbines are mainly synchronous machine based generators [2].

Non-traditional DG sources mainly consist of electrochemical devices (such as fuel cells) and renewable energy devices. Of particular interest is the increase in the utilization of renewable sources such as wind farms (induction and converter based) and photovoltaics (converter based) [3]. Wind energy is becoming an increasingly popular resource following the global trend towards promoting the integration of green initiatives [4] and substantial investment in investigating the

viability of this form of energy generation. Although higher levels of wind penetration are being integrated into modern utility grids [5], the effect on protection coordination is not as significant as those in synchronous based generators [2]. This in part is due to the configuration of Doubly Fed Induction Generator (DFIG) type wind turbines (most common [3]) as shown in Figure 1.1.

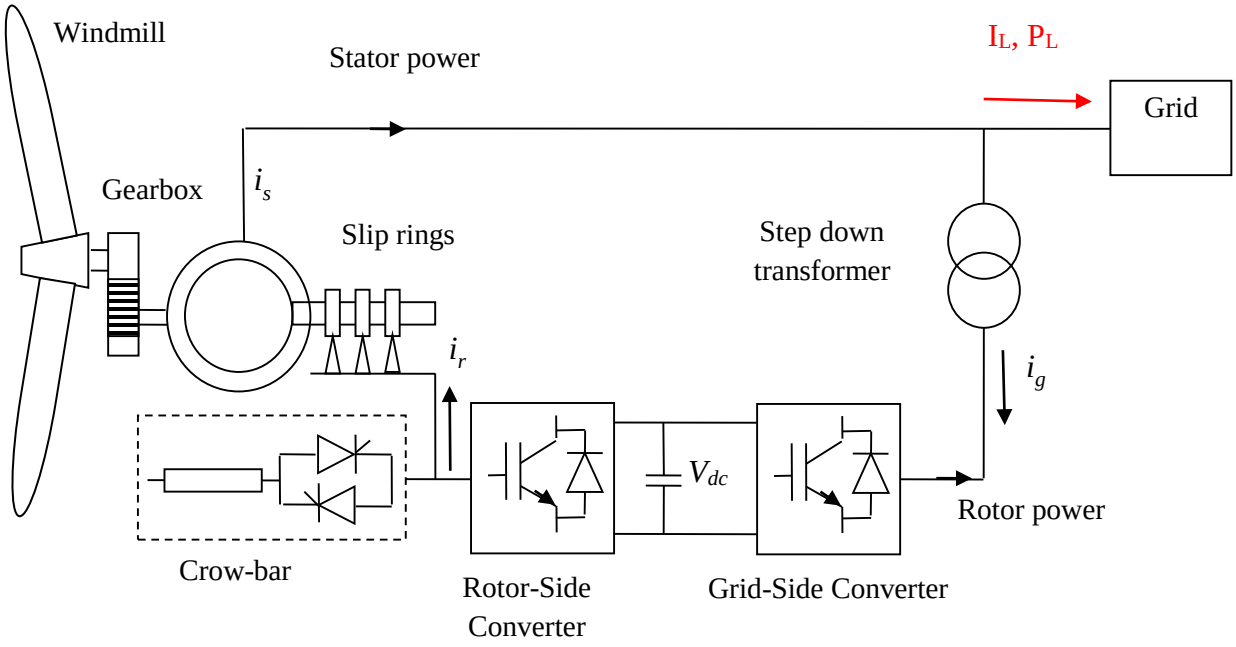

Figure 1.1: A basic configuration of a DFIG wind turbine [6].

For DFIG type wind turbines, the stator of the induction machine is connected to the grid while the rotor windings are connected through slip rings and an AC-AC converter system. A crowbar is used to protect the power electronics converter against overvoltage or thermal breakdown whilst also limiting the rotor inrush current when a voltage dip occurs [7]. When a grid fault occurs the rotor windings are shorted by the crowbar turning the wind turbine into a squirrel cage induction generator with an increased rotor resistance. This in turn has the effect that for a persistent fault, the current contribution from the wind farm will decrease exponentially over time until it reaches near zero after a few cycles (2 to 3) [12, 13, 14]. Given this fault behavior in conjunction with the fact that synchronous machine based DG has a more severe effect on system operation, only synchronous machine based DG sources are used in this thesis.

1.1.1 Interconnection of Distributed Resources

A typical interconnecting scheme for DG sources to the existing network consists of an inter-collecting feeder and inter-connecting transformer as shown in Figure 1.2 [8].

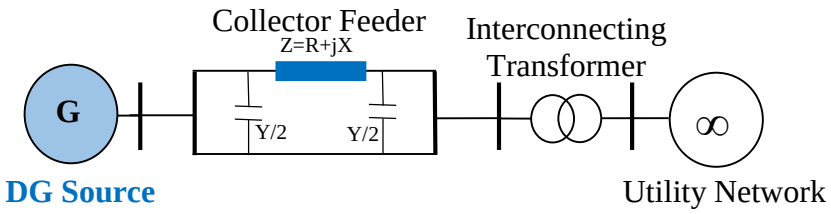

Figure 1.2: A typical DG interconnecting scheme.

One critical aspect of the interconnection is related to the transformer. Each type of connection comes with advantages and disadvantages. Currently there are five connections that are most commonly used: the advantages and disadvantages are summarized in Table 1.1.

Table 1.1: Advantages and disadvantages of interconnecting transformers.

Low Voltage Side	High Voltage Side	Disadvantages	Advantages
Delta	Delta	Supplies network from ungrounded source even if utility breaker trips.	Provides no fault current for a ground fault on the HV side of the transformer. Main network breakers will not react to ground faults on the LV side of the transformer.
Ground-Wye	Delta		
Delta	Wye		
Delta	Ground-Wye	Provides an unwanted ground current for network faults.	Main network breakers will not react to ground faults on the LV side of the transformer. No overvoltages for faults on main feeder.
Ground-Wye	Ground-Wye	Allows main feeder relaying to respond to ground faults on the LV side.	No overvoltages for ground faults on main feeder if the DG source is grounded.

There is no universal agreement amongst utilities about the most effective connection [8], but a range of utilities have set preferences for DG interconnection in relation to DG size. Table 1.2 specifies the preferences for the Hydro One distribution utility [9].

Table 1.2: Hydro One preferred interconnection transformer connections.

System Voltage (kV)	DG size (MW)	Preferred Interconnection Transformer High voltage: Low voltage
27.6	1-2	Gnd-Wye:Delta Delta:Gnd-Wye Gnd-Wye:Gnd-Wye
27.6/12/8	0.2-1	Gnd-Wye:Gnd-Wye Gnd-Wye:Delta Delta:Gnd-Wye
27.6/12/8/4	0.05-0.2	Gnd-Wye:Gnd-Wye
27.6/12/8/4	0.02-0.05	Gnd-Wye:Gnd-Wye

1.2 Power System Protection

When faults occur, the implications for a power system can be catastrophic as it potentially yields system failure and equipment damage. Faults may occur when equipment insulation fails, overvoltages occur due to lightning and switching surges, and due to other natural or mechanical causes [10].

Power system protection can be defined as "the science, skill and art of applying and setting relays and/or fuses to provide maximum sensitivity to faults and undesirable conditions, but to avoid their operation on all permissible or tolerable conditions" [10]. In modern protection schemes, it is desirable to remove only sections of the power system that have a faulted condition, leaving the rest of the network to operate as normal. Additionally it is preferred that devices that are closer to the fault should operate before those that are further away [10, 11, 15]. This will be discussed further in this chapter.

1.2.1 Protective Devices

Fuses are the simplest and oldest forms of system protection that are capable of interrupting current in a power network [11]. A fuse can be defined as "an overcurrent protective device with a circuit-opening fusible part that is heated and severed by the passage of overcurrent through it" [11]. Fuses are installed in series on the lines they are assigned to protect and are able to carry normal load currents without interrupting supply. Fuses have two distinct time-current characteristic (TCC) curves, namely minimum melt time (MMT) and total clearing time (TCT). The MMT is the minimum time required for the fuse link to melt for a designated short circuit

level. The TCT is the maximum time required for the fuse link to melt and the arc to clear for a designated short circuit level [15]. A typical fuse time current characteristic is shown in Figure 1.3.

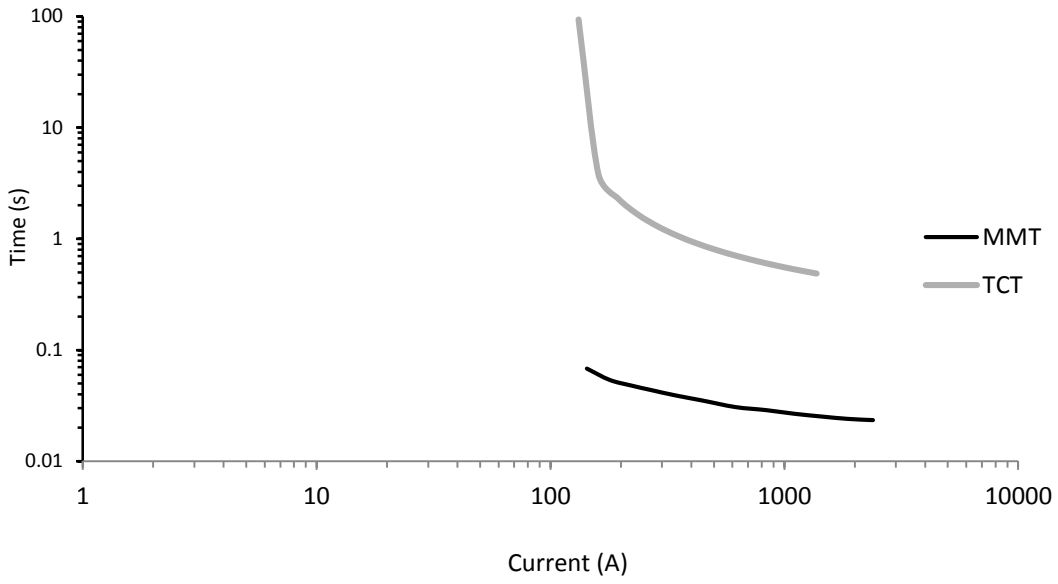

Figure 1.3: Time-Current Characteristic of a Kearney 100T fuse [16].

A recloser is an overcurrent device that is set to trip (by opening points of contact and then reclosing a specified amount of time after) a designated number of times in order to clear temporary faults or isolate sections of a network in the presence of a permanent fault [15]. The sequence followed by a recloser will vary depending on the respective standards adopted by utilities/countries. However a common sequence is the 'two fast and two slow before lockout' (contacts are permanently opened) [17, 18]. The fast (often called TCC1) and slow (often called TCC2) sequences of the recloser are dependent on both the manufacturer and the TCC curve that is used in the programming of the recloser [11]. For the typical 'two fast two slow' scheme the recloser first reacts to a fault twice using its fast characteristic before switching to its slow characteristic. If the fourth attempt at clearing a fault is unsuccessful, the recloser locks out [11]. A typical recloser TCC curve is shown in Figure 1.4.

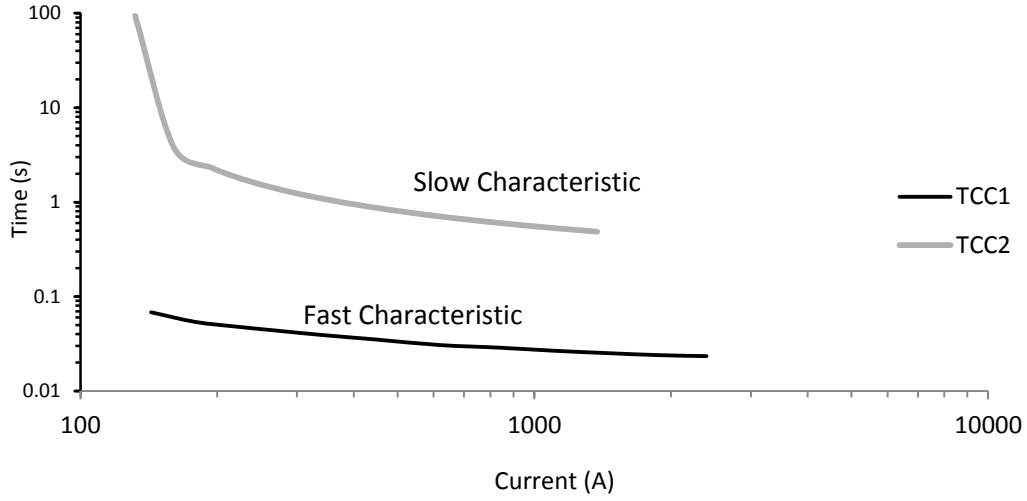

Figure 1.4: Time-Current Characteristics of an ABB PCD 2000 Recloser [19].

Circuit breakers are devices that automatically interrupt or reclose for a system in a faulted or steady state condition [15]. The main purpose of a circuit breaker is to extinguish the arc that develops when the breaker's contact opens during fault conditions. In general, circuit breakers are equipped with a relay that senses the level of current flowing through the system. The relay is programmed to activate the circuit breaker if a fault is sensed [11]. Typically, the relays that are used are overcurrent electronic type with inverse, very inverse or extremely inverse time-current characteristics. The time-current characteristic of any relay curve can be modeled by [20].

$$t(I) = \left(\frac{D}{M^{u}-1} + B\right) \times TDS \tag{1.1}$$

With time *t(I)* expressed in seconds for a current I in Amperes, M is the I_{input}/I_{pickup} ratio, I_{pickup} is the pickup current of the relay (lowest current that is detected as a fault) in Amperes, TDS is the time dial setting of the relay, and D, B, and u are the constants to provide the curve with its characteristic. These inverse time characteristics can be depicted graphically in Figure 1.5.

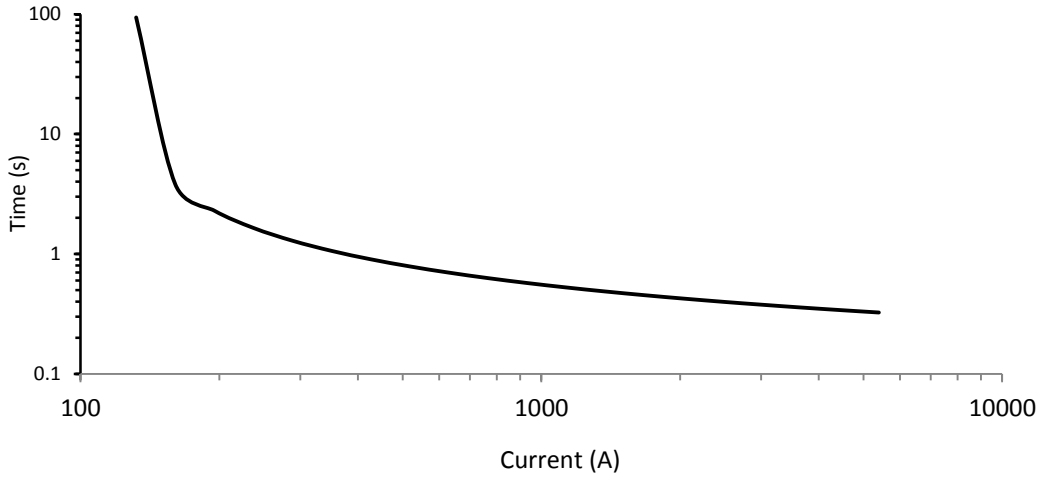

Figure 1.5: Time-Current Characteristics of a relay with D, B, u, TDS, and pickup current being 19.61, 0.491, 2, 1 and 1A respectively [20].

Current transformers (CTs) are devices that reproduce a current in the secondary windings that is directly proportional to the primary windings. During steady state conditions, the secondary windings of the CT will be representative of the load current of the protected network and will flow consistently into the relay. Most relays in industrial applications have a current rating of 5 A hence most CT ratios are designed to output 5 A to the relay during steady state conditions [11]. This allows for the utilization of the same relays in different applications whereby the fault level and steady state current for separate systems do not necessarily need to be the same to attain identical relay operations. Some typical CT ratios are given in Table 1.3 [11, 21].

Table 1.3: Typical CT current ratios.

50:5	300:5	800:5
100:5	400:5	900:5
150:5	450:5	1000:5
200:5	500:5	1200:5
250:5	600:5	

1.2.2 Protection Coordination of Radial Distribution Networks

In a typical radial type distribution network, feeders have fuses, reclosers and circuit breakers installed to prevent damage to the system when fault conditions occur. Fuses only operate for permanent faults (known as the fuse saving scheme). In the event of a temporary fault, the recloser opens quickly to allow the fault to self-clear, or slowly if the fuse fails to clear a permanent fault. In the event that the recloser and fuse both fail to clear the fault, the feeder relay will operate to prevent system damage [11, 22].

Traditional protection coordination in radial distribution networks requires the determination of minimum and maximum fault currents that may be experienced by the feeder. These fault levels allow for the fast characteristic curve of the recloser to be determined and set below the fuse's minimum melting time, while the slow characteristic is placed above the total clearing time curve. This allows the recloser to operate before the fuse is activated, allowing temporary faults time to self-clear. In the case of a permanent fault, the fuse will operate before the recloser utilizes the slow characteristic curve application. The characteristic curve of the relay resides above the recloser slow characteristic and serves as a backup protection. The implications are that for coordination to be maintained it is imperative that the fault current levels experienced by the feeder remain in the predetermined minimum and maximum range [11, 22]. This scheme can be depicted graphically via Figure 1.6.

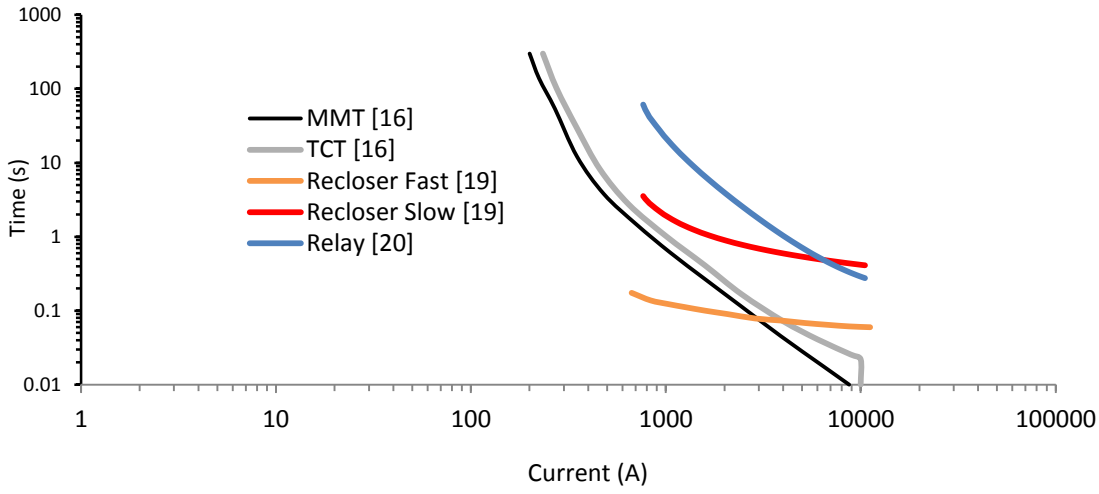

Figure 1.6: Typical characteristic curves for protection coordination in radial distribution networks.

1.3 Fault Current Limiters

Fault current limiters (FCLs) limit the amount of short circuit current that is allowed to flow into a power network enabling continual operation of systems despite faulted conditions [23]. FCLs are series devices that have very low impedances (near zero) during steady state system operation (normal mode) but rapidly introduce high impedance into the protected line to restrain the short circuit current (superconducting mode) to a desirable level during fault conditions [24].

FCLs can be classified into quench, non-quench and composite type, depending on their operating characteristics. Quench FCLs can be resistive, inductive or hybrid and act to limit the fault level through control of the conversion between the normal and superconducting states. Non-quench type FCLs can be iron core, bridge or active types, and control the fault level by controlling the conductor current. Composite type FCLs combine the principles of the quench and non-quench types [25].

An alternate type of FCL is known as the resonant FCL. The resonant FCL, as the name suggests, is a component that makes use of the series resonant circuit in a system to limit the short circuit level during fault conditions. For resonant FCLs, the short circuit current increases gradually, (not instantaneously during a fault condition, the effect being that the fault can be interrupted at a lower magnitude, preventing damage to the system [26, 27].

1.4 Literature Review

With the anticipation that various types of DG's are set to be introduced into distribution grids with increasing levels of penetration [28], there is scope for engineers to investigate viable methods of solving the coordination issues associated with DG introduction. Research into adaptions which will limit the influences of DG on existing protection systems is still in its infancy. IEEE Std. 1547 was the first standard of its kind, promoting the disconnection of all DGs from the system following fault detection [29]. This design prevents fault current contribution through disconnection during fault conditions, solving coordination issues. The inefficiency associated with this practice is that the DG would have to resynchronize to the grid for reconnection and decrease the capacity of the network, even for temporary faults.

Abdel-Galil and team [2] demonstrate that inverter based DG has little effect on existing protection coordination when compared to synchronous machine based DG sources. Reference [2]

also determines a method to ascertain the DG penetration level at which coordination is no longer maintained. The solution presented in [2] would obviate the need for protection system redesign, but it is not feasible long term, as it limits the amount of DG that is able to be introduced. An alternative solution offered in [2] is to redesign the protective schemes, again not feasible long term due to high re-engineering costs.

A proposal for the use of microprocessor based reclosers to prevent loss of coordination is one of a range of possible recommended solutions [22, 30]. These solutions are based on the use of multiple recloser curves which are selected following analysis of current system operating conditions and output of recloser algorithms. Williams [31] proposes the use of inverse time admittance relays which have an admittance factor rather than pick up current to determine trip conditions.

Other solutions that have been developed involve the use of communications based protocols. A selection is outlined in [32, 33]. Although this type of solution is reliable, the methodology requires protective device upgrades and changes to existing settings. These additions come at a high capital cost, and the buyback period of the DG may affect economic unfeasibility.

A recently developed solution is presented in [12] where it is proposed that inverter based DGs are used to limit the fault current contribution of the DG. Although this solution is effective it is limited to the capabilities of the inverters.

One possible response to re-evaluation of existing protection infrastructure following DG integration is to utilize FCLs. FCLs are series devices that have very low impedance (considered zero) during steady state operation but change following a fault to a high impedance value in order to limit the short circuit current [26]. Some research has been conducted in the use of FCLs for DG integration. El-Khattam [34] presents a method of restoring relay coordination in a loop based system using FCLs. It demonstrates that FCLs have the ability to limit the fault current contribution of the DG and maintain relay original coordination. However, it does not investigate fuse-recloser coordination.

A solution presented in [35] demonstrates the use of FCLs in limiting the overvoltages and additional fault current experienced by the introduction of DG. This paper does not outline the type of DG used nor does it thoroughly investigate the implications of DG integration into multiple locations in a distribution system. Reference [35] only investigates DG integration for locations

between the utility and the load, whereas in a realistic distribution system the load is not confined to a single location but is rather spread throughout the network [11, 15, 21]. Additionally, the results presented do not investigate the implications of increased DG on the system's steady state operation.

1.5 Research Objective and Scope of the Thesis

Due to the increasing size of energy demand by the consumer, utility companies around the world are investigating the efficiencies of integrating distributed resources to curb the additional stresses that will be experienced by existing generating units [2]. The introduction of DG sources offers a method of expanded generating capacity and increased reliability in power supply; however it also offers its own challenges with regards to aspects of system operation. This has led to growing research in the field of DG integration, as utilities look to mitigate the detrimental operational effects DG sources can have on power networks.

Alteration of the adequacy of existing protective schemes is one of these detrimental effects of DG integration. Other critical issues that have been identified with regard to protection systems are: the alterations made by DG integration on fuse-recloser coordination, recloser sensitivity and recloser bi-directionality [2]. Although the use of FCLs has been employed in some research [30, 34], no research has been reported on the effects of FCL use on synchronous machine based DG source integration for the purposes of the mitigation of fuse-recloser mis-operation.

The main objective of this research is to determine the feasibility of use of superconducting FCLs to mitigate short circuit currents that can affect fuse-recloser coordination, recloser sensitivity, and recloser bi-directionality during fault conditions. The approach utilizes FCLs at the DG side of the interconnection transformer in conjunction with some characteristics from [2] to determine the effectiveness of using FCLs to mitigate the effects of synchronous machine based DG sources on fuse-recloser protection infrastructure in a typical radial distribution network. The approach demonstrates the use of FCLs to restore the effectiveness of the original fuse-recloser characteristics with the presence of synchronous machine based DG sources without the requirement of DG disconnection as per IEEE Std. 1547 or alteration to existing protection infrastructure.

This thesis is organized into five chapters, a list of references section and two appendices. Chapter 1 introduces the fundamentals of protection coordination, generation source interconnection and distributed generation. An introduction into FCLs is also included. Objectives are also presented.

In Chapter 2, the system under study is introduced along with the details associated with the modelling of individual components. A sample case study is also presented in this chapter.

Chapter 3 outlines the approach taken for DG impact assessment on fuse-recloser loss of coordination, recloser loss of sensitivity and recloser bi-directionality. Case studies are also presented for each problem.

Chapter 4 presents results in the validation of the use of FCLs in mitigating the effects of synchronous machine based DG integration on distribution networks during fault conditions. A critical analysis of results is also presented in this chapter.

Chapter 5 summarizes the research described in this thesis and presents conclusions and recommendations for future research.

The data of the systems under investigation are provided in Appendix A.

Fault current characteristics of the system under study are provided in Appendix B

2. MODELING OF POWER SYSTEMS FOR DISTRIBUTED GENERATION IMPACT ASSESSMENTS

2.1 Introduction

This chapter presents a discussion of the system under study with particular reference to the protection settings and mathematical models of individual components. Results of a digital time-domain simulation of the system during a three-phase fault are presented at the end of this chapter.

2.2 System under Study

2.2.1 Network

A modified version of the suburban distribution network presented in [2] and shown in Figure 2.1 is used in the investigations in this thesis. The system comprises of a connection to the utility (modeled as a source behind impedance) connected to a double ended substation, with a transformer on each side with a rating of 100 MVA. The rated bus voltage is 25kV. Each transformer feeds six feeders and a tie breaker is connected to allow for all twelve feeders to be supplied by a single transformer. For the main feeder, a 2 Ω series reactor is placed on the head end to limit the highest fault current to approximately 6 kA. There are two suburban loads of 5 MVA, each connected at bus 1. These loads are considered as lateral feeders and their protective elements are not under investigation in this thesis. Bus 2 and bus 3 have 2.1 MVA residential loads. Bus 4 has a 1 MVA industrial load connected which is modelled by a 1 MVA induction motor. Bus 5 has a 1 MVA commercial load connected through a delta/wye transformer. More details on the loads, components and cables are presented in APPENDIX A.

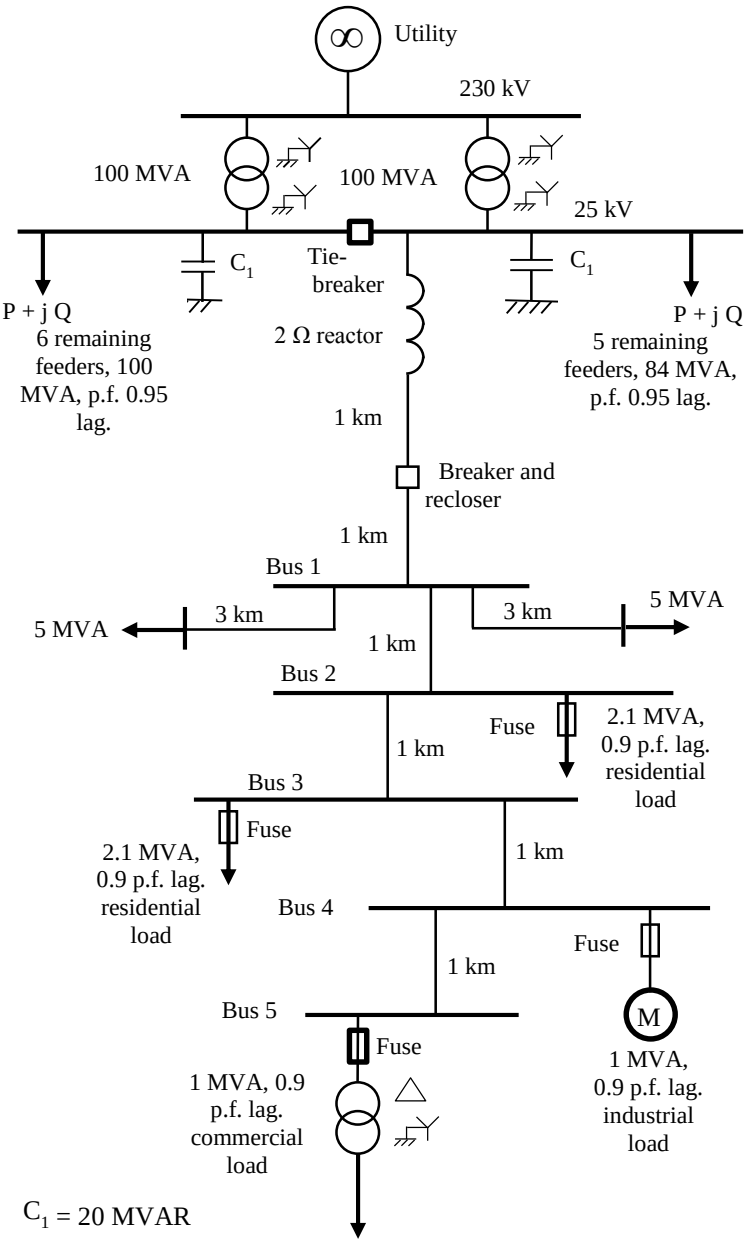

Figure 2.1: Single line diagram of the suburban distribution system under study [2].

2.2.2 Protection Coordination Paths

As per Figure 2.1, loads connected to buses 2 to 5 are fuse protected at the connections to the feeder backbone. The feeder backbone has a recloser and relay present on the head end. Four coordination paths are therefore present, each with a fuse-recloser-relay scheme (fuse is most

downstream device). These paths are feeder to bus 2, feeder to bus 3, feeder to bus 4, and feeder to bus 5. These coordination paths are shown in Figures 2.2 to 2.5.

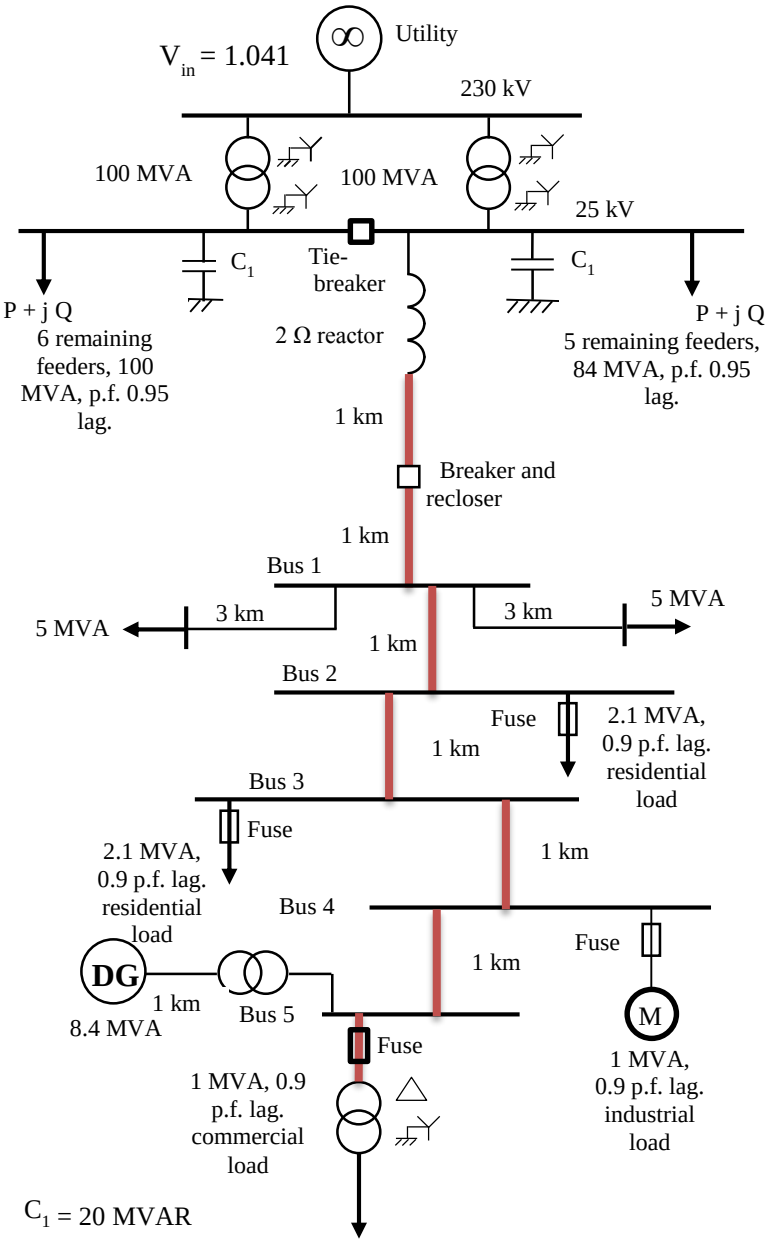

Figure 2.2: Single line diagram of the suburban distribution system bus 5 coordination path.

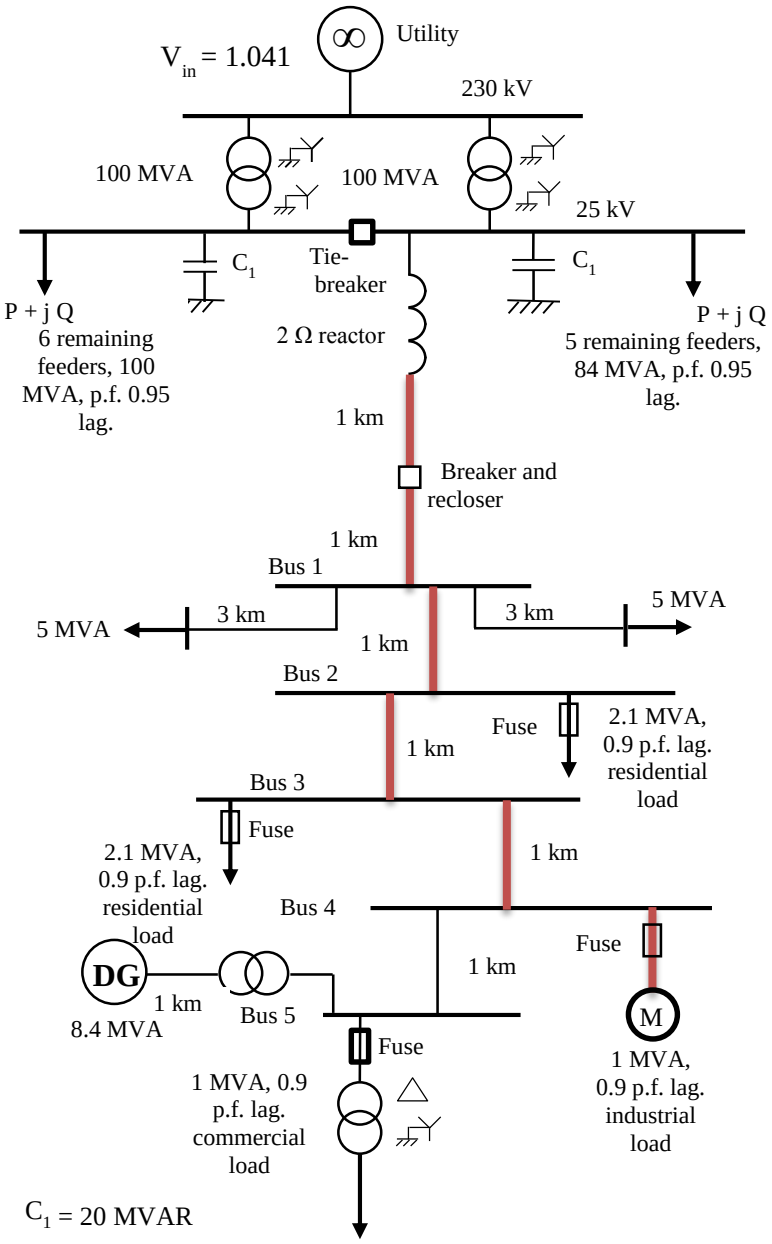

Figure 2.3: Single line diagram of the suburban distribution system bus 4 coordination path.

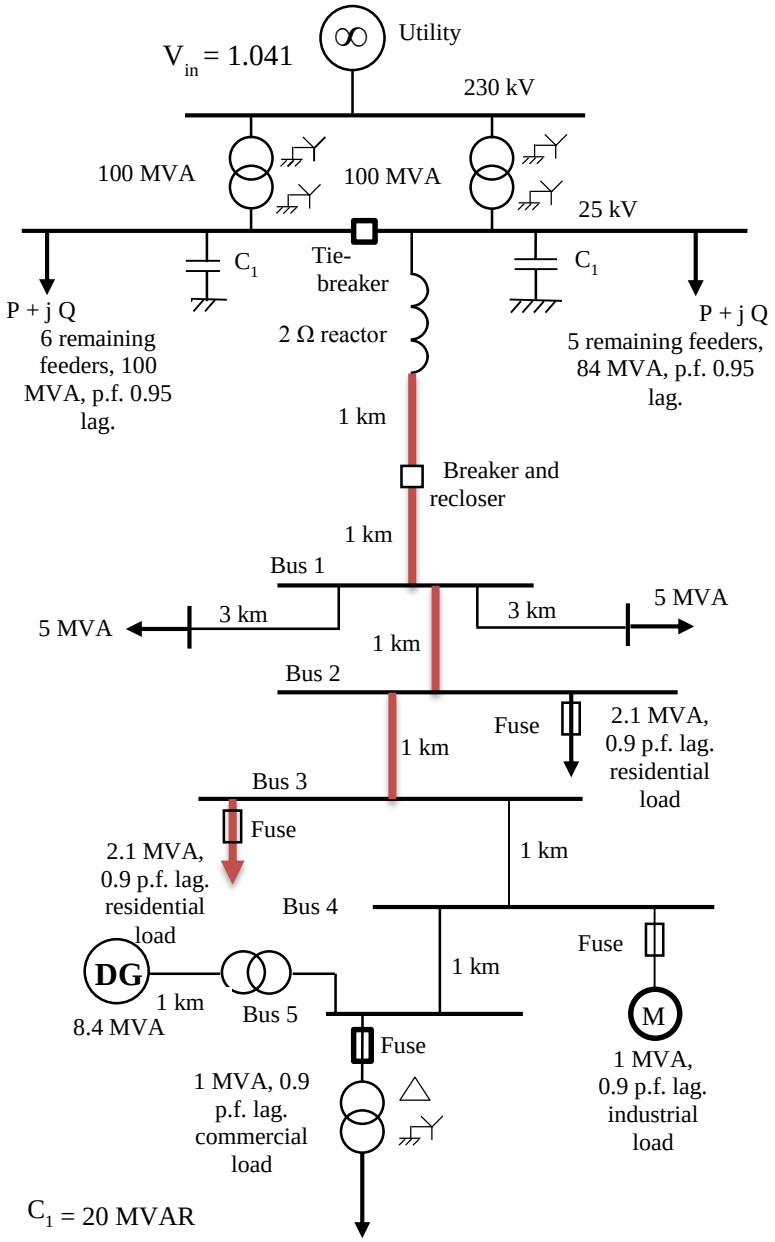

Figure 2.4: Single line diagram of the suburban distribution system bus 3 coordination path.

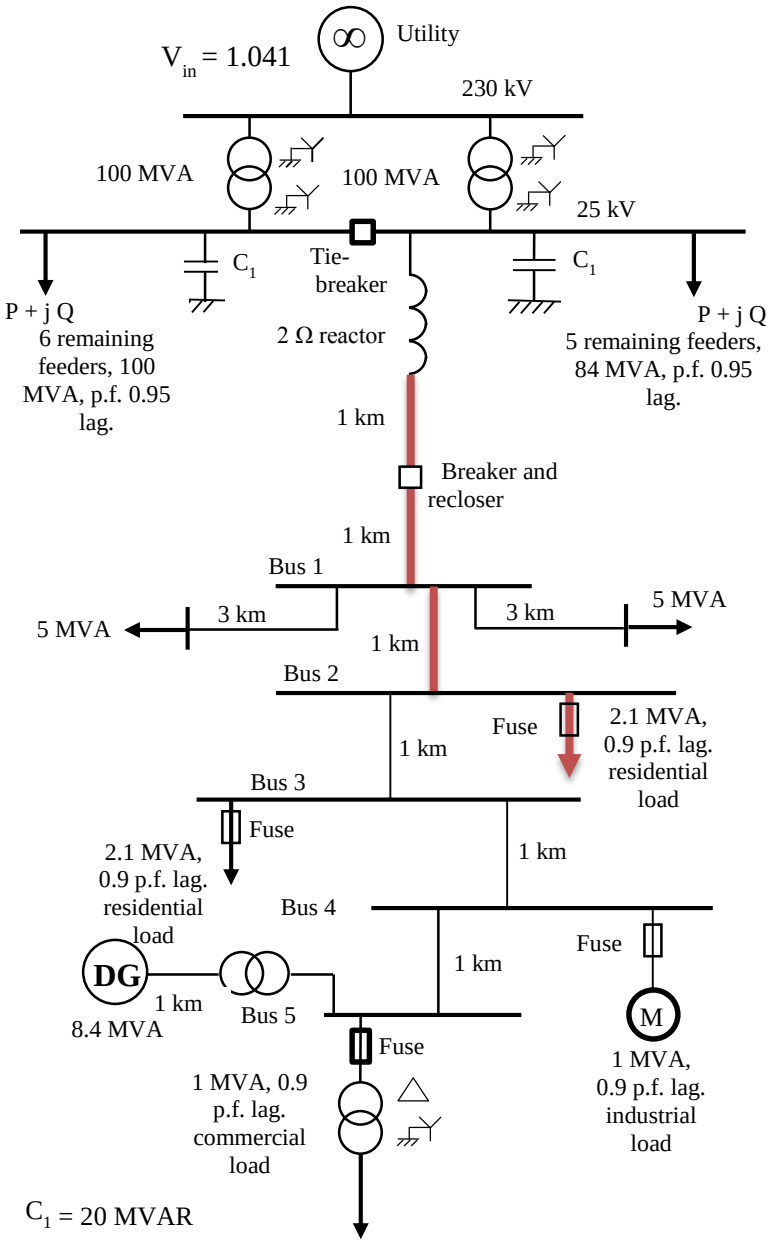

Figure 2.5: Single line diagram of the suburban distribution system bus 2 coordination path.

2.2.3 Protection Settings

As specified in Section 1.2.2, most modern radial distribution networks employ a fuse saving scheme. This is to prevent excessive maintenance costs on lines where there are temporary faults [11].

2.2.3.1 Utility to 1 MVA Commercial Load (Bus 5)

As per Figure 2.1, the coordination path extends from the utility source to the last load of the system. The coordination path includes the main feeder relay, the recloser, and the lateral fuse connected on the high voltage side of the load transformer. The most downstream device is the lateral fuse protecting the 1 MVA load. The rating of this fuse is selected through the use of Equation 2.1 [21].

$$I = \frac{S_{load}}{\sqrt{3} \times V_{LL}} \times Multiplying\ factor \tag{2.1}$$

In the case of a fuse, the multiplying factor used is 1.75 so as to account for the transformer inrush current as well as coordination with the transformer damage curve [2].

This gives a rating of:

$$I = \frac{10^6}{\sqrt{3} \times 25000} \times 1.75 = 40.4 \text{ A}$$

A Kearney 40T fuse is adequate. It should be noted that T fuses are more preferable than K in this context due to the slower response times of the T fuses, allowing for easier coordination with the upstream recloser [11].

For the recloser rating, Equation 2.1 can also be used with a multiplying factor: the recloser phase and ground setting being 1.5 and 0.75 respectively [21]. As per Section 2.2.1, the overall load of the main feeder is 16.2 MVA. This gives a phase trip setting of:

$$I = \frac{16.2 \times 10^6}{\sqrt{3} \times 25000} \times 1.5 = 561.2 \text{ A}$$

The nearest standard recloser rating that is adequate is 560 A [10].

The ground trip setting is given as:

$$I = \frac{16.2 \times 10^6}{\sqrt{3} \times 25000} \times 0.75 = 280.6 \text{ A}$$

The nearest standard recloser rating that is adequate is 280 A [10].

The head end feeder relay pick up settings are found using the same calculations as those for the recloser [11]. From this the phase and ground pick up settings of the relay are 600 A and 300 A, respectively. Given that the relay phase pick up current is 600 A, the CT ratio is selected to be 600:5 as per Table 1.3.

It is necessary to determine the time-current characteristic curves for the relay and recloser for both the ground and phase operations.

The recloser is coordinated with the fuse such that a fuse saving scheme is employed for the network. This means that the recloser fast TCC needs to react faster to a fault than that of the fuse for the most severe fault current experienced by the system. The fault current experienced by the system for faults at varying locations is given in APPENDIX B. As can be seen from the results in APPENDIX B, the maximum phase short circuit current experienced for a fault at the bus 5 load is 1059 A which equates to 1171 A experienced by the recloser/relay. When performing recloser-fuse coordination for fuse saving it is recommended that for adequate system operation, the recloser fast clearing time be at least 75% lower than that of the minimum melt time of the fuse and that the recloser slow clearing time be at least double that of the fuse maximum clearing time [11]. Given this, the recloser phase fast TCC is selected to be the ANSI INV INST-1 curve. This characteristic yields a trip time for a current of 1171 A at 0.0461 seconds while the fuse reacts in 0.0976 seconds, well within the 75% tolerance. The recloser phase slow TCC is selected to be the ANSI INV-2 curve. This characteristic yields a trip time for a current of 1171 A at 1.56 seconds while the fuse reacts in 0.1567 seconds, well within tolerance.

Similarly for the ground setting, the maximum ground short circuit current experienced during a fault at the bus 5 load is 657 A, which equates to 889 A for the recloser/relay. The recloser ground fast TCC is selected again to be the ANSI INV INST-1 curve. This characteristic yields a trip time for a current of 889 A at 0.0382 seconds while the fuse reacts in 0.2476 seconds, well within the 75% tolerance. The recloser ground slow TCC is selected to be the ANSI LTEI-1 curve. This characteristic yields a trip time for a current of 889 A at 7.48 seconds, while the fuse reacts in 0.3762 seconds, well within tolerance.

For the recloser to relay coordination, it is recommended that the difference in clearing times between the recloser slow TCC and relay be 0.2 to 0.3 seconds. Given this recommendation the relay is selected as an ABB DPU 2000R LT EI with a time dial setting (TDS) of 1 and a tap setting of 5 (scale: 1/12) for the phase settings, and a TDS of 1 with a tap of 2.5 (scale: 1/12) for the ground settings. For the maximum phase fault current of 1171 experienced by both the relay and recloser, the relay operates in 23.46 seconds while the recloser slow TCC yields operation in 1.56 seconds. For the maximum ground fault current of 889 A experienced by both the relay and recloser, the relay operates in 21.89 seconds while the recloser slow TCC yields operation in 7.48 seconds. These large margins are due to other coordination paths.

Given these settings, Figure 2.6 displays the phase coordination TCC curves while Figure 2.7 displays the ground coordination TCC curves [16, 19, 20].

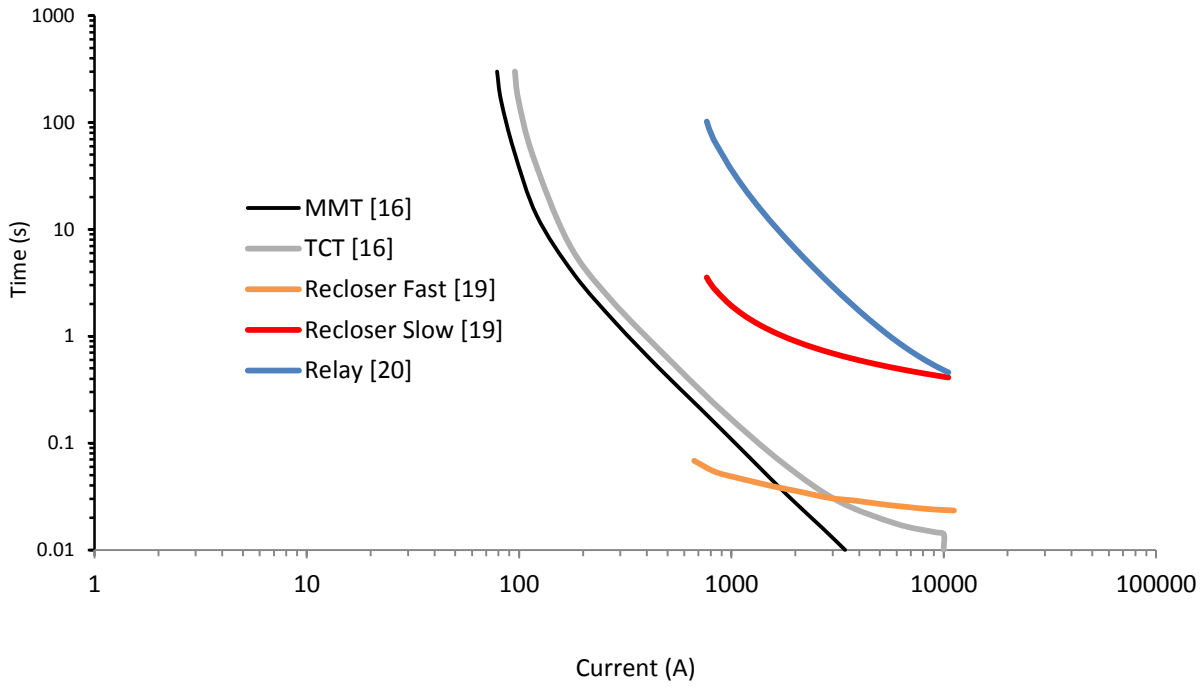

Figure 2.6: Phase coordination chart for the suburban distribution system bus 5 path.

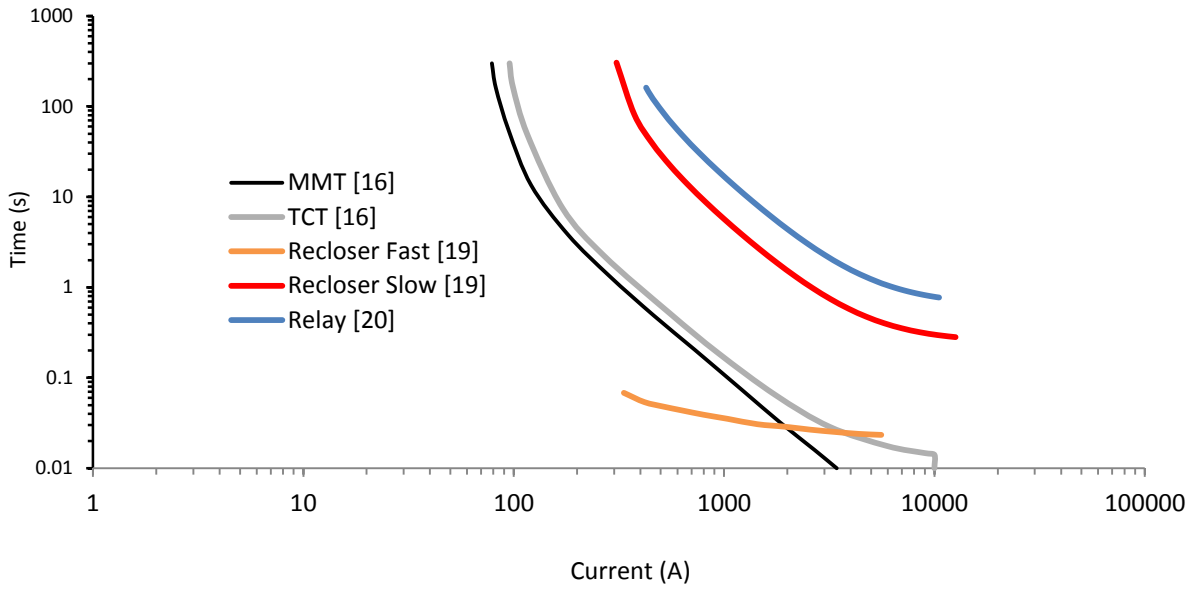

Figure 2.7: Ground coordination chart for the suburban distribution system bus 5 path.

2.2.3.2 Utility to 1 MVA Industrial Load (Bus 4)

As per Figure 2.1, the coordination path extends from the utility source to the industrial load located at bus 4. The coordination path includes the main feeder relay, the recloser, and the lateral fuse connected to bus 4. The most downstream device is the lateral fuse protecting the 1 MVA load. As per Equation 2.1, the rating of the fuse can be determined by [21]:

$$I = \frac{10^6}{\sqrt{3} \times 25000} \times 1.75 = 40.4 \text{ A}$$

A Kearney 40T fuse should be adequate. The recloser and relay are the same as those specified in Section 2.2.3.1. From here it is necessary to check for coordination between the recloser/relay and the 50T fuse.

As per the results in APPENDIX B, the maximum phase short circuit current experienced for a fault at bus 4 is 3869 A which equates to 3917 A experienced by the recloser/relay. The recloser phase fast TCC is the ANSI INV INST-1 curve. This characteristic yields a trip time for a current of 3869A at 0.0292 seconds while the fuse reacts in 0.025 seconds, indicating that the

fuse needs to be increased in size. A Kearney 50T fuse is adequate as it is close enough to 1.5 times the load current and will still allow for at least one recloser operation. The recloser phase slow TCC is the ANSI INV-2 curve. This characteristic yields a trip time for a current of 3917 A at 0.6086 seconds while the fuse reacts in 0.0317 seconds, well within tolerance.

Similarly for the ground setting, the maximum ground short circuit current experienced for a fault at bus 4 is 3402 A, which equates to 3516 A for the recloser/relay. The recloser ground fast TCC is the ANSI INV INST-1 curve. This characteristic yields a trip time for a current of 3516 A at 0.0253 seconds while the fuse reacts in 0.0369 seconds. This is marginally outside the 75% tolerance recommendation, which should still be within operational tolerance levels. The recloser ground slow TCC is the ANSI LTEI-1 curve. This characteristic yields a trip time for a current of 3516 A at 0.672 seconds while the fuse reacts in 0.3762 seconds, marginally outside the twice operating time recommendation but still considered adequate.

For the maximum phase fault current of 3917 A experienced by both the relay and recloser, the relay operates in 1.8 seconds while the recloser slow TCC yields operation in 0.6117 seconds. For the maximum ground fault current of 3516 A experienced by both the relay and recloser, the relay operates in 1.87 seconds while the recloser slow TCC yields operation in 0.672 seconds. Given the settings, Figure 2.8 displays the phase coordination TCC curves while Figure 2.9 displays the ground coordination TCC curves [16, 19, 20].

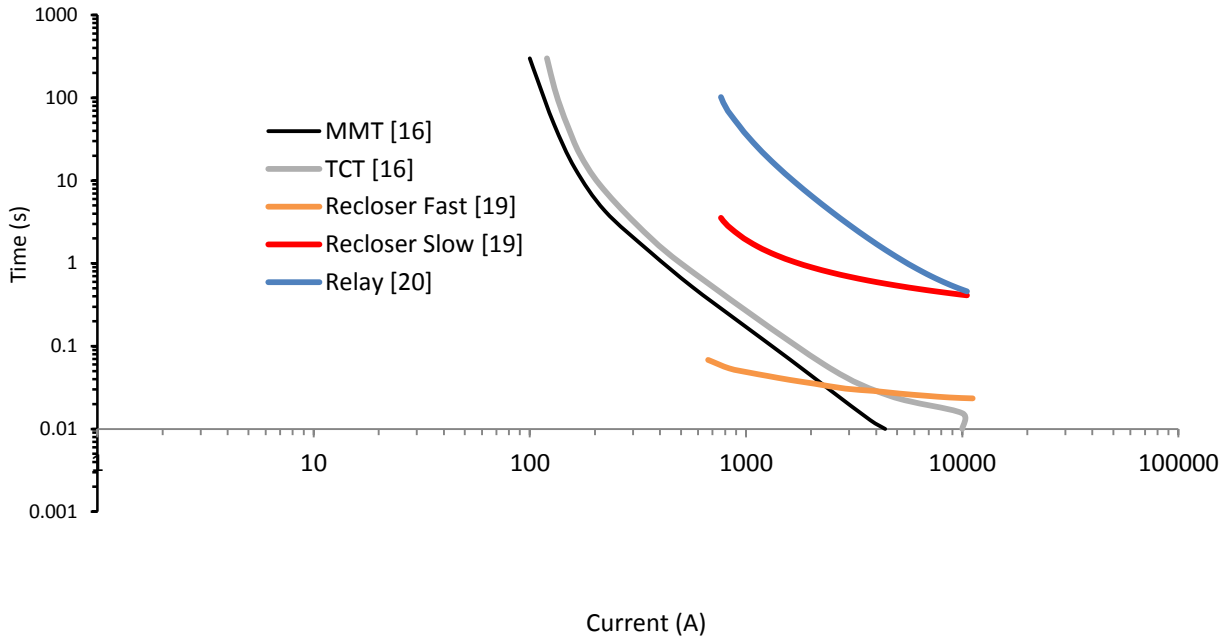

Figure 2.8: Phase coordination chart for the suburban distribution system bus 4 path.

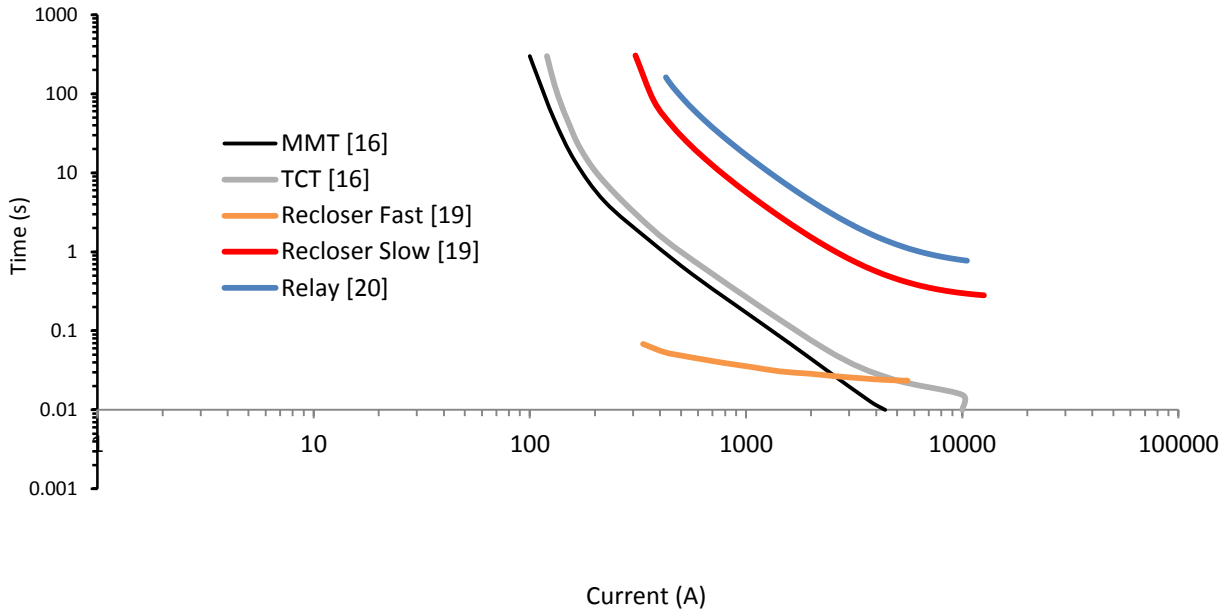

Figure 2.9: Ground coordination chart for the suburban distribution system bus 4 path.

2.2.3.3 Utility to 2.1 MVA Industrial Load (Bus 2/3)

The load for bus 2 and bus 3 are identical in magnitude and are both residential loads hence their coordination paths will be the same. Bus 2 will have the highest fault level due to it being located closer to the utility [11]. As per Figure 2.1, the coordination path extends from the utility source to the residential loads located at bus 2/3. The coordination path includes the main feeder relay, the recloser, and the lateral fuse connected to bus 2/3. The most downstream device is the lateral fuse protecting the 2.1 MVA load. As per Equation 2.1, the rating of the fuse can be determined by:

$$I = \frac{2.1 \times 10^6}{\sqrt{3} \times 25000} \times 1.75 = 84.9 \text{ A}$$

A Kearney 100T fuse should be adequate.

The recloser and relay are the same as those specified in Section 2.2.3.1. At this point it is necessary to check for coordination between the recloser/relay and the 100T fuse.

The results in APPENDIX B demonstrate that the maximum phase short circuit current experienced for a fault at bus 2 is 4707 A, which equates to 4724 A experienced by the recloser/relay. The recloser phase fast TCC is the ANSI INV INST-1 curve. This characteristic yields a trip time for a current of 4724 A at 0.0277 seconds while the fuse reacts in 0.032 seconds, which is just outside the 75% tolerance, which should be within operational limits. The recloser phase slow TCC is the ANSI INV-2 curve. This characteristic yields a trip time for a current of 4724 A at 0.5585 seconds while the fuse reacts in 0.0581 seconds, well within tolerance.

Similarly for the ground setting, the maximum ground short circuit current experienced for a fault at bus 2 is 4256 A which equates to 4313A for the recloser/relay. The recloser ground fast TCC is the ANSI INV INST-1 curve. This characteristic yields a trip time for a current of 4313 A at 0.0244 seconds while the fuse reacts in 0.0384 seconds, well within the 75% tolerance range. The recloser ground slow TCC is the ANSI LTEI-1 curve. This characteristic yields a trip time for a current of 4313 A at 0.531 seconds while the fuse reacts in 0.0673 seconds, well within tolerance.

For the maximum phase fault current of 4724 A experienced by both the relay and recloser, the relay operates in 1.32 seconds while the recloser slow TCC yields operation in 0.5585 seconds. For the maximum ground fault current of 4313 A experienced by both the relay and recloser, the

relay operates in 1.43 seconds while the recloser slow TCC yields operation in 0.531 seconds.

Given the settings, Figure 2.10 displays the phase coordination TCC curves while Figure 2.11 displays the ground coordination TCC curves [16, 19, 20].

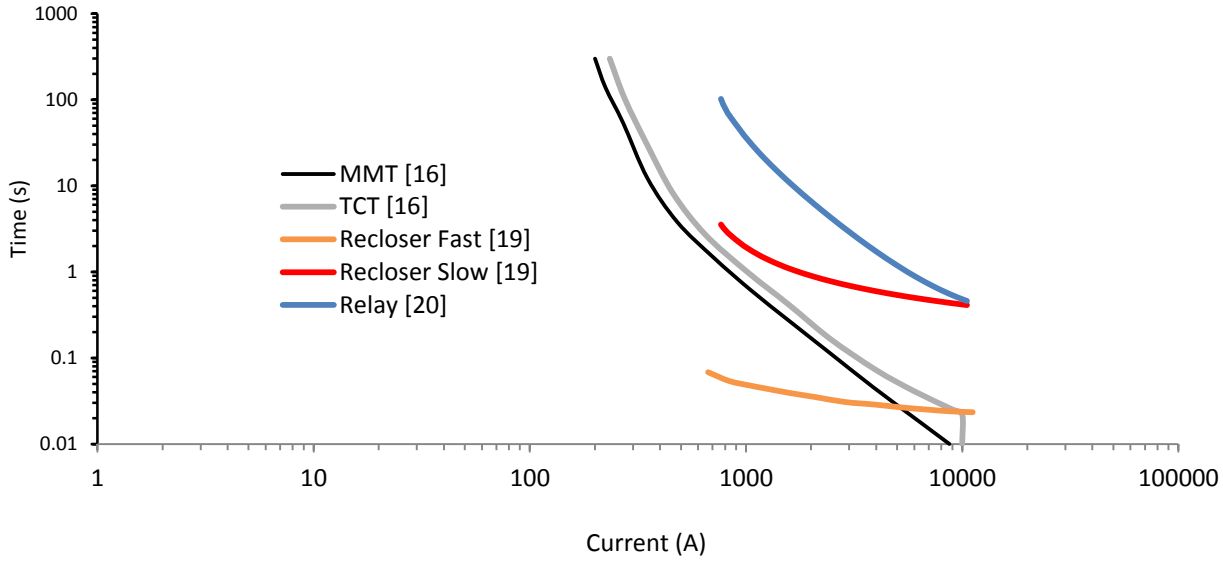

Figure 2.10: Phase coordination chart for the suburban distribution system bus 2/3 path.

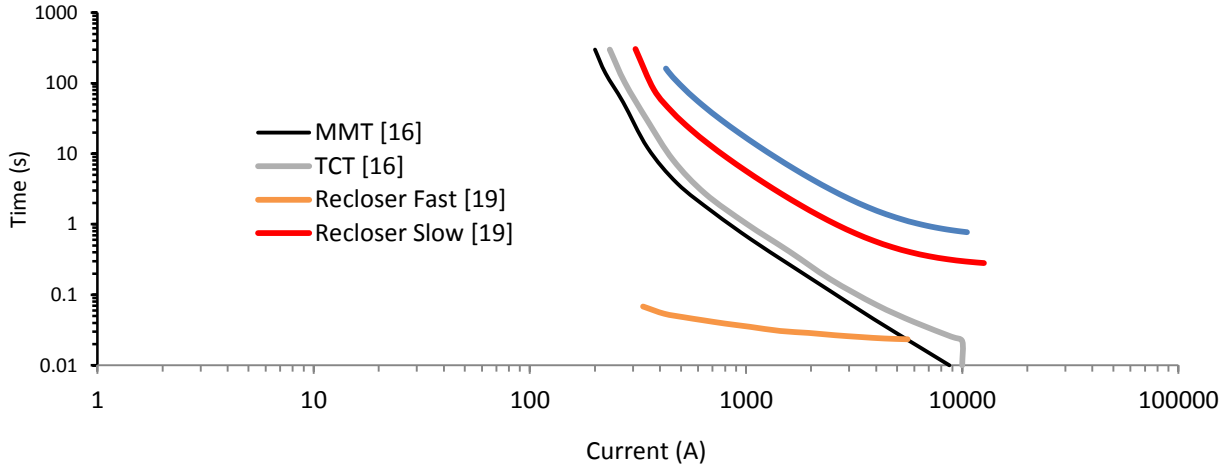

Figure 2.11: Ground coordination chart for the suburban distribution system bus 2/3 path.

2.2.4 Candidate DG Interconnection Points

As per [2], the candidate DG connection points of the system used in this thesis are bus 1, bus 2, bus 3, bus 4, and bus 5. The coordination paths for bus 2 and 3 are similar, hence bus 3 is not investigated as a DG connection point in this study. These DG connection locations can be dictated by system studies or client requirements [2].

2.3 Power System Modeling

The nonlinear differential equations of the system under study are derived through the development of individual mathematical models representative of multiple components of the network. This includes modeling of the utility, distribution lines, transformers, system loads, the synchronous generator (DG source), and the fault current limiters.

2.3.1 Modeling of the Utility

The utility connection shown in Figure 2.1 is modelled as a voltage source of constant voltage and angle behind a small impedance. The voltage is kept at 1.041 per unit so as to maintain the most downstream voltage (bus 5) above 0.95 per unit, as per most utility standards [21].

2.3.2 Modeling of Distribution Lines

Transmission/distribution lines can be classed into three different categories [10]:

1. Short lines: lines smaller than 80 km in length.
2. Medium lines: lines equal to or longer than 80 km in length but smaller than 240 km.
3. Long lines: lines longer than 240 km in length.

In the PSCAD environment, there are several distribution line models that can be used. Three of these models can be described as;

1. Beregon Model: This model is the traditional nominal PI model of a distribution line where admittance and impedance are manually input at a specific frequency. The suitability of the model is limited to constant frequency operations where studies such as relay coordination are being conducted [36].

2. Frequency Dependent (Mode) Model: This model is used to represent the frequency dependence of the line models using modal techniques to solve the line constants while assuming constant transformation. The issue with this model is that it requires ideally transposed conductor spacing geometry, hence tower configurations must be known for this model to be used accurately [36].
3. Frequency Dependent (Phase) Model: This model is used to represent the frequency dependence of all the parameters (similar to the mode model). It does not require constant transformation since solving occurs in the phase domain. The model is therefore accurate in all studies, including unbalanced line geometry. The limitation comes from the requirement for the tower configuration to be known [36].
4. PI Models: This model is suitable when the frequency is kept constant. It is very precise in keeping admittance and impedance constant, however precision can be inadequate for long lines. The model is mainly used in short and underground lines [37].

Considering that the longest line in the suburban distribution system in Figure 2.1 is 5 kilometers and the test is being conducted using short circuit studies, the PI model is selected as the model for this thesis. The PI model can be visually represented by Figure 2.12.

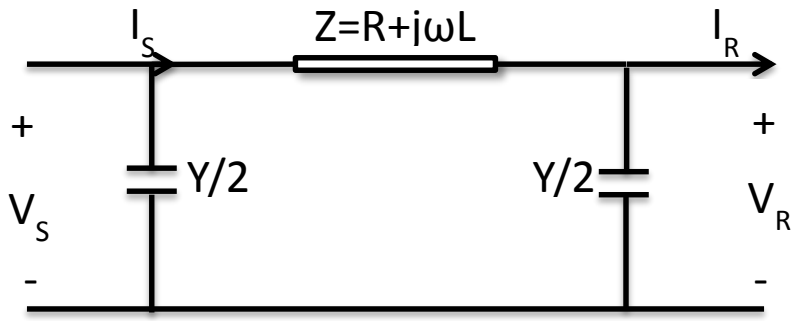

Figure 2.12: The nominal PI model for distribution lines [10].

Where:

- V_S is the sending voltage (V)
- V_R is the receiving voltage (V)
- I_S is the sending current (A)
- I_R is the receiving current (A)

- Y is the total shunt admittance (S)
- Z is the total series impedance (Ω)

An important aspect of a distribution line in short circuit studies is the zero sequence impedance. Positive sequence components are those that consist of three phasors of equal magnitude with 120 degree spacing that rotate in the same direction as the phasors in the network. The negative sequence components are the same as positive except that the phasors are in the reverse sequence. Zero sequence components are three phasors of equal magnitude that are in phase with one another that rotate in the same direction as the positive sequence phasors. The zero sequence impedance of a line differs from the positive and negative sequence, as the magnetic field that creates the positive and negative sequence currents is different to that of the zero sequence. (Positive and negative sequence impedances are of the same magnitude of the given impedance of the line). In the case of single circuit lines, the zero sequence impedance can be up to 3.5 times more than the positive and negative, while for underground cables it can be between 3 and 5 times larger for triplex core underground cables [38, 39]. Given this, the zero sequence impedances of the lines in this thesis are taken to be three times larger than the positive and negative. Cable impedances are given in APPENDIX A.

2.3.3 Modeling of transformers

Two modelling options are available for transformers in the PSCAD simulation environment: the UMEC and classical approach model. The classical approach model utilizes the IEEE equivalent circuit given in [14], using equivalent lumped components to represent internal impedances of the equipment. The Unified Magnetic Equivalent Circuit (UMEC) model is based primarily on the core of the transformer and deals with the magnetic coupling of the different phases [36]. Considering that the key features required from the transformer for the studies in this thesis are impedances and voltage transformation, the IEEE (classical) model is used.

The three phase transformer connected to the bus 5 load in Figure 2.1 is a delta, wye solidly grounded for the high voltage and low voltage sides respectively. All other transformers are wye solidly grounded connections. Each transformer consists of winding resistance, winding reactance and winding impedance as specified in APPENDIX A.

2.3.4 Modeling of system loads

System loads can be modeled by Equations 2.2 and 2.3 [40]

$$P_{Load} = P_0 \left(\frac{V}{V_0}\right)^a \tag{2.2}$$

$$Q_{Load} = Q_0 \left(\frac{V}{V_0}\right)^b \tag{2.3}$$

Where

P_{Load} = real load power at V

Q_{Load} = reactive load power at V

a = real load constant equal to the slope $\frac{dP}{dV}$

b = reactive load constant equal to the slope $\frac{dQ}{dV}$

V_0 = initial voltage

V = current voltage

Loads can be grouped into different categories, each dependent on variation in demand according to voltage [40];

1. Constant Power Loads are loads that demand fixed power supply levels regardless of voltage. The constants a and b are both 0. Examples include induction motors and tap changing transformers.
2. Constant Current Loads are loads for which power demand is proportional to the voltage. The constants a and b are both 1. Examples include thyristor application drives.
3. Constant Impedance Loads are loads where power demand is proportional to the square of the voltage. The constants a and b are both 2. Examples include residential and commercial loads.
4. Composite System Loads are those that have combinations of the other three load types. The constant 'a' usually ranges between 0.5 and 1.8 while 'b' usually ranges between 1.5 and 6.

Considering that the loads connected to every bus in Figure 2.1 are residential or commercial (excluding bus 4) [2], the loads are modeled as constant impedance loads. The load at bus 4 load can be modeled as a constant current load since an induction motor is utilized, however PSCAD does have the capability of modeling induction motors [36].

2.3.5 Induction Motor Model

The model is available in the PSCAD library as a wound rotor induction motor. Both the stator and the rotor are similar to the synchronous machine model specified in Section 2.3.6, in that it can also be represented in the d-q axis frame. The impedance matrix of the induction motor can be expressed as [41];

$$[L] = \begin{bmatrix} r_1 + (L_m + L_1)p & r_1 + (L_m + L_1)p & L_m & L_m p \\ L_m p & L_m \omega_r & r_2 + (L_m + L_2)p & (L_m + L_2)\omega_r \\ -L_m \omega_r & L_m p & -(L_m + L_2)\omega_r & r_2 + (L_m + L_2)p \end{bmatrix} \quad (2.4)$$

$$\begin{bmatrix} v_{1d} \\ v_{1q} \\ v_{2d} \\ v_{2q} \end{bmatrix} = [L] \begin{bmatrix} i_{1d} \\ i_{1q} \\ i_{2d} \\ i_{2q} \end{bmatrix} \quad (2.5)$$

Where r_1 and r_2 are stator and rotor resistances respectively and L_1 and L_2 are stator and rotor reactances respectively.

Additionally, the transient reactance of the induction machine can be expressed as

$$X' = X_1 + \frac{X_m X_2}{X_m + X_2} \quad (2.6)$$

Where X' is the transient reactance, X_1 and X_2 are the stator and rotor reactances respectively X_m is the magnetizing reactance [41]. Induction machine short circuit current can be calculated as

$$i_{SC} = i_{ac} + i_{dc} = \frac{E}{X'} \exp\left(-\frac{t}{T'}\right) + \frac{\sqrt{2}E}{X'} \exp\left(-\frac{t}{T_{dc}}\right) \quad (2.7)$$

Where E is the prefault voltage behind the transient reactance X', T' is the short circuit transient time constant expressed in Equation 2.8, and T_{dc} is the time constant for the decay of the DC component expressed in Equation 2.9.

The time constants are given as:

$$T' = \frac{X'}{\omega r_2} \tag{2.8}$$

$$T_{dc} = \frac{X'}{\omega r_1} \tag{2.9}$$

The nature of the short circuit current is identical to that of a synchronous machine, the main difference being that the current of the induction machine will decay rapidly and can often be ignored after six cycles [41].

2.3.6 Modeling of the Synchronous DG

In this thesis the DG source is modeled as a synchronous generator. In a standard synchronous machine, the stator circuit that consists of a three-phase winding, produces a magneto motive force. The field winding, located on the rotor, is excited by a DC voltage. A synchronous machine can be modeled by the equations given below in the d-q reference frame depicted in Figure 2.13. The convention adopted for the signs of the voltages and currents in the equations below is that *v* is the impressed voltage at the terminals, and the direction of positive current *i* corresponds to generation [42].

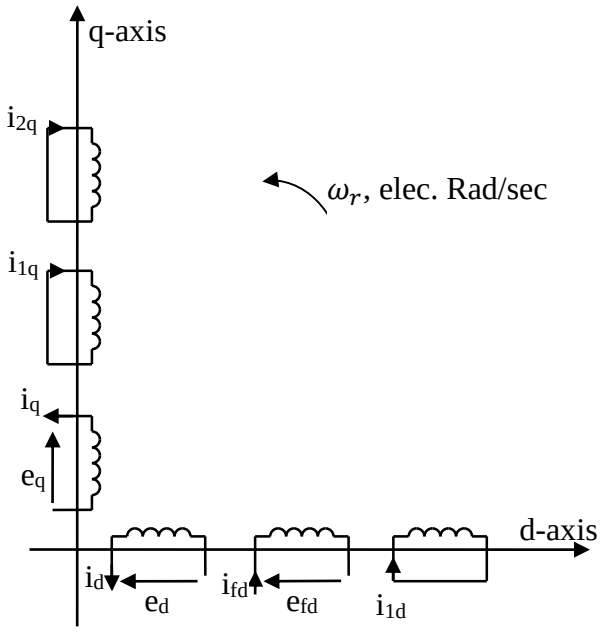

Figure 2.13: Modeling of the synchronous machine in the d-q reference frame.

With time t expressed in seconds, the angular velocity ω expressed in rad/s ($\omega_0 = 377 rad/\text{sec}$) and the other quantities expressed in per unit, the stator equations become:

$$e_d = \frac{1}{\omega_0}\frac{d\Psi_d}{dt} - \frac{\omega}{\omega_0}\Psi_q - R_a i_d \tag{2.10}$$

$$e_q = \frac{1}{\omega_0}\frac{d\Psi_q}{dt} + \frac{\omega}{\omega_0}\Psi_d - R_a i_q \tag{2.11}$$

The rotor equations:

$$e_{fd} = \frac{1}{\omega_0}\frac{d\Psi_{fd}}{dt} + R_{fd} i_{fd} \tag{2.12}$$

$$0 = \frac{1}{\omega_0}\frac{d\Psi_{1d}}{dt} + R_{1d} i_{1d} \tag{2.13}$$

$$0 = \frac{1}{\omega_0}\frac{d\Psi_{1q}}{dt} + R_{1q} i_{1q} \tag{2.14}$$

$$0 = \frac{1}{\omega_0}\frac{d\Psi_{2q}}{dt} + R_{2q} i_{2q} \tag{2.15}$$

The stator flux linkage equations:

$$\Psi_d = -L_d i_d + L_{ad} i_{fd} + L_{ad} i_{1d} \tag{2.16}$$

$$\Psi_q = -L_q i_q + L_{aq} i_{1q} + L_{aq} i_{2q} \tag{2.17}$$

The rotor flux linkage equations:

$$\Psi_{fd} = L_{ffd} i_{fd} + L_{ad} i_{1d} - L_{ad} i_d \tag{2.18}$$

$$\Psi_{1d} = L_{ad} i_{fd} + L_{11d} i_{1d} - L_{ad} i_d \tag{2.19}$$

$$\Psi_{1q} = L_{11q} i_{1q} + L_{aq} i_{2q} - L_{aq} i_q \tag{2.20}$$

$$\Psi_{2q} = L_{aq} i_{1q} + L_{22q} i_{2q} - L_{aq} i_q \tag{2.21}$$

The electromagnetic torque equation:

$$T_e = \Psi_d i_q - \Psi_q i_d \tag{2.22}$$

The overall differential equations which describe the transient performance of the synchronous machine are given by the following matrix equation:

$$\left[\frac{dX_{syn}}{dt}\right] = \left[At_{syn}\right]\left[X_{syn}\right] + \left[Bt_{syn}\right]\begin{bmatrix} V_{td} \\ V_{tq} \\ e_{fd} \end{bmatrix} \tag{2.23}$$

where

$$\left[X_{syn}\right] = [i_d \quad i_q \quad i_{fd} \quad i_{1q} \quad i_{1d} \quad i_{2q}]^T$$

$$\left[At_{syn}\right] = [L]^{-1}[Qt]$$

$$\left[Bt_{syn}\right] = [L]^{-1}[Rt]$$

$$[L] = \begin{bmatrix} -L_d & 0 & L_{ad} & 0 & L_{ad} & 0 \\ 0 & -L_q & 0 & L_{aq} & 0 & L_{aq} \\ -L_{ad} & 0 & L_{ffd} & 0 & L_{ad} & 0 \\ 0 & -L_{aq} & 0 & L_{11q} & 0 & L_{aq} \\ -L_{aq} & 0 & L_{ad} & 0 & L_{11d} & 0 \\ 0 & -L_{aq} & 0 & L_{aq} & 0 & L_{22q} \end{bmatrix} \tag{2.24}$$

$$[Qt] = \begin{bmatrix} \omega_0 R_a & -\omega L_q & 0 & \omega L_{aq} & 0 & \omega L_{aq} \\ \omega L_d & \omega_0 R_a & -\omega L_{ad} & 0 & -\omega L_{ad} & 0 \\ 0 & 0 & -\omega_0 R_{fd} & 0 & 0 & 0 \\ 0 & 0 & 0 & -\omega_0 R_{1q} & 0 & 0 \\ 0 & 0 & 0 & 0 & -\omega_0 R_{1d} & 0 \\ 0 & 0 & 0 & 0 & 0 & -\omega_0 R_{2q} \end{bmatrix}$$

$$[Rt] = \begin{bmatrix} \omega_0 & 0 & 0 \\ 0 & \omega_0 & 0 \\ 0 & 0 & \omega_0 \\ 0 & 0 & 0 \\ 0 & 0 & 0 \\ 0 & 0 & 0 \end{bmatrix}$$

Here, the superscript ^{T} means matrix transpose.

The interconnection of the DG to the network in Figure 2.1 is as shown in Figure 1.2 in Section 1.1.1.

2.3.7 Modeling of the Fault Current Limiters

Fault current limiter models are required to have no influence on steady state system operations (invisible to the system) but are also required to produce a high impedance during fault periods in order to limit the short circuit current. Three FCL models are considered in this thesis, designated FCL_R, FCL_L and FCL_LC. Individual values for components in Sections 2.3.7.1, 2.3.7.2 and 2.3.7.3 are given in APPENDIX A.

2.3.7.1 Resistive FCL Model

The resistive type FCL (FCL_R) model's elements consist of a superconducting resistor in parallel with a regular resistor. When steady state conditions are present, the superconducting element of the FCL is in a superconductive state, allowing normal load currents to pass through with virtually no losses. When a fault occurs, the current will sharply rise and will surpass a critical current of the FCL. At this point the FCL will transition into its normal resistive state, applying high impedance to the connection point (R_{FCL}). This in turn limits the short circuit level. In practical FCLs, a parallel resistance (R_P) is present to protect the FCL during the transition period from "hot spots". It also adjusts the limited current and, in the event the FCL resistance rises too rapidly, avoids overvoltages [24]. This can be represented graphically via Figure 2.14.

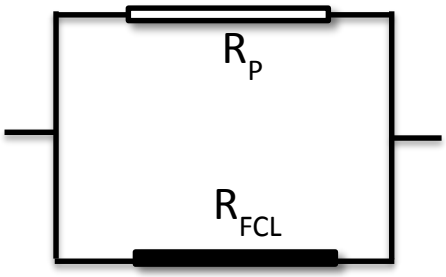

Figure 2.14: Resistive type superconducting FCL.

Superconducting FCLs are required to limit the fault current to at least between three and five times the rated line current [24]. Three values of R that will allow for this to occur at 60, 50 and 20 Ω respectively. Figure 2.15 illustrates the fuse protecting the bus 5 for a three phase fault at bus 5 with and without the FCL_R in service respectively.

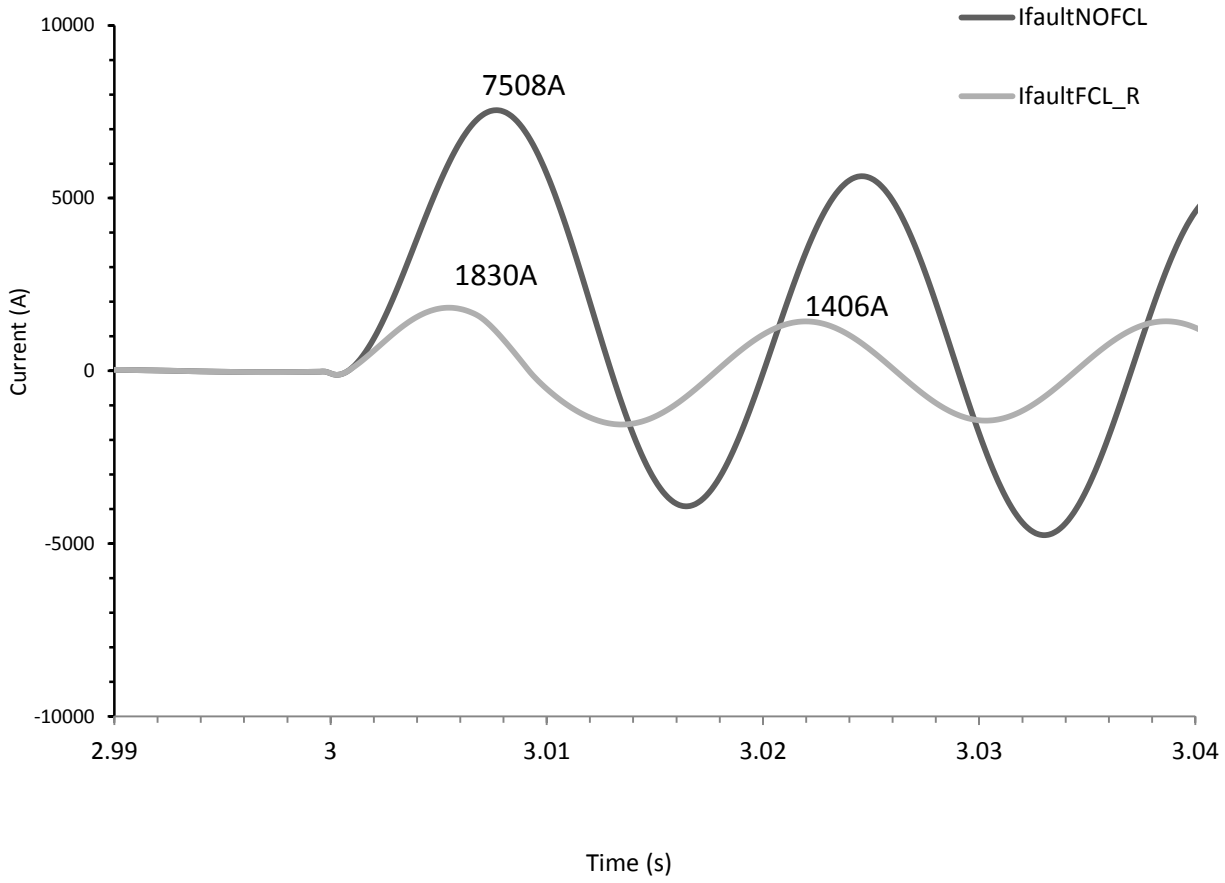

Figure 2.15: Current through fuse 2 during a three phase to ground fault at bus 5 with and without a 60 Ω FCL_R.

As can be seen in Figure 2.15, when the FCL is disabled the peak current is 7508 A. In contrast, the peak current for the FCL system is 1830 A in the first half cycle, which reduces to 1406 A in the second (less than 5 times the peak load current). Observations demonstrate that the

fault current is reduced by 76% in the first half cycle, demonstrating that the models being used for the FCL are operating as expected.

2.3.7.2 Inductive FCL Model

Similarly for the inductive type FCL (FCL_L) model, two coils are connected in parallel as depicted in Figure 2.16. Under steady state conditions, currents flow through L_{TC} until a fault condition occurs. In the presence of the fault condition, L_{TC} transitions to the L_{FCL} state, limiting the fault current [24]. Similar to Section 2.3.7.3, the inductance values used in this thesis are 0.16, 0.13 and 0.05 H respectively.

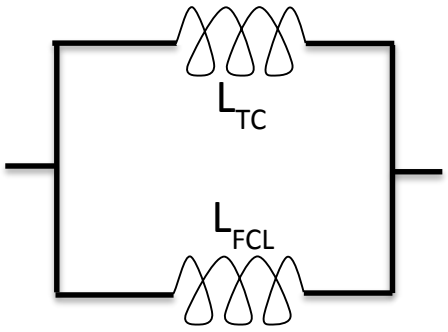

Figure 2.16: Inductive type superconducting FCL.

2.3.7.2 Resonant FCL Model

For the resonant FCL model (FCL_LC), an inductor is placed in series with a capacitor as depicted in Figure 2.17. The capacitor is protected via a metal oxide varistor (MOV). Similar to FCL_R and FCL_L, during steady state operation the FCL is virtually invisible to the system. The resonant frequency of this circuit given by Equation 2.25 is tuned to the frequency of the power (60 Hz) such that under steady state conditions the FCL is virtually invisible to the system [27].

$$f_c = \frac{1}{2\pi\sqrt{LC}} \tag{2.25}$$

Where f_c is the resonant frequency (Hertz), L is inductance (H) and C is capacitance (F)

When a short circuit occurs, the FCL has a characteristic that increases the current gradually. This is due to the activation of the MOV across the capacitor when the capacitor protection voltage level is reached [27]. L and C are 0.187 H and 37.665 μF respectively.

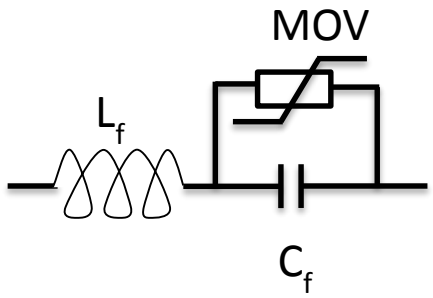

Figure 2.17: Resonant type superconducting FCL.

2.4 A Sample Case Study: Effects of DG Integration on Short Circuit Level

The following sample case study demonstrates the effect of DG integration on short-circuit levels of a power network. It shows results for a three phase fault at bus 4 in Figure 2.1 for both bus 1 synchronous machine based DG integrated and non-DG systems. Further results are presented in APPENDIX B for differing fault types, DG locations and fault locations with results presenting the same conclusions as the sample case study. The studies conducted in this thesis utilize the PSCAD/EMTDC program to model a variety of system components to produce time-domain simulation results. It should be noted that faults are assumed to occur 9 seconds into the simulation to ensure steady state system operation has occurred.

Figure 2.18 shows the voltage load flow results (in per unit voltage) for the suburban distribution system without DG integration while Figure 2.19 depicts the time-domain short circuit level for a fault at bus 4 experienced by the bus 4 fuse and feeder recloser respectively. Figure 2.20 presents a summary of the varying three phase fault currents experienced by the recloser and fuse at each bus without DG integration.

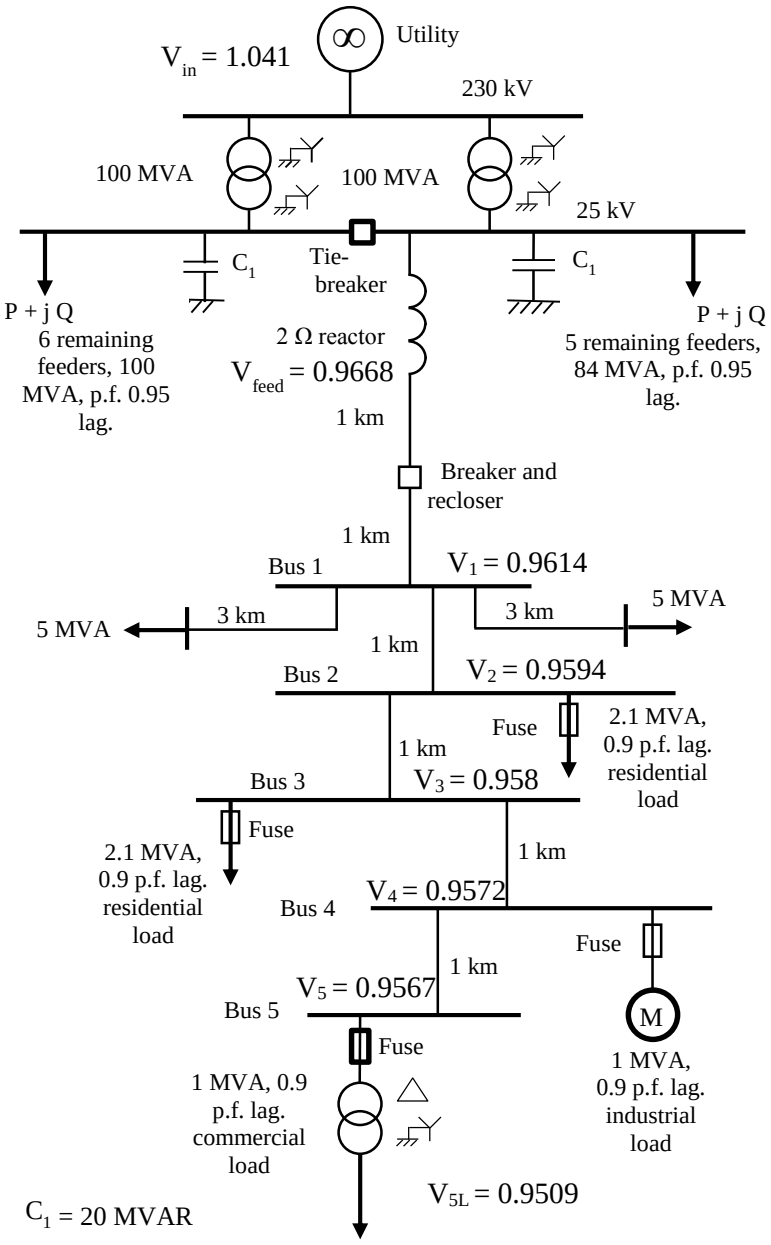

Figure 2.18: Suburban distribution system bus voltages without DG integration.

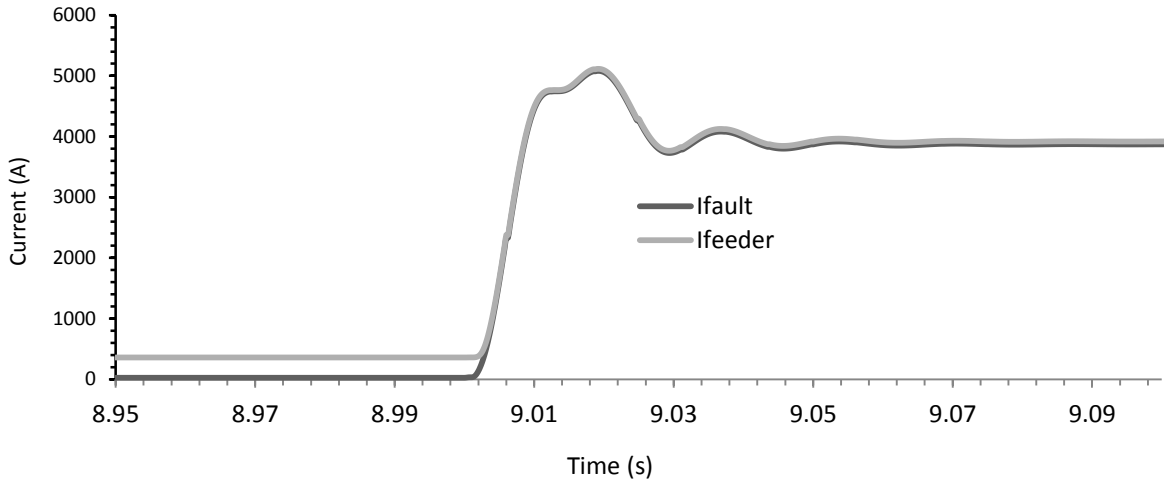

Figure 2.19: Time-domain RMS current simulation for a fault applied at bus 4.

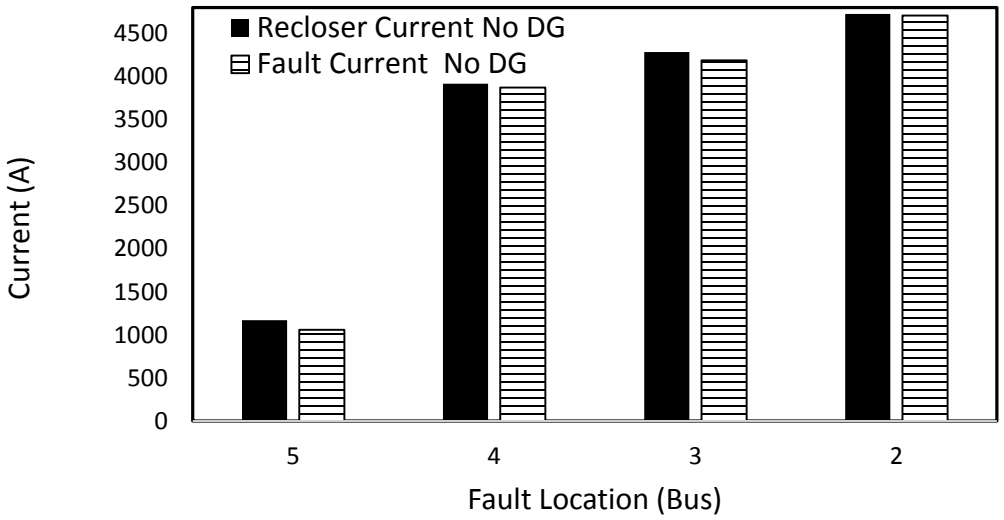

Figure 2.20: Fault current experienced by the relay and respective bus fuse for a three phase fault.

As can be observed in Figure 2.20, there is a correlation between the distance from the utility source and the size of the fault. This is as expected, since the further the fault is from the source, the larger the impedance that is available in the lines to limit the fault level [10].

Figure 2.21 shows the voltage load flow results (in per unit voltage) for the suburban distribution system with an 8.4 MVA DG integration at bus 1 while Figure 2.22 depicts the time-domain short circuit level for a fault at bus 4 experienced by the bus 4 fuse and feeder recloser respectively. Figure 2.23 presents a summary of the varying fault currents experienced by the recloser and fuse at each bus with an 8.4 MVA DG integration at bus 4 while being compared to those that were obtained in Figure 2.20. An 8.4 MVA DG size was selected as it has the capacity to supply over half the local load demand.

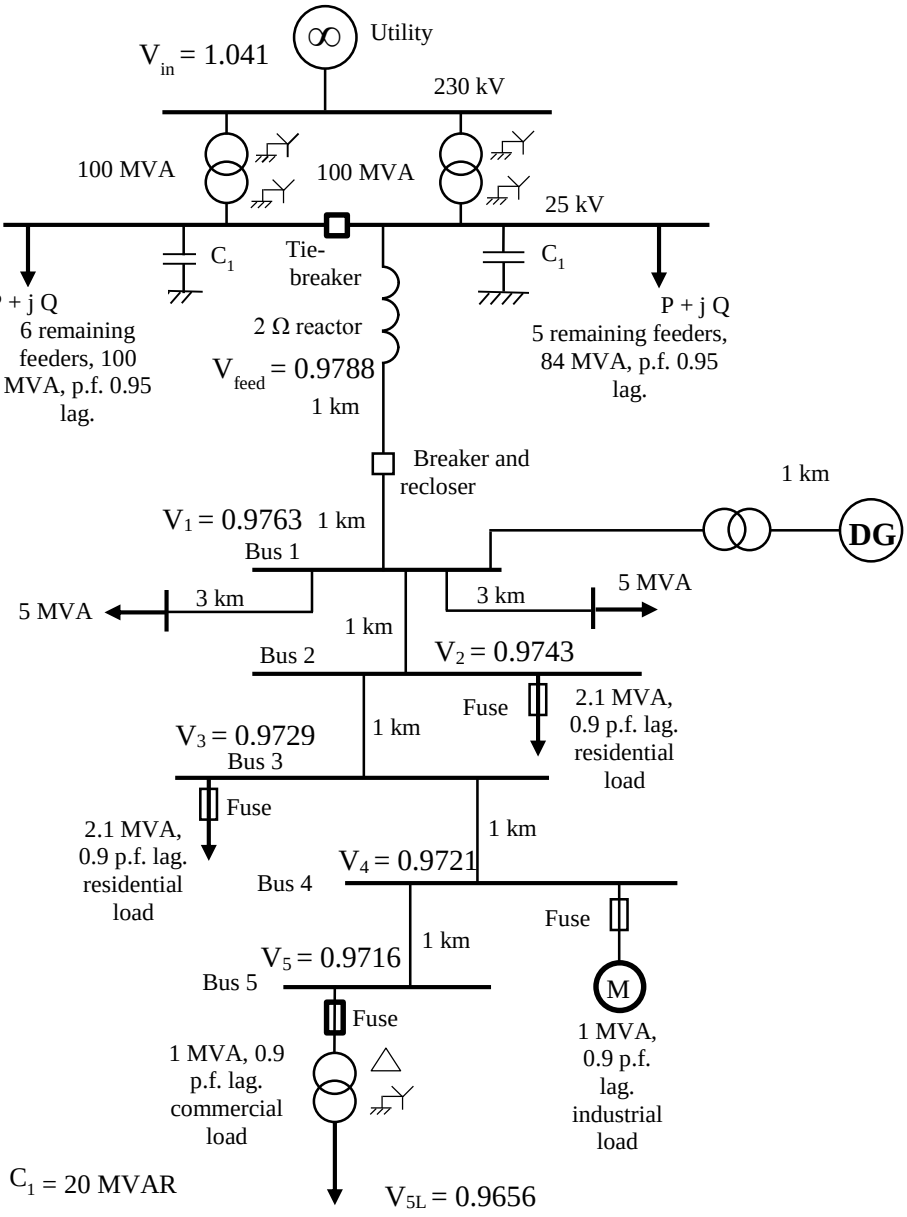

Figure 2.21: Suburban distribution system bus voltages with DG integration at bus 1.

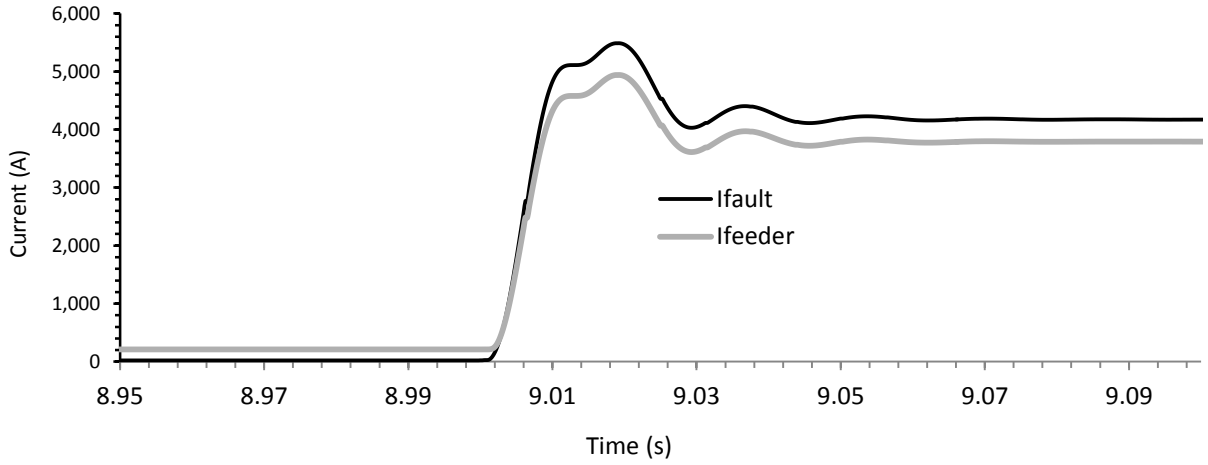

Figure 2.22: Time-domain RMS current simulation for a fault applied at bus 4 with 8.4 MVA DG integration at bus 1.

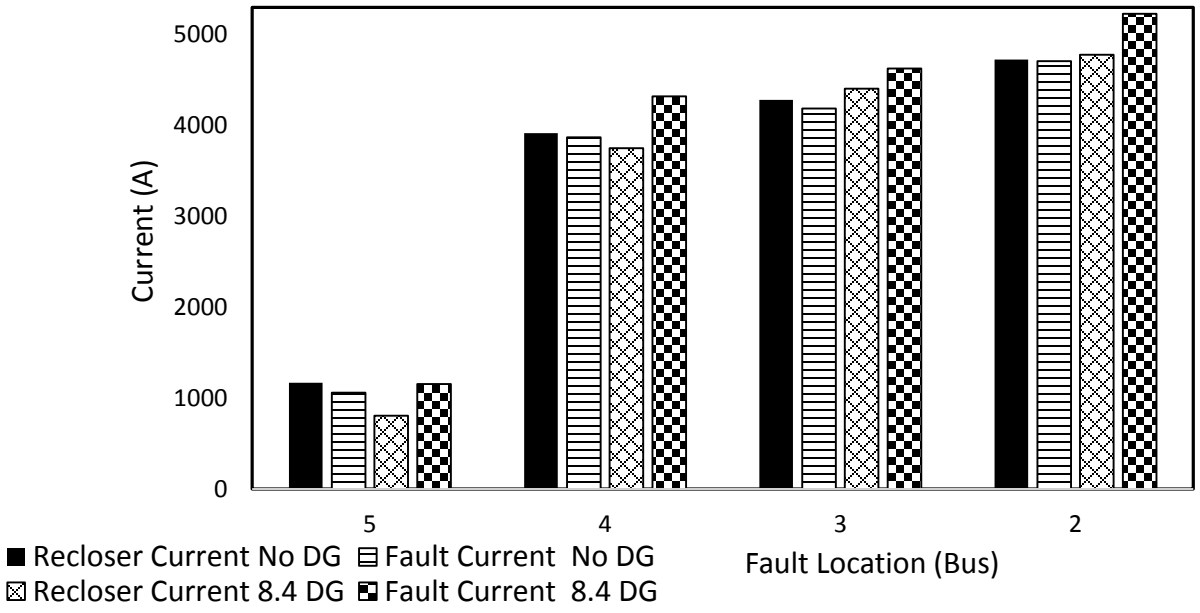

Figure 2.23: Fault current experienced by the relay and respective bus fuse for a three phase fault at bus 4 for both 8.4 MVA DG integrated at bus 1 and non-DG integrated systems.

Observation of Figure 2.21 in conjunction with Figure 2.18 makes it apparent that DG integration can aid in the improvement of the voltage profile of a power network [1-9] with an average of 1.54% increase in voltage is generated when DG is present. When the 8.4 MVA DG is

connected at bus 5 this voltage profile improves by up to 3%, demonstrating the capacity for the DG source to supplement the voltage of a power system, enhancing the voltage of the network.

Comparison of Figure 2.19 in conjunction with Figure 2.22 highlights that in the event of a fault condition, the fault current contribution from the utility decreases with the presence of DG. In the case study presented, the contribution to the fault current by the utility can decrease by as much as 32% in some cases meaning that the recloser located on the main feeder will detect a lower fault current than what is present. Although there is less stress on the utility during the fault condition, this lower short circuit level being detected may cause the protection infrastructure to fail to perform as expected.

Analysis of Figure 2.23 demonstrates that the inclusion of a small DG can have a significant effect on the short circuit levels experienced by a power system. In some cases the fault current increased by as much as 16% for a DG that can supply 52% of the total load of the system. This means that the lateral fuses experience heavier currents than when there is no DG presence and can result in the fuse clearing the fault before the feeder's recloser has time to operate. Observations make it apparent that the initial coordination scheme outlined in Section 2.2.3 may no longer be adequate.

From results obtained it is apparent that the introduction of a DG source can significantly change the behavior of a power system under faulted conditions. This gives rise to the need for determination of frameworks to analyze and assess the level of effect that DG sources of varying size may have on the operational characteristics of power systems, and an investigation into how to best mitigate the detrimental changes.

2.5 Summary

Chapter 2 has provided an introduction into the suburban distribution system under consideration, in addition to an investigation into the models employed for the variety of components implemented in the PSCAD software environment. A digital time-domain simulation is presented of a case study of the system under three phase fault conditions both with and without synchronous machine based DG source integration. Results obtained highlight the effect that synchronous machine based DG source integration can have on the short circuit levels of a power system, demonstrating its capacity to adversely affect normal system operations and behaviors.

3. STRATEGIES FOR DG INTEGRATION IMPACT ASSESSMENTS ON PROTECTION INFRASTRUCTURE IN DISTRIBUTION NETWORKS

3.1 Introduction

This chapter presents methods for assessment of DG integration on existing fuse-recloser infrastructure. The proposed impact assessment approach considers effects associated with increasing levels of synchronous machine based DG penetration on previously installed fuse-recloser protection. These effects considered can be classed as [2]:

1. Loss of Coordination: The level of DG penetration that will cause the original fuse-recloser coordination to become inadequate or ineffective at clearing fault conditions for fuse saving schemes.
2. Loss of Sensitivity: The level of DG penetration that will render protective elements unable to detect fault conditions.
3. Bi-Directionality: The level of DG penetration that will cause the original directionality of a fault to reverse

3.2 Loss of Fuse-Recloser Coordination Assessment due to DG Source Interconnection

3.2.1 Loss of Fuse-Recloser Coordination Definition and Method of Assessment

Increasing the size of a DG source can lead to downstream protective devices experiencing greater fault levels than those that are upstream [11, 30]. These devices have previously been coordinated for a system that has excluded this DG source. This can create inadequacy in the original fuse-recloser coordination (current protection settings), causing alterations in behavior under faulted conditions, including loss of fuse-recloser coordination and incorrect performance of fuse saving schemes [30]. In order to determine when fuse-recloser loss of coordination will occur, the following method adapted from the ideas in [2] and presented in Figure 3.1 is useful. This can be explained by:

1. Firstly a synchronous machine based DG source is connected to a previously determined candidate connection point.
2. A load bus is selected with a fault that yields the highest short circuit current being applied to the selection.
3. The algorithm allows the engineer to determine if loss of fuse-recloser coordination has occurred, through analysis of the time overcurrent characteristics of the equipment for the given coordination path.

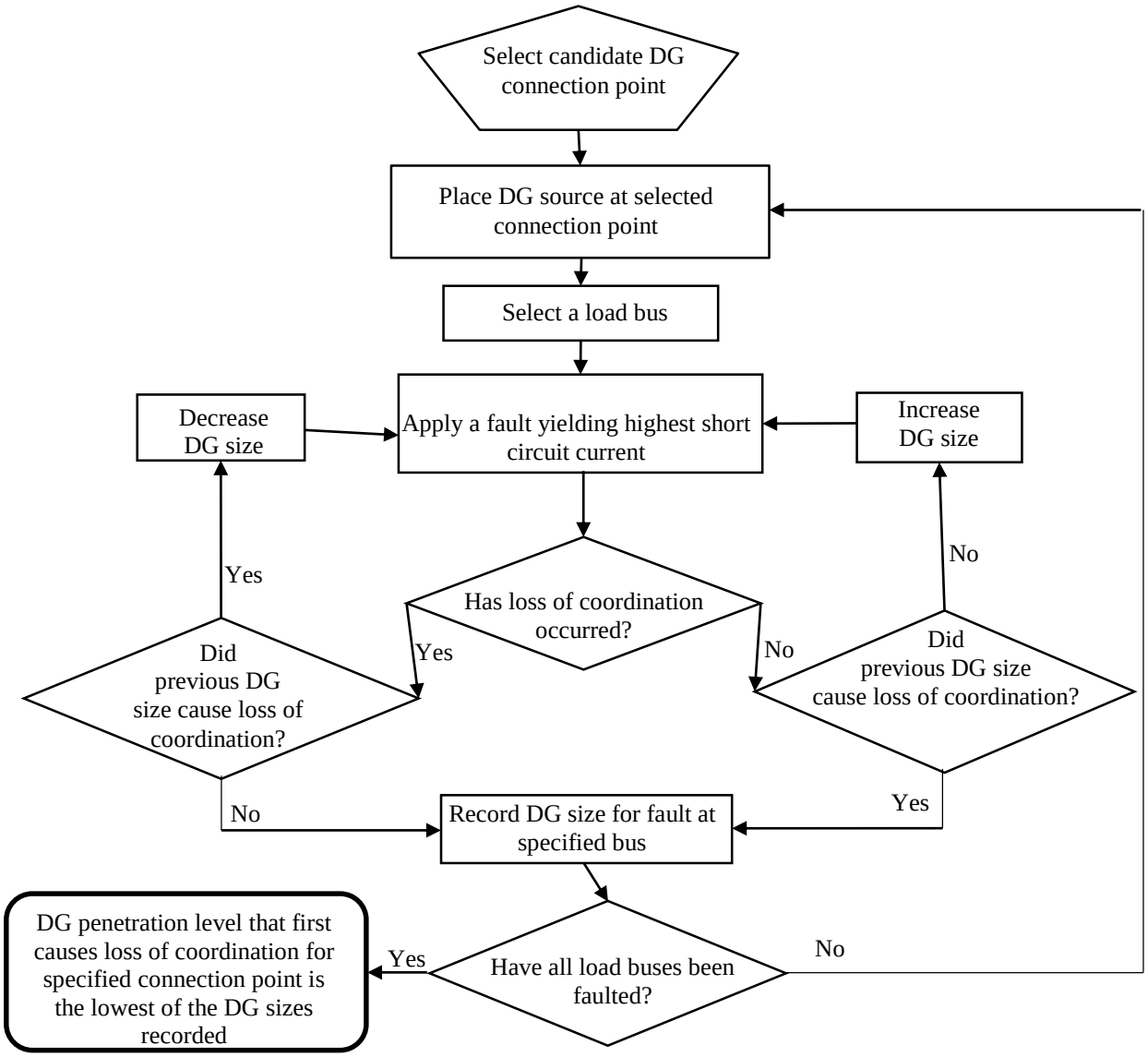

Figure 3.1: Algorithm for the determination of DG penetration level before the occurrence of loss of fuse-recloser coordination.

4. If loss of fuse-recloser coordination has occurred, then it is necessary to look at the previous iteration of the algorithm. If this is the first iteration, or the previous iteration caused loss of coordination, then the DG size needs to be decreased. Otherwise the DG size must be recorded for future use.
5. If loss of fuse-recloser coordination has not occurred, then it is necessary to look at the previous iteration of the algorithm. If this is the first iteration, or the previous iteration did not cause loss of coordination, then the DG size needs to be increased. Otherwise the DG size must be recorded for future use.
6. After the DG size has been recorded, the algorithm needs to be repeated for all coordination paths.
7. The algorithm ends with the result being the lowest DG size recorded from the analysis, since this will be the largest DG size for the selected candidate point before a severe fault will cause mis-operation of the previously determined fuse-recloser coordination.

It should be noted that the algorithm assumes that the protection coordination for the distribution system has been completed as well as the increase/decrease of DG levels being limited so as to accurately capture the penetration level. This algorithm is applied to all DG candidate connection points.

3.2.2 Loss of Fuse-Recloser Coordination Case Study

In regular overcurrent protection coordination for radial distribution networks, it is desirable for the primary protection (for temporary and permanent faults. In this case it is the recloser and fuse respectively) to operate before the backup [11]. As demonstrated in Section 2.4, the integration of DG sources can have an adverse effect on the short circuit characteristics of distribution networks.

3.2.2.1 Bus 1 DG Connection

In order to illustrate the effect of DG integration on fuse-recloser coordination, the case study presented in Section 2.4 should be considered. As depicted in Figure 2.22, the short circuit current experienced by the load lateral fuse at bus 4 increases to 4319 A (11% increase) for a three phase fault at bus 4 with 8.4 MVA synchronous machine based DG integration at bus 1. In contrast,

for the same fault conditions, the short circuit current experienced by the recloser located on the main feeder decreases to 3750 A (5% decrease). This will result in the recloser and load fuse reacting to the faulted condition at differing times than what was previously determined in Section 2.2.3.2. Through the utilization of the coordination chart presented in Figure 2.8, it is apparent that the synchronous machine based DG integrated suburban distribution system, yields a recloser operating time (fast curve) of 0.0294 seconds. In contrast, the lateral fuse protecting the bus 4 load will operate in 0.0274 seconds (10% faster), meaning that it will blow before the recloser has time to attempt to clear the fault. In addition, for this level of synchronous machine based DG penetration, the characteristics determined in Section 2.2.3.2 can no longer be characterized as a fuse saving scheme hence fuse-recloser coordination is no longer present, highlighting the importance of assessment methods such as those presented in Figure 3.1.

In order to assess the level of synchronous machine based DG penetration that the suburban distribution system is able to receive before loss of fuse-recloser coordination occurs, the algorithm present in Figure 3.1 is utilized. In the suburban distribution system presented, there are a total of four coordination paths with fuse-recloser protection as outlined in Section 2.2.2. Each of these paths need to be considered, hence faults need to be placed separately at bus 5, 4, 3 and 2 for each of the candidate connection points. As shown in APPENDIX B, for both the 8.4 MVA DG connected and non DG suburban distribution systems the most severe type of fault is three phase [10]. This results in the three phase fault yielding loss of fuse-recloser coordination before other fault types in the presence of synchronous machine based DG sources.

It is apparent from results given in APPENDIX B that an 8.4 MVA synchronous machine based DG source causes loss of fuse-recloser coordination, with three phase faults at bus 2 and bus 4 having the most severe effect. This means that the DG source needs to be reduced in size in order to be able to determine the penetration level before loss of coordination.

Following the steps presented in Figure 3.1, a synchronous machine based DG size of 5.2 MVA is found to cause the recloser fast characteristic to yield the same trip time as the fuse along the bus 4 coordination path. The time response for this condition and level of DG penetration can be depicted graphically via Figure 2.22 in Section 2.4.

Observations of Figure 2.22 in conjunction with Figure 2.8 demonstrate that at a synchronous machine based DG penetration level of 5.2 MVA, the short circuit characteristics of the suburban distribution system will yield simultaneous operation of the bus 4 coordination paths recloser and fuse hence coordination is lost.

In order to determine if the bus 4 fault presents the lowest synchronous machine based DG penetration level before loss of fuse-recloser coordination, the bus 1 DG connected suburban distributed system in Figure 2.21 is faulted at bus 2 (three phase fault). As per APPENDIX B, a bus 2 fault yields a short circuit current of 4776 A experienced by the recloser. Through the use of Figure 2.10 a recloser current of 4776 A yields an operating time (time) of 0.0273 seconds. The fuse along the bus 2 coordination path in Figure 2.5 will operate at 0.0273 seconds once the short circuit level reaches 5115 A. For a 5.2 MVA synchronous machine based DG at bus 1, the fault current at bus 2 is 4955 A, less than the required 5115 A, meaning that coordination between the fuse and recloser is maintained along the bus 2 coordination path. The time response for this condition and level of DG penetration can be depicted graphically via Figure 3.2.

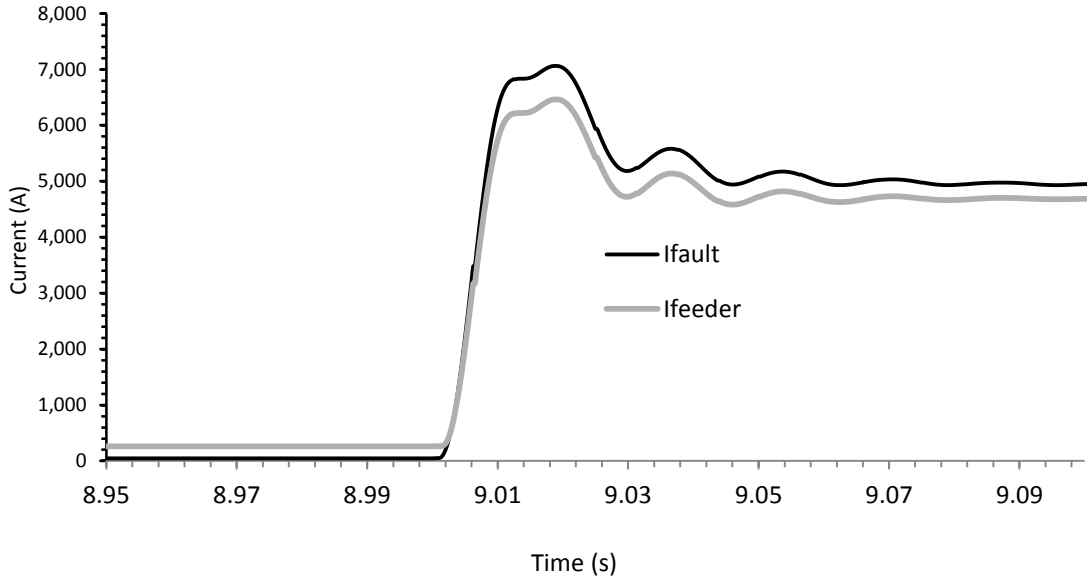

Figure 3.2: Time-domain RMS current simulation for a three phase fault applied at bus 2 with a 5.2 MVA synchronous machine based DG source integrated at bus 1.

Observations of Figure 3.2 in conjunction with Figure 2.10 demonstrate that at a synchronous machine based DG penetration level of 5.2 MVA, the short circuit characteristics of the suburban distribution system along the bus 2 coordination path will yield a trip time of 0.0273 and 0.0282 seconds for the recloser and fuse respectively, hence fuse coordination is maintained. From this it is apparent that the synchronous machine based DG penetration level before loss of coordination between fuse and recloser of at least one coordination path occurs, is 5.2 MVA.

3.2.2.2 Bus 2 DG Connection

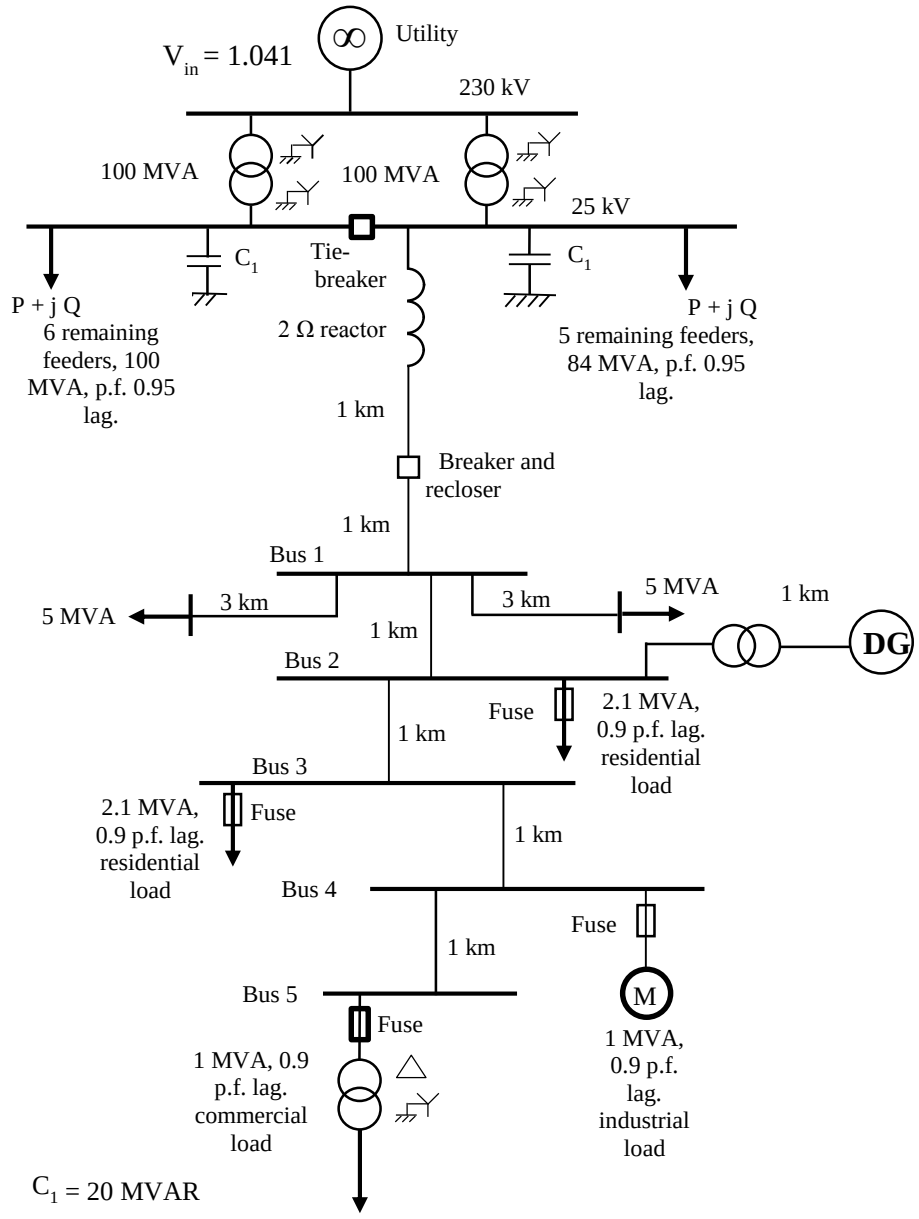

Figure 3.3: Suburban distribution system with DG integration at bus 2.

The bus 2 DG connected (synchronous machine based source) suburban distribution system can be depicted by Figure 3.3.

As observed in APPENDIX B, for a three phase fault at bus 4 of the system depicted in Figure 3.3, the short circuit current experienced by the recloser is 4041 A. Through the use of Figure 2.8, a recloser current of 4041 A yields an operating time (fast) of 0.0287 seconds. The fuse along the bus 4 coordination path in Figure 2.3 will operate at 0.0287 seconds once the short circuit level reaches 4176 A. In order for the fault current to lower to 4176 A, the DG source connected at bus 2 needs to be reduced. Following the steps presented in Figure 3.1, a synchronous machine based DG size of 5.5 MVA is found to cause the recloser fast characteristic to yield the same trip time as the fuse along the bus 4 coordination path. The time response for this condition and level of DG penetration can be depicted graphically via Figure 3.4.

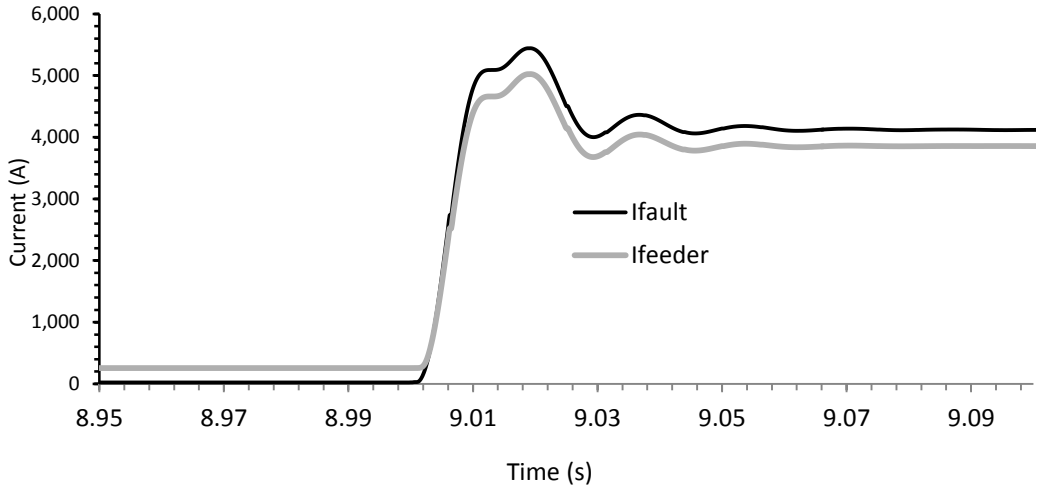

Figure 3.4: Time-domain RMS current simulation for a three phase fault applied at bus 4 with a 5.5 MVA synchronous machine based DG source integrated at bus 2.

Observations of Figure 3.4 in conjunction with Figure 2.8 demonstrate that at a synchronous machine based DG penetration level of 5.5 MVA, the short circuit characteristics of the suburban distribution system will yield simultaneous operation of the bus 4 coordination paths recloser and fuse, resulting in coordination loss.

In order to determine if the bus 4 fault presents the lowest synchronous machine based DG penetration level before loss of fuse-recloser coordination, the bus 2 DG connected suburban distribution system in Figure 3.3 is faulted at bus 2 (three phase fault). As per APPENDIX B, a bus 2 fault yields a short circuit current of 4724 A experienced by the recloser. Through the use of Figure 2.10, a recloser current of 4724 A yields an operating time (time) of 0.0274 seconds. The fuse along the bus 2 coordination path in Figure 2.5 will operate at 0.0274 seconds once the short circuit level reaches 5084 A. For a 5.5 MVA synchronous machine based DG at bus 2, the fault current at bus 2 is 5028 A, less than the required 5084 A, meaning that coordination between the fuse and recloser is maintained along the bus 2 coordination path. The time response for this condition and level of DG penetration can be depicted graphically via Figure 3.5.

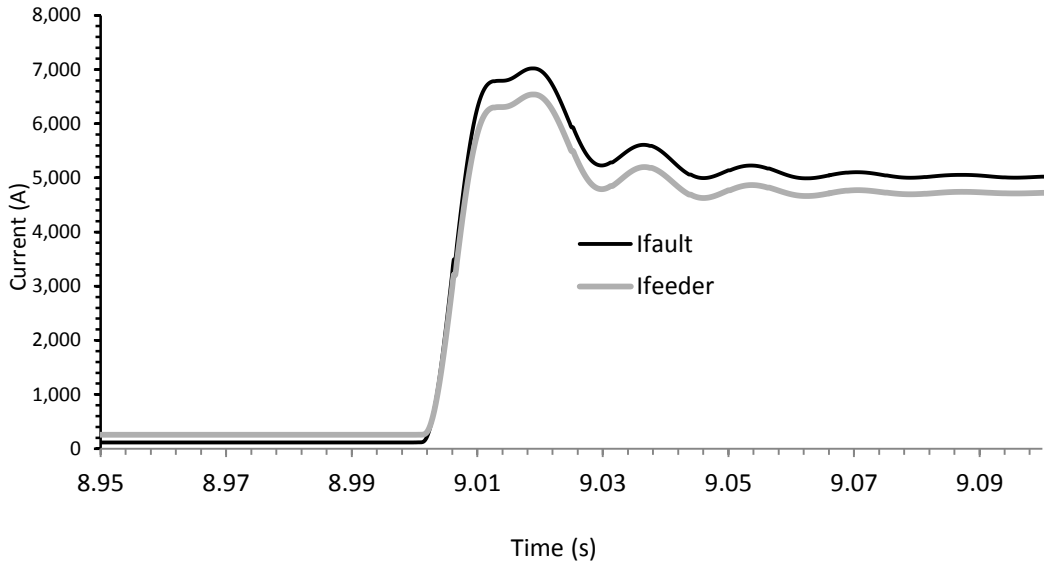

Figure 3.5: Time-domain RMS current simulation for a three phase fault applied at bus 2 with a 5.5 MVA synchronous machine based DG source integrated at bus 2.

Observations of Figure 3.5 in conjunction Figure 2.10 demonstrate that at a synchronous machine based DG penetration level of 5.5 MVA, the short circuit characteristics of the suburban distribution system along the bus 2 coordination path will yield a trip time of 0.0274 and 0.0281 seconds for the recloser and fuse respectively, hence fuse coordination is maintained.

From this it is apparent that the synchronous machine based DG penetration level of the suburban distribution system depicted in Figure 3.3 is 5.5 MVA, before loss of coordination occurs between the fuse and recloser of at least one coordination path.

3.2.2.3 Bus 4 DG Connection

Similar to Section 3.2.2.2, the bus 4 DG connected (synchronous machine based source) suburban distribution system can be depicted by Figure 3.6.

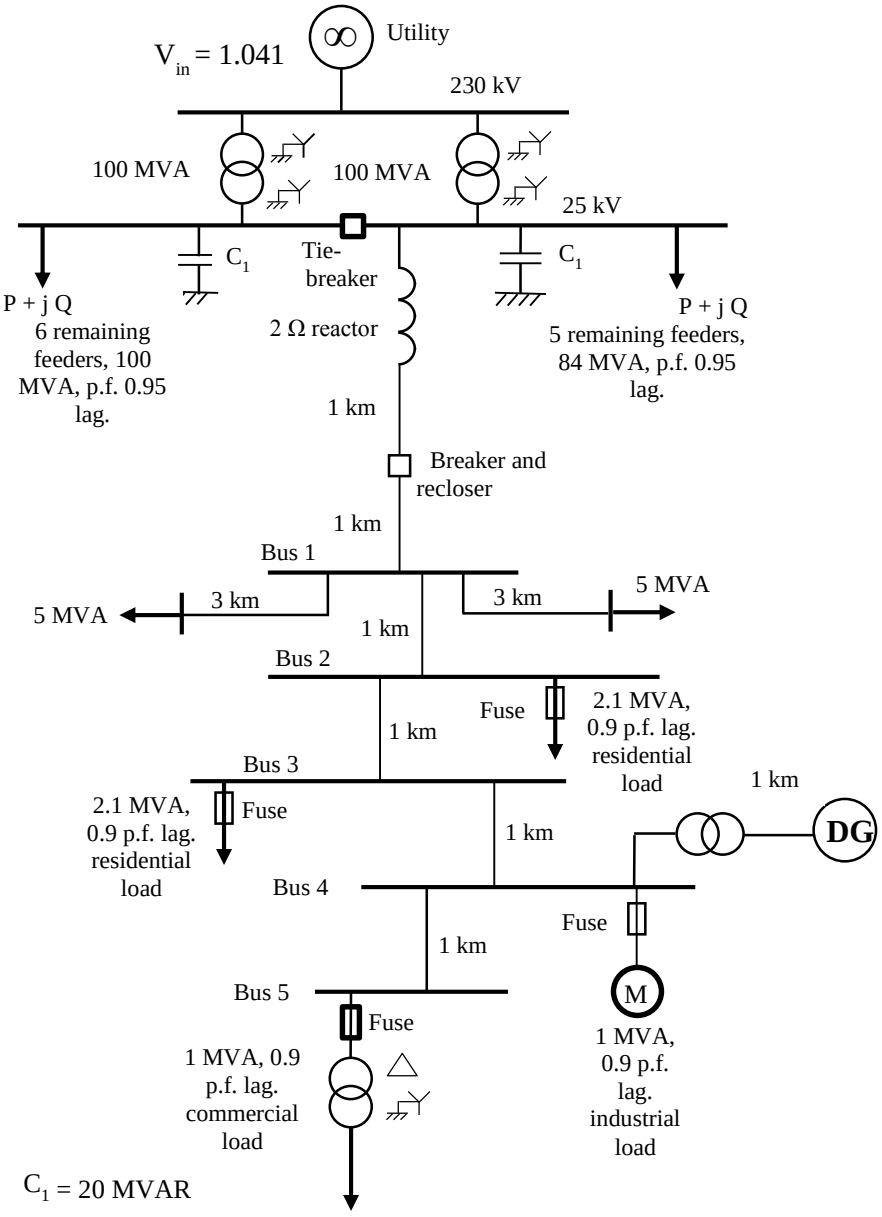

Figure 3.6: Suburban distribution system with DG integration at bus 4.

As observed in APPENDIX B, for a three phase fault at bus 4 of the system depicted in Figure 3.6, the short circuit current experienced by the recloser is 3917 A. As illustrated in Figure 2.8, a recloser current of 3917 yields an operating time (fast) of 0.0292 seconds. The fuse along the bus 4 coordination path in Figure 2.3 will operate at 0.0292 seconds once the short circuit level reaches 4152 A. In order for the fault current to lower to 4152 A, the DG source connected at bus 4 needs to be reduced. Following the steps presented in Figure 3.1, a synchronous machine based DG size of 3.8 MVA is found to cause the recloser fast characteristic to yield the same trip time as the fuse along the bus 4 coordination path. The time response for this condition and level of DG penetration can be depicted graphically via Figure 3.7.

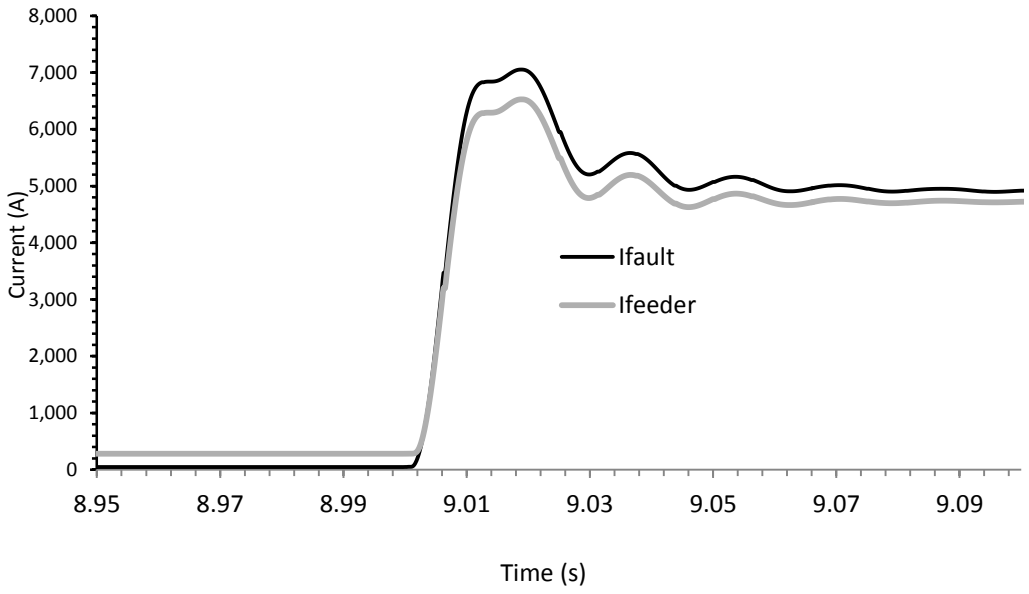

Figure 3.7: Time-domain RMS current simulation for a three phase fault applied at bus 4 with a 3.8 MVA synchronous machine based DG source integrated at bus 4.

Observations of Figure 3.7 in conjunction with Figure 2.8 demonstrate that at a synchronous machine based DG penetration level of 3.8 MVA, the short circuit characteristics of the suburban distribution system will yield simultaneous operation of the bus 4 coordination path recloser and fuse, resulting in coordination loss.

In order to determine if the bus 4 fault presents the lowest synchronous machine based DG penetration level before loss of fuse-recloser coordination, the bus 4 DG connected suburban distributed system in Figure 3.6 is faulted at bus 2 (three phase fault). As per APPENDIX B, a bus 2 fault yields a short circuit current of 4724 A experienced by the recloser. Through the use of Figure 2.10, a recloser current of 4724 A yields an operating time (time) of 0.0274 seconds. The fuse along the bus 2 coordination path in Figure 2.5 will operate at 0.0274 seconds once the short circuit level reaches 5084 A. For a 3.8 MVA synchronous machine based DG at bus 4, the fault current at bus 2 is 4919 A, less than the required 5084 A, meaning that coordination between the fuse and recloser is maintained along the bus 2 coordination path. The time response for this condition and level of DG penetration can be depicted graphically via Figure 3.8.

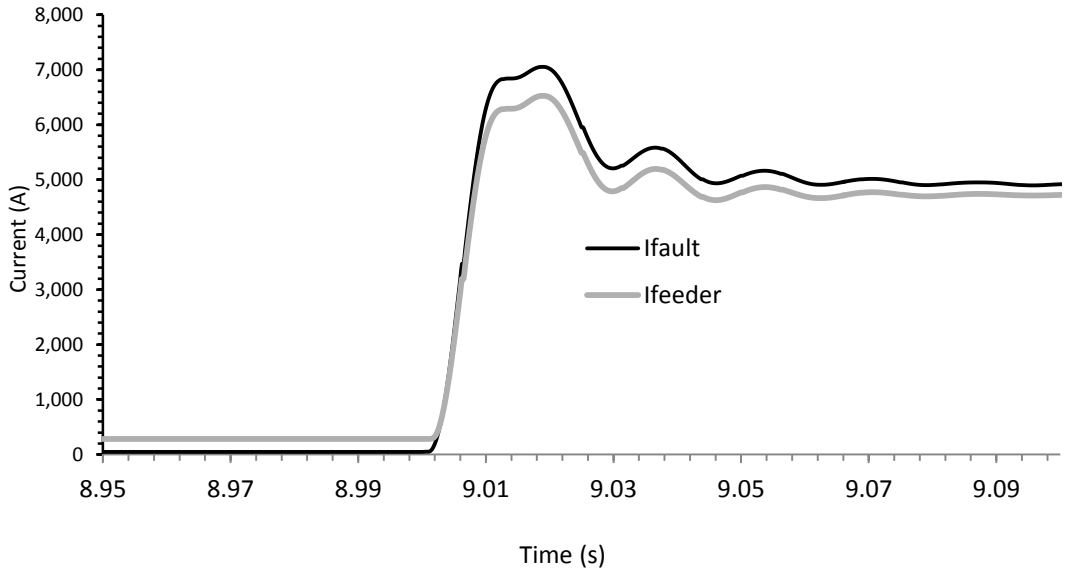

Figure 3.8: Time-domain RMS current simulation for a three phase fault applied at bus 2 with a 3.8 MVA synchronous machine based DG source integrated at bus 4.

Observations of Figure 3.8 in conjunction with Figure 2.10 demonstrate that at a synchronous machine based DG penetration level of 3.8 MVA, the short circuit characteristics of the suburban distribution system along the bus 2 coordination path will yield a trip time of 0.0274 and 0.0282 seconds for the recloser and fuse respectively, hence fuse coordination is maintained.

From this it is apparent that the synchronous machine based DG penetration level of the suburban distribution system depicted in Figure 3.6 is 3.8 MVA, before loss of coordination between the fuse and recloser of at least one coordination path occurs.

3.2.2.4 Bus 5 DG Connection

The bus 5 DG connected (synchronous machine based source) suburban distribution system can be depicted by Figure 3.9.

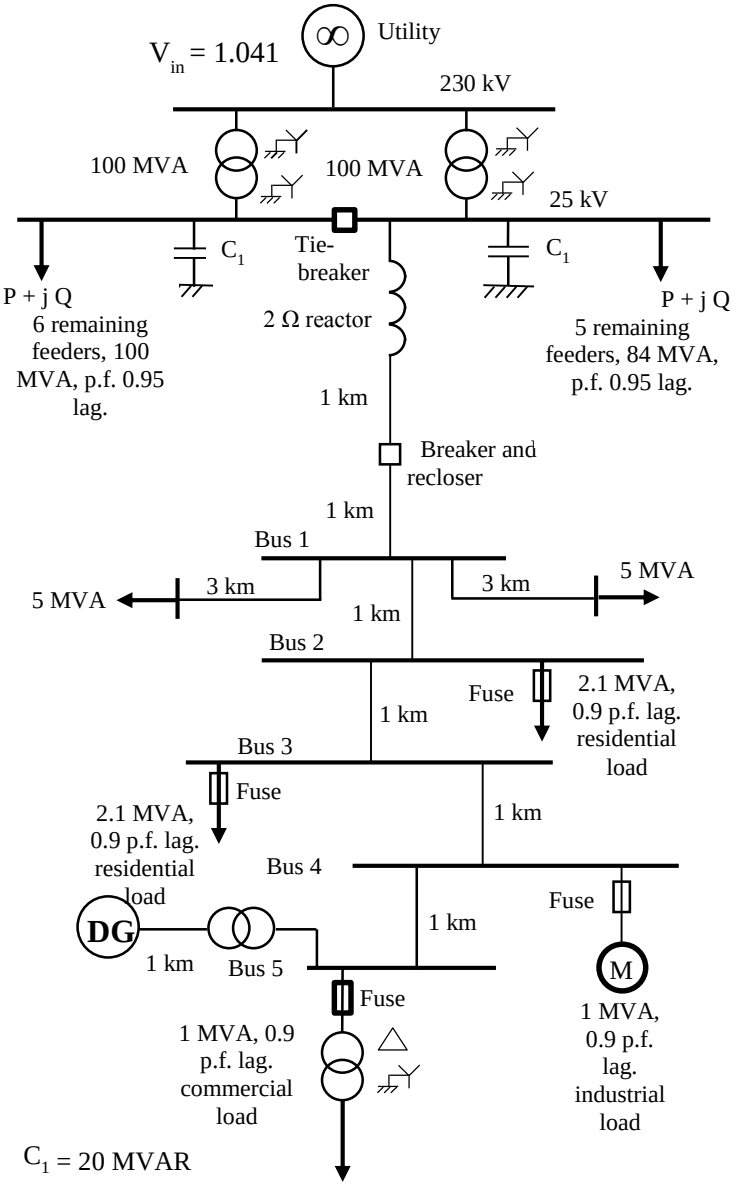

Figure 3.9: Suburban distribution system with DG integration at bus 5.

As observed in APPENDIX B, for a three phase fault at bus 4 of the system depicted in Figure 3.9, the short circuit current experienced by the recloser is 3917 A. Through the use of Figure 2.8, a recloser current of 3917 yields an operating time (fast) of 0.0292 seconds. The fuse along the bus 4 coordination path in Figure 2.3 will operate at 0.0292 seconds once the short circuit level reaches 4152 A (342 A lower than the 8.4 MVA DG). In order for the fault current to lower to 4152 A, the DG source connected at bus 5 needs to be reduced. Following the steps presented in Figure 3.1, A synchronous machine based DG size of 3.8 MVA is found to cause the recloser fast characteristic to yield the same trip time as the fuse along the bus 4 coordination path. The time response for this condition and level of DG penetration can be depicted graphically via Figure 3.10.

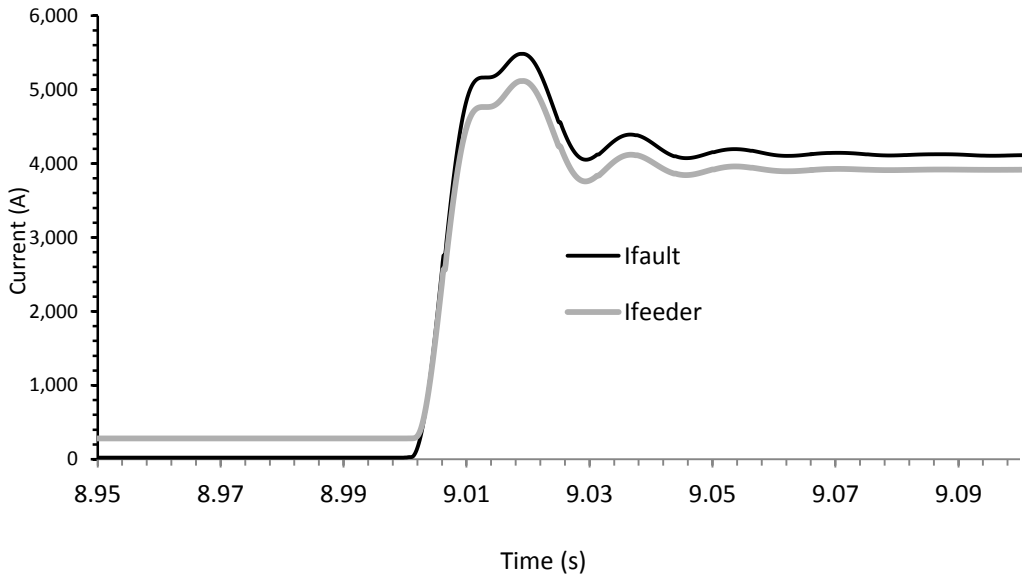

Figure 3.10: Time-domain RMS current simulation for a three phase fault applied at bus 4 with a 3.8 MVA synchronous machine based DG source integrated at bus 5.

Observations of Figure 3.10 in conjunction with Figure 2.8 demonstrate that at a synchronous machine based DG penetration level of 3.8 MVA, the short circuit characteristics of the suburban distribution system will yield simultaneous operation of the bus 4 coordination paths recloser and fuse hence coordination is lost.

In order to determine if the bus 4 fault presents the lowest synchronous machine based DG penetration level before loss of fuse-recloser coordination, the bus 5 DG connected suburban distribution system in Figure 3.9 is faulted at bus 2 (three phase fault). As per APPENDIX B, a bus 2 fault yields a short circuit current of 4724 A experienced by the recloser. Through the use of Figure 2.10, a recloser current of 4724 A yields an operating time (time) of 0.0274 seconds. The fuse along the bus 2 coordination path in Figure 2.5 will operate at 0.0274 seconds once the short circuit level reaches 5084 A. For a 3.8 MVA synchronous machine based DG at bus 5, the fault current at bus 2 is 4909 A, less than the required 5084 A, meaning that coordination between the fuse and recloser is maintained along the bus 2 coordination path. The time response for this condition and level of DG penetration can be depicted graphically via Figure 3.11.

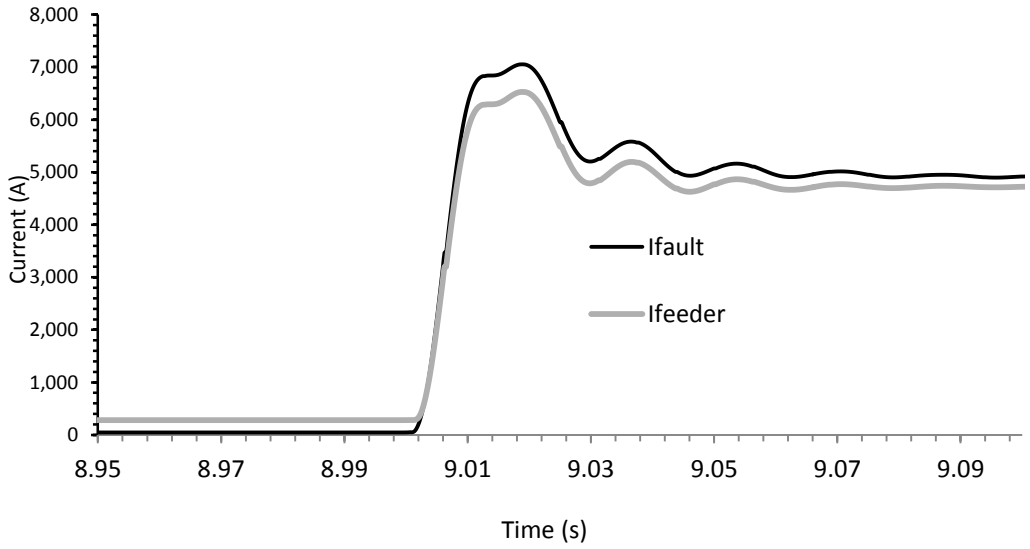

Figure 3.11: Time-domain RMS current simulation for a three phase fault applied at bus 2 with a 3.8 MVA synchronous machine based DG source integrated at bus 5.

Observations of Figure 3.11 in conjunction with Figure 2.10 demonstrate that at a synchronous machine based DG penetration level of 3.8 MVA, the short circuit characteristics of the suburban distribution system along the bus 2 coordination path will yield a trip time of 0.0274 and 0.0286 seconds for the recloser and fuse respectively, hence coordination is maintained.

From this it is apparent that the synchronous machine based DG penetration level the suburban distribution system depicted in Figure 3.9 is 3.8 MVA before loss of coordination between the fuse and recloser of at least one coordination path occurs.

3.2.2.5 DG Connection Summary

The results for Sections 3.2.2.1 to 3.2.2.4 can be summarized as per Figure 3.12.

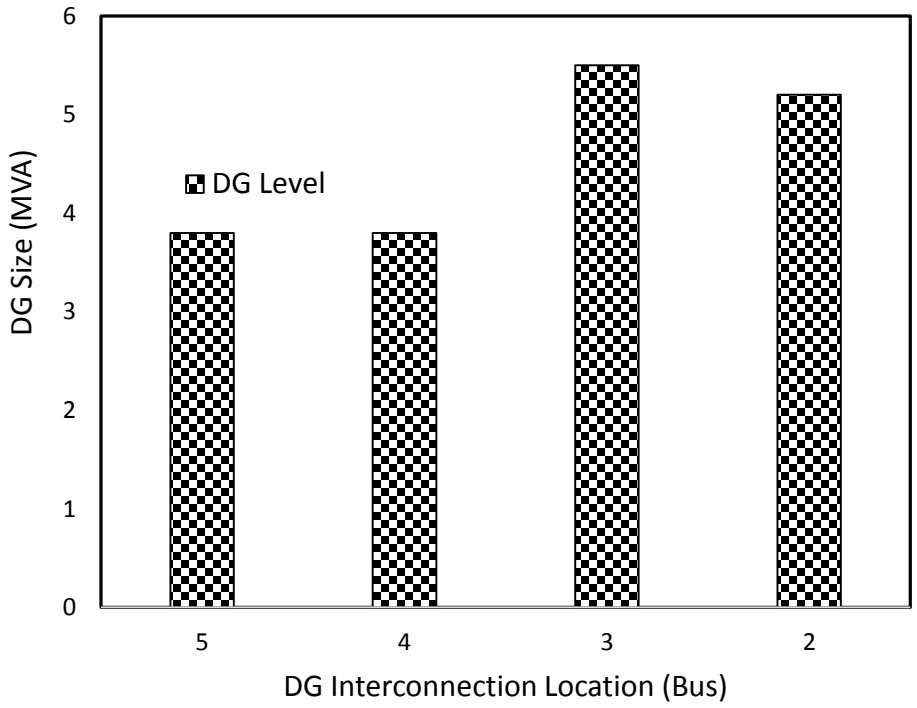

Figure 3.12: Synchronous machine based DG penetration levels for differing interconnection points in the suburban distribution system before loss of fuse-recloser coordination occurs.

Observations of Figure 3.12 in conjunction with Figure 2.1 makes it apparent that loss of fuse-recloser coordination will occur for the suburban distribution system for relatively low levels of synchronous machine based DG (24% of load demand) of interconnection types specified in APPENDIX B. At these levels of penetration, the DG source supplements power delivered by the utility, improving system supply quality. However, the increased short circuit level due to the fault current contribution by the DG source nullifies existing fuse saving protection schemes.

3.3 Loss of Sensitivity Assessment due to Interconnection of DG sources

3.3.1 Loss of Sensitivity Definition and Method of Assessment

Increasing the size of a DG source can lead to downstream protective devices experiencing greater fault levels than those that are upstream [11, 30]. The issue with this in the context of sensitivity is that if the fault current contribution from the DG surpasses that of the contribution from the utility then the main feeder circuit breaker may not be able to detect the fault condition. In order to determine when a loss of sensitivity will occur, the algorithm adapted from the ideas in [2] and presented in Figure 3.13 is useful. This can be explained by:

1. Firstly a synchronous machine based DG source is connected to a previously determined candidate connection point.
2. A load bus is selected with a fault that yields the lowest short circuit current being applied to the selection.
3. The algorithm allows the engineer to determine if loss of recloser sensitivity has occurred, through analysis of the time overcurrent characteristics of the equipment for the given coordination path.
4. If loss of recloser sensitivity has occurred then it is necessary to look at the previous iteration of the algorithm. If this is the first iteration, or the previous iteration caused loss of sensitivity, then the DG size needs to be decreased. Otherwise the DG size must be recorded for future use.
5. If loss of recloser coordination has not occurred then it is necessary to look at the previous iteration of the algorithm. If this is the first iteration or the previous iteration did not cause loss of sensitivity then the DG size needs to be increased. Otherwise the DG size must be recorded for future use.
6. After the DG size has been recorded, the algorithm needs to be repeated for all coordination paths.
7. The algorithm ends with the result being the lowest DG size recorded from the analysis, since this will be the largest DG size for the selected candidate point before the recloser will no longer be sensitive to the smallest phase fault.

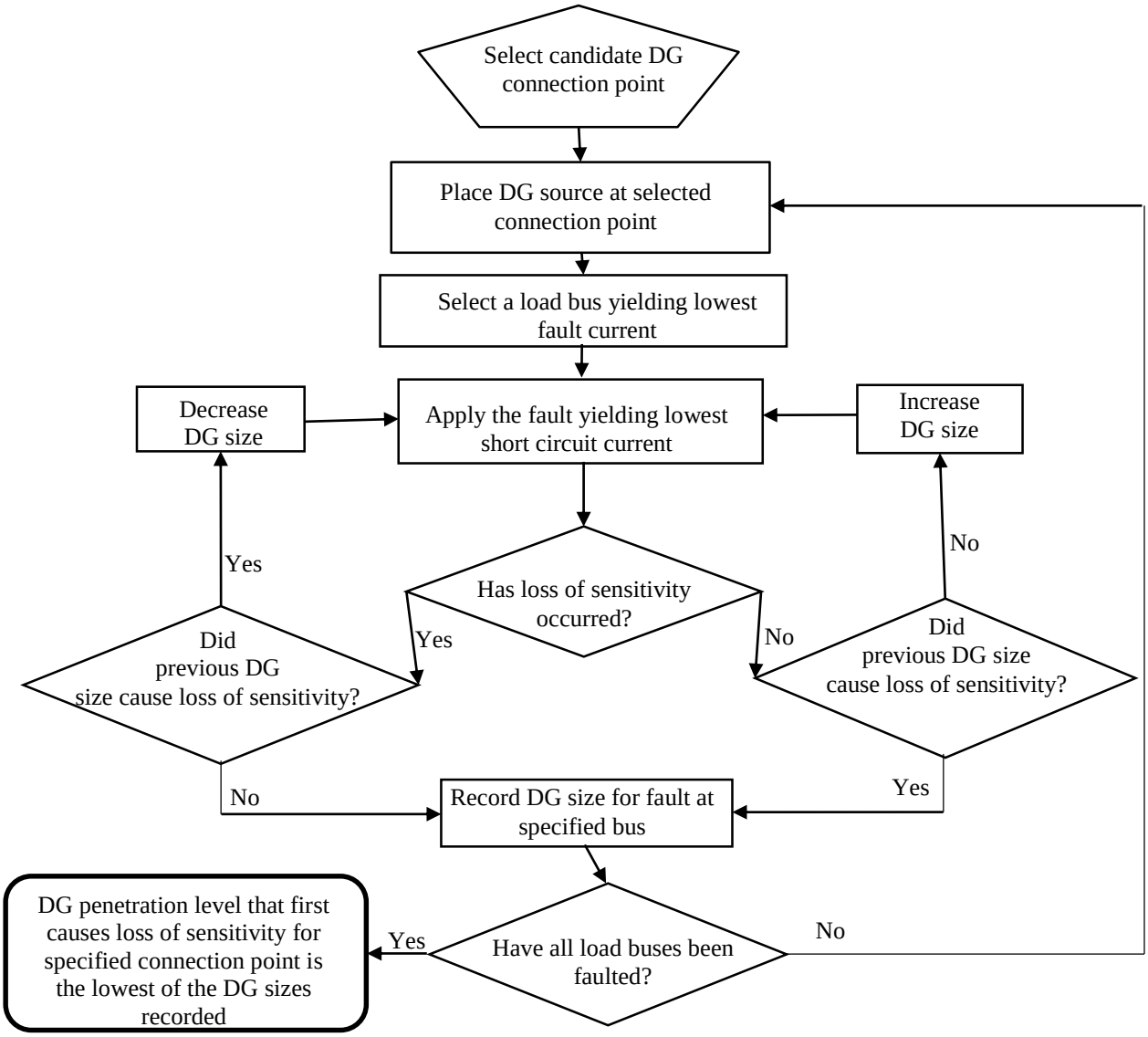

Figure 3.13: Algorithm for the determination of DG penetration level before the occurrence of recloser loss of sensitivity.

3.3.2 Loss of Recloser Sensitivity Case Study

For faults between the utility and the DG source, the utility contribution becomes independent of DG size. If the DG is connected in between the substation and a fault, the utilities contribution to the short circuit current is decreased based on DG interconnection and source type. The most extreme effect of the DG source connection is that it can have the capacity to decrease the main feeder short circuit current to a point where the head end recloser/relay is no longer able to sense fault conditions [2].

Observation of results given in APPENDIX B makes it apparent that for the suburban distribution system given in Figure 2.1, the lowest short circuit current experienced by the network is a line to line fault at the bus 5 load corresponding to the coordination path in Figure 2.6. For this coordination path the recloser pick up current is 560 A. Observation of APPENDIX B demonstrates that the penetration level for a synchronous machine based DG source, with a wye ground/wye ground transformer, needs to be increased for each connection point before loss of recloser sensitivity will occur. Interconnection data is given in APPENDIX A.

3.3.2.1 Bus 1 DG Connection

Following the steps presented in Figure 3.13, a synchronous machine based DG size of 55.6 MVA is found to cause the recloser to become insensitive to a line to line faulted condition at the bus 5 load. The time response for this condition and level of DG penetration as well as 8.4 MVA and no DG can be depicted graphically via Figure 3.14.

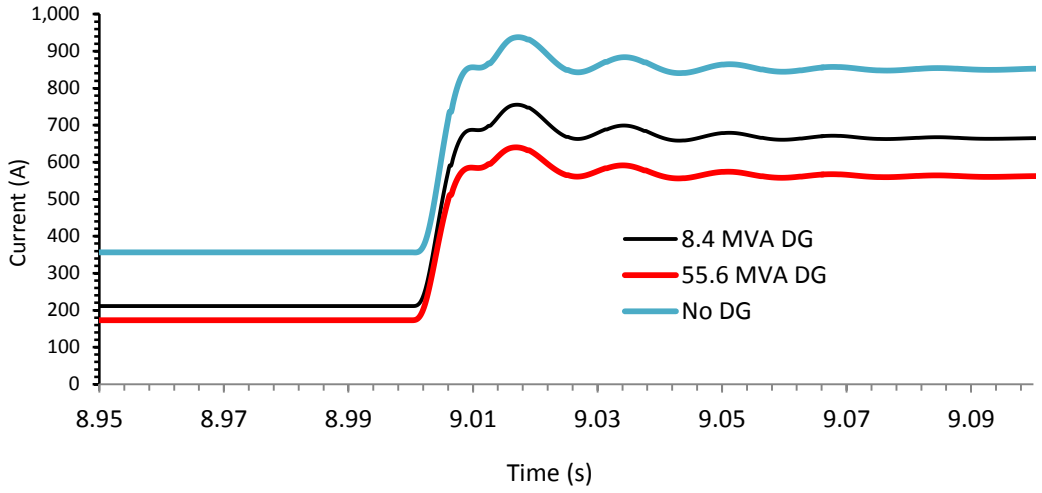

Figure 3.14: Time-domain recloser RMS current simulation for a line to line fault applied at the bus 5 load with synchronous machine based DG sources integrated at bus 1.

Through observation of Figure 3.14 in conjunction with the recloser pick up setting of 560 A, it is apparent that for a synchronous machine based DG penetration level of 55.6 MVA, the head end recloser is no longer able to detect every fault condition.

3.3.2.2 Bus 2 DG Connection

In order to assess the level of synchronous machine based DG penetration at bus 2 that the suburban distribution system is able to receive before loss of recloser sensitivity occurs, the algorithm present in Figure 3.13 is utilized.

Following the steps presented in Figure 3.13, a synchronous machine based DG size of 55.5 MVA is found to cause the recloser to become insensitive to a line to line faulted condition at the bus 5 load. The time response for this condition and level of DG penetration as well as 8.4 MVA and no DG can be depicted graphically via Figure 3.15.

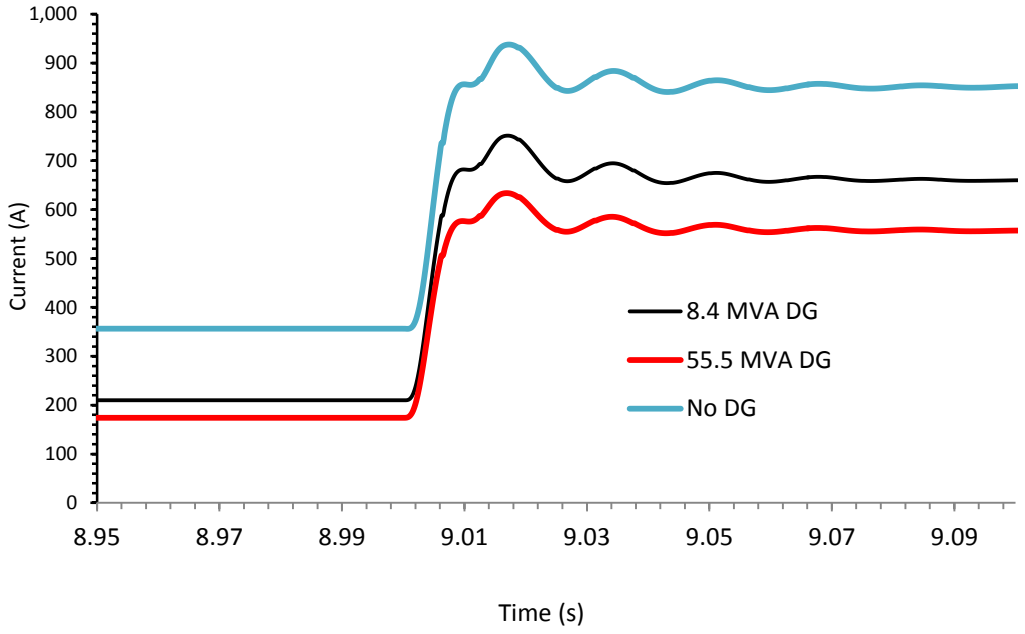

Figure 3.15: Time-domain recloser RMS current simulation for a line to line fault applied at the bus 5 load with synchronous machine based DG sources integrated at bus 2.

Through observation of Figure 3.15 in conjunction with the recloser pick up setting of 560 A, it is apparent that for a synchronous machine based DG penetration level 55.5 MVA, the head end recloser is no longer able to detect every fault condition.

3.3.2.3 Bus 4 DG Connection

In order to assess the level of synchronous machine based DG penetration at bus 4 that the suburban distribution system is able to receive before loss of recloser sensitivity occurs, the algorithm present in Figure 3.13 is utilized.

Following the steps presented in Figure 3.13, a synchronous machine based DG size of 50.5 MVA is found to cause the recloser to become insensitive to a line to line faulted condition at the bus 5 load. The time response for this condition and level of DG penetration as well as 8.4 MVA and no DG can be depicted graphically via Figure 3.16.

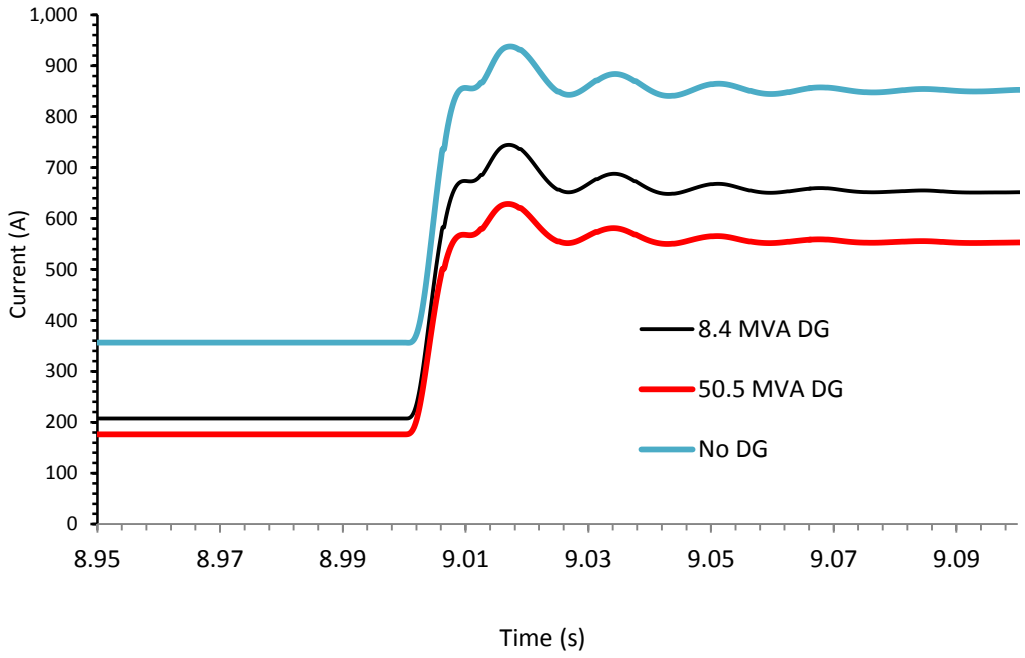

Figure 3.16: Time-domain recloser RMS current simulation for a line to line fault applied at the bus 5 load with synchronous machine based DG sources integrated at bus 4.

Through observation of Figure 3.16 in conjunction with the recloser pick up setting of 560 A, it is apparent that for a synchronous machine based DG penetration level 50.5 MVA, the head end recloser is no longer able to detect every fault condition.

3.3.2.4 Bus 5 DG Connection

In order to assess the level of synchronous machine based DG penetration at bus 5 that the suburban distribution system is able to receive before loss of recloser sensitivity occurs, the algorithm present in Figure 3.13 is utilized.

Following the steps presented in Figure 3.13, a synchronous machine based DG size of 48.8 MVA is found to cause the recloser to become insensitive to a line to line faulted condition at the bus 5 load. The time response for this condition and varying level of DG penetration can be depicted graphically via Figure 3.17.

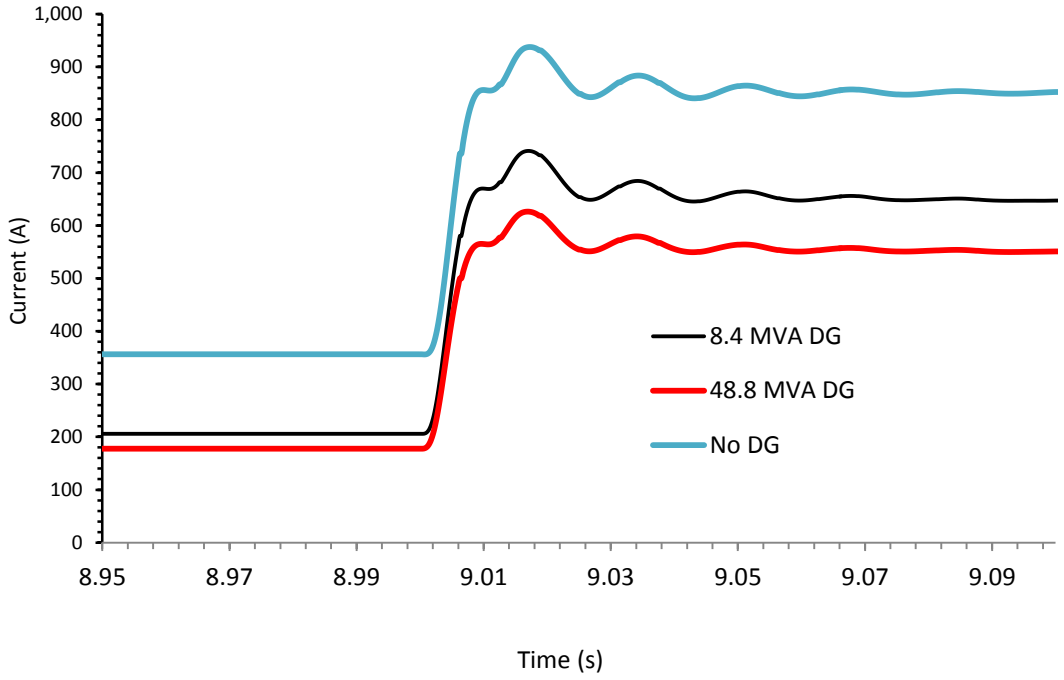

Figure 3.17: Time-domain recloser RMS current simulation for a line to line fault applied at the bus 5 load with synchronous machine based DG sources integrated at bus 5.

Through observation of Figure 3.17 in conjunction with the recloser pick up setting of 560 A, it is apparent that for a synchronous machine based DG penetration level of 48.8 MVA, the head end recloser is no longer able to detect every fault condition.

3.3.2.5 DG Connection Summary

The results for Sections 3.3.2.1 to 3.3.2.4 can be summarized as per Figure 3.12.

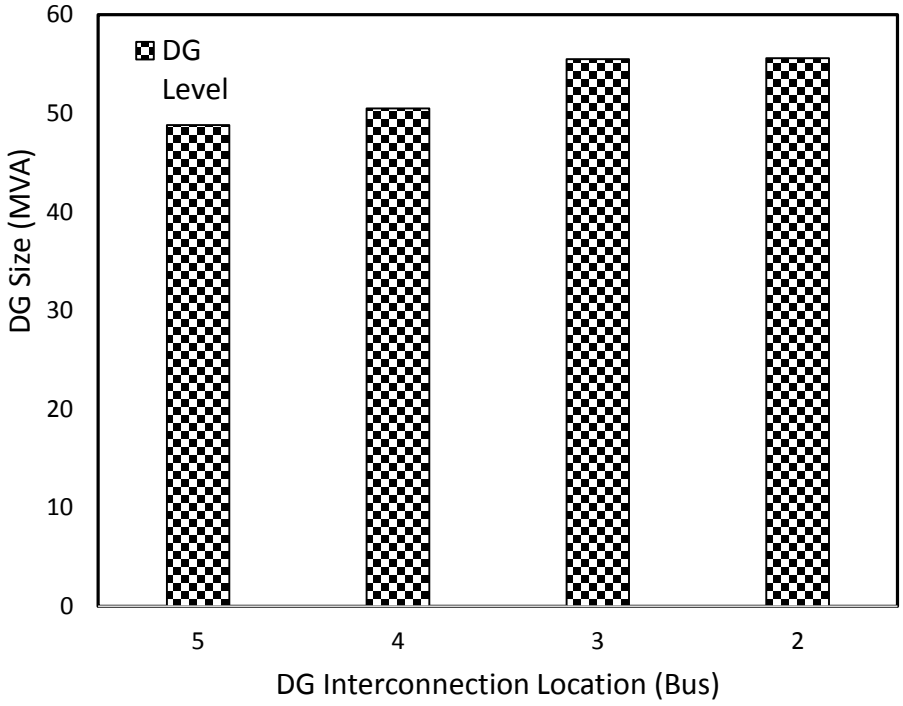

Figure 3.18: Synchronous machine based DG penetration levels for differing interconnection points in the suburban distribution system before loss of recloser sensitivity occurs.

Observation of Figure 3.12 in conjunction with Figure 2.1 makes it apparent that loss of recloser sensitivity will occur for the suburban distribution system for high levels of synchronous machine based DG (at least 300% of the load demand) of interconnection types specified in APPENDIX A. At these levels of penetration, the DG source supplies power to the utility, removing the unidirectional power flow scheme typical of radial distribution networks (utility to load direction). This loss of sensitivity violates the fuse-saving scheme employed in radial distribution networks due to the failure of the recloser to detect short circuit conditions, leaving the utility susceptible to feeding faulted lines should the fuse protection fail to operate for permanent faults.

Additionally, comparison of varying DG source levels in Figures 3.14, 3.15, 3.16 and 3.17 makes it apparent that increasing levels of synchronous machine based DG penetration yield lower

short circuit currents experienced by the head end recloser for faults downstream of the utility and DG connection point.

3.4 Bi-Directionality Assessment due to Interconnection of DG sources

3.4.1 Bi-Directionality Definition and Method of Assessment

Increasing the size of a DG source can lead to unwanted bi-directionality behavior of the main system, while adjacent feeders experience faulted conditions [2]. This situation can be observed via Figure 3.19.

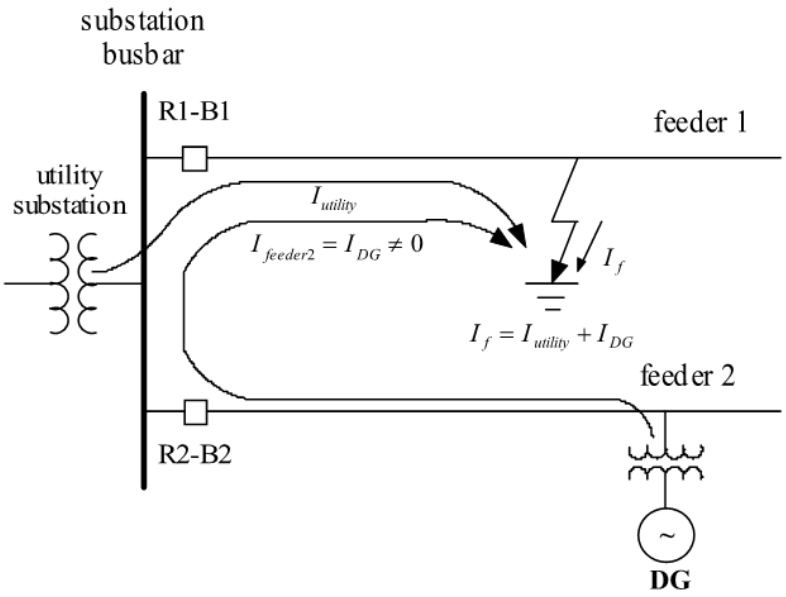

Figure 3.19: Short circuit contribution for a radial distribution network with DG integration [2].

In regular radial distribution networks, when a fault occurs on a feeder, the short circuit current source is purely from the utility connection [11], hence the current level experienced by feeder 2 is zero. This is no longer the case for DG integrated networks as the fault can be fed from multiple sources [2], resulting in additional short circuit current in the fault level.

As per Figure 3.19, if the short circuit current contribution from the DG source at feeder 2 to a fault on feeder 1 (adjacent) is sufficient, there is a possibility that the relay/recloser (B2) protecting feeder 2 will operate faster than that at B1 for a fault on feeder 1. This results in

unnecessary interruption of the healthy feeder (2) which can degrade power quality [2]. In order to determine when bi-directionality will occur, the following algorithm adapted from the ideas in [2] and presented in Figure 3.20 is useful. This can be explained by:

1) Firstly a DG source is connected to a previously determined candidate connection point.
2) An adjacent feeder is created that is of a larger size than the main feeder. Double the load size will be adequate [2]
3) If the steady state current of the system exceeds the rating of the network equipment then the DG needs to decrease in size. The steady state current analysis is repeated until the DG size does not cause currents to exceed equipment ratings.
4) A three phase fault is applied to the adjacent feeder.
5) The algorithm then requires the engineer to determine if bi-directionality has occurred. This can be done through analysis of the time overcurrent characteristics of the protective devices of both the adjacent and main feeder. If the main feeder trips before the adjacent feeder, then bi-directionality has occurred at an unacceptable level.
6) If bi-directionality has occurred, it is necessary to look at the previous iteration of the algorithm. If this is the first iteration or the previous iteration caused bi-directionality then the DG size needs to be decreased. Otherwise the DG size must be recorded and the algorithm terminates.
7) If bi-directionality did not occur following a three phase fault on the adjacent feeder then the previous steady state solution must be observed. If the previous iteration of the algorithm caused the steady state current of the system to exceed rated capacity then the DG size needs to be recorded and the algorithm terminates. If the previous iteration did not cause exceeded capacity and did not cause bi-directionality then the DG size needs to be increased. If the previous iteration did not cause exceeded capacity but did cause bi-directionality then the DG size needs to be recorded and the algorithm terminates. If this was the first iteration then the DG size is required to be increased.

This algorithm is applied to all DG candidate connection points.

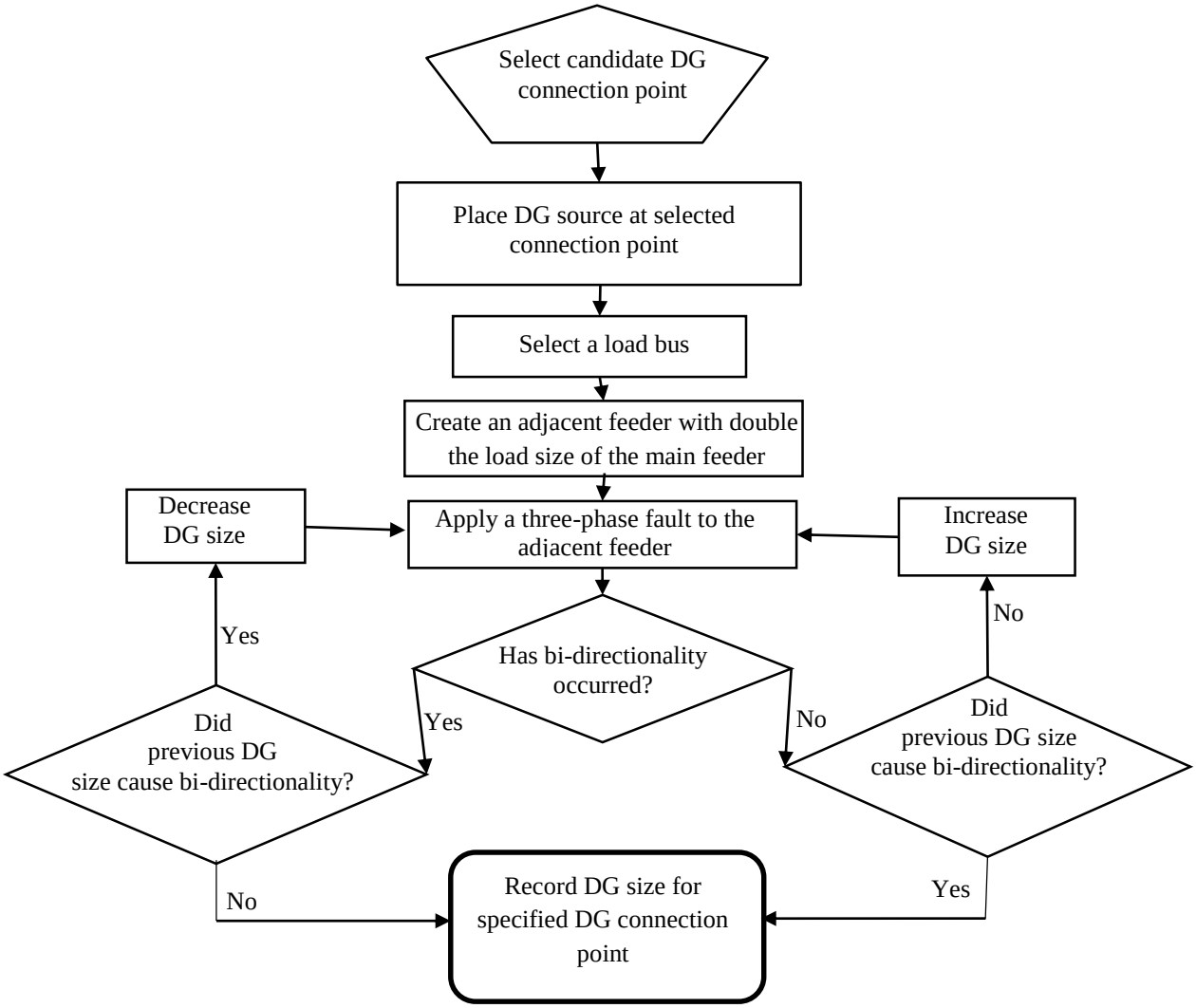

Figure 3.20: Algorithm for the determination of DG penetration level before the occurrence of recloser bi-directionality.

3.4.2 Bi-Directionality Case Study

For all coordination paths in the suburban distribution network, the recloser pick up current is 560 A and 280 A for the phase and ground respectively. In accordance with Figure 3.20, to perform a recloser bi-directionality assessment of the suburban distribution network a PQ load of 32.4 MVA is placed parallel to the main feeder. The head end recloser of the adjacent feeder is

assumed to be a Schweitzer 351R G&W VIPER, Phase trip: 1120 A, Fast curve: 101, Slow curve: 132, Ground Trip: 560 A, Fast curve: 101, Slow curve: 138. The TCC curves of both the phase and ground are shown in Figures 3.21 and 3.22 superimposed over the recloser TCC curves for the main feeder [11, 18].

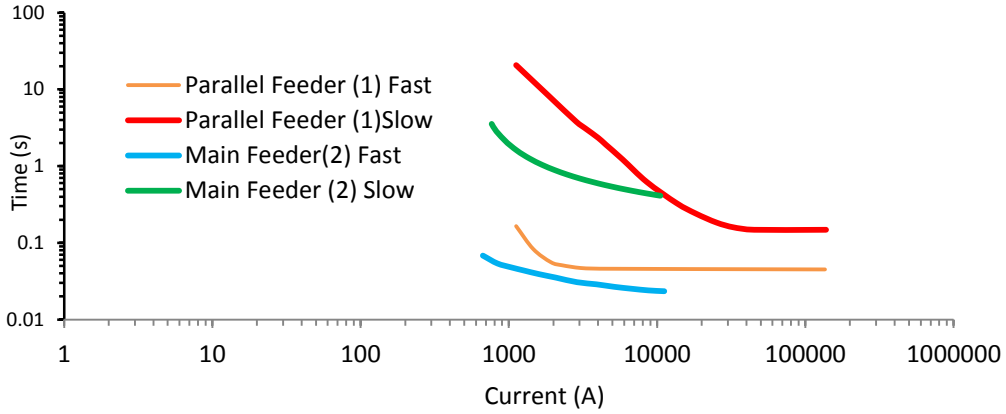

Figure 3.21: Phase Time-Current Characteristics of the main and parallel feeder head end recloser.

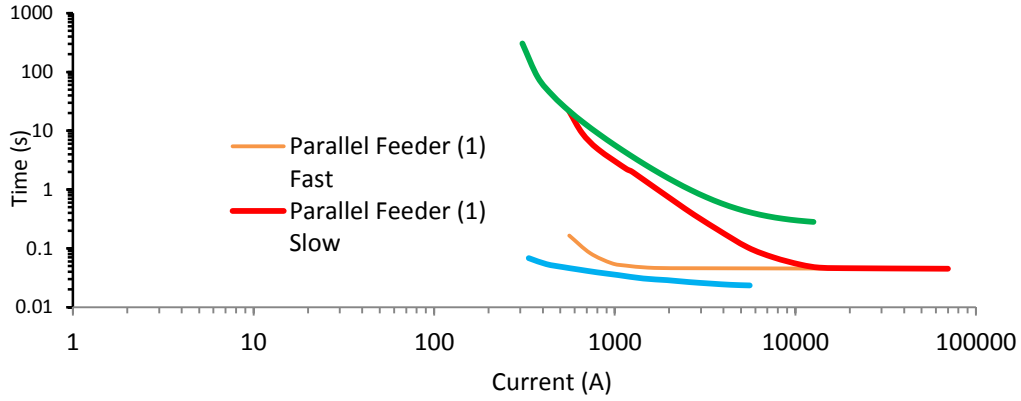

Figure 3.22: Ground Time-Current Characteristics of the main and parallel feeder head end recloser.

Observation of Figures 3.21 and 3.22 makes it apparent that the recloser of the main feeder will operate simultaneously with the recloser on the parallel when the short circuit current exceeds 1151 A and 624 A for the phase and ground respectively. The most severe fault in the suburban distribution system is three phase and double line to ground for the phase and ground respectively.

3.4.2.1 Bus 1 DG Connection

In order to assess the level of synchronous machine based DG penetration at bus 1 that the suburban distribution system is able to receive before recloser bi-directionality occurs for a fault on a parallel feeder, the algorithm present in Figure 3.20 is utilized.

Following the steps presented in Figure 3.20, a synchronous machine based DG size of 4.7 MVA is found to cause the recloser to operate for a parallel feeder double line to ground fault before primary protection is able to react. The time response for the main feeder head end recloser following a double line to ground fault on the adjacent feeder with a 4.7 MVA and 8.4 MVA level of DG penetration can be depicted graphically via Figure 3.23.

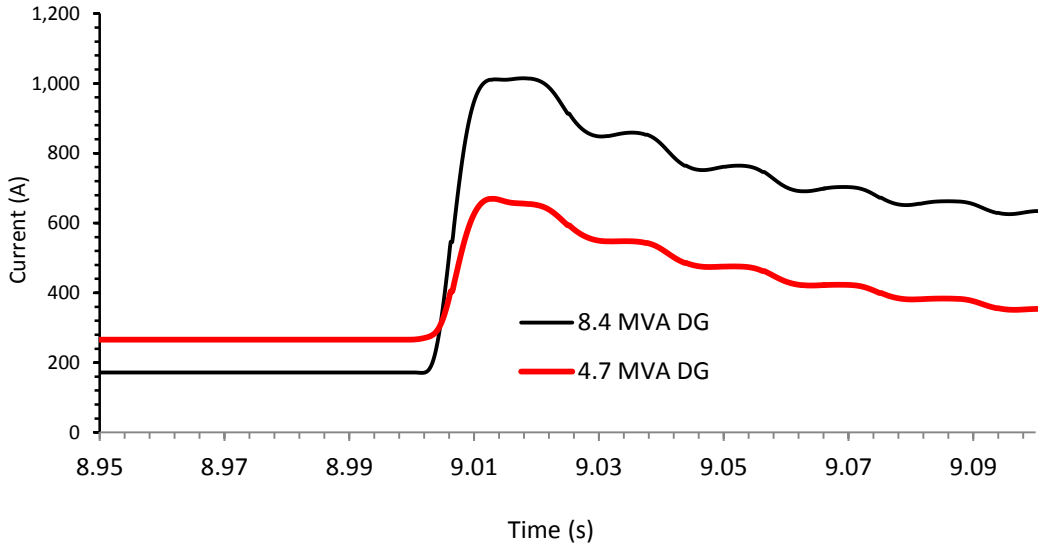

Figure 3.23: Time-domain primary feeder recloser RMS current simulation for a line to line to ground fault applied at the parallel feeder with main feeder synchronous machine based DG source integration at bus 1.

In order to determine if the double line to ground fault presents the lowest synchronous machine based DG penetration level before the occurrence of bi-directional operation, a three phase fault is applied to the parallel feeder. The time response for the main feeder head end recloser following a three phase fault on the adjacent feeder with a 4.7 MVA and 8.4 MVA level of DG penetration can be depicted graphically via Figure 3.24.

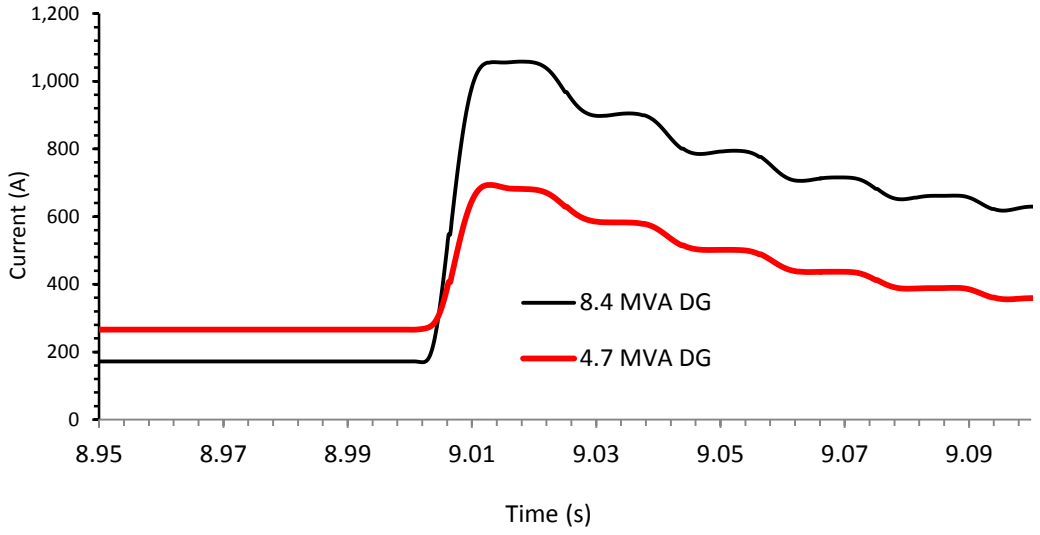

Figure 3.24: Time-domain primary feeder recloser RMS current simulation for a three phase fault applied at the parallel feeder with main feeder synchronous machine based DG source integration at bus 1.

Through observation of Figures 3.23 and 3.24 in conjunction with the recloser pick up settings, it is apparent that for a synchronous machine based DG penetration level of 4.7 MVA, the head end recloser of the main feeder will operate before the parallel feeder protection for a double line to ground fault but not for a three phase. For a DG penetration level of 8.4 MVA the main feeder recloser current exceeds the 1151 A and 624 A for three phase and double line to ground faults respectively, yielding main feeder recloser operation before the parallel feeder. From this it is apparent that the ground fault characteristic is what will cause bi-directionality behavior before the phase. Note that the parallel feeder fault current exceeds 30 kA.

3.4.2.2 Bus 2 DG Connection

In order to assess the level of synchronous machine based DG penetration at bus 2 that the suburban distribution system is able to receive before recloser bi-directionality occurs for a fault on a parallel feeder, the algorithm present in Figure 3.20 is utilized.

Following the steps presented in Figure 3.20, a synchronous machine based DG size of 5 MVA is found to cause the recloser to operate for a parallel feeder double line to ground fault

before primary protection is able to react. The time response for the main feeder head end recloser following a double line to ground fault on the adjacent feeder with a 5 MVA and 8.4 MVA level of DG penetration can be depicted graphically via Figure 3.25.

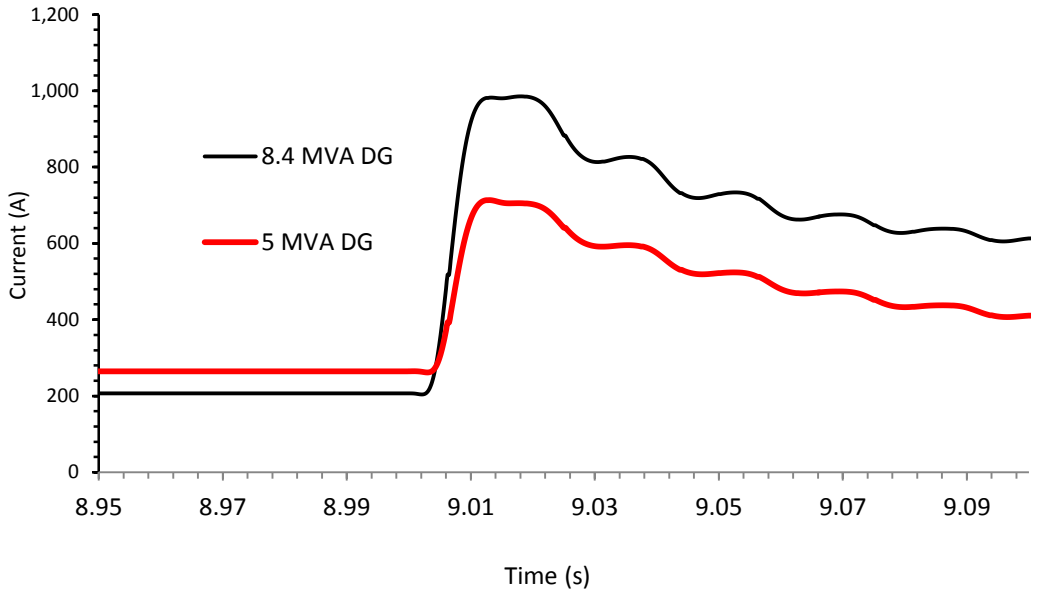

Figure 3.25: Time-domain primary feeder recloser RMS current simulation for a line to line to ground fault applied at the parallel feeder with main feeder synchronous machine based DG source integration at bus 2.

Through observation of Figure 3.25 in conjunction with the recloser ground settings, it is apparent that for a synchronous machine based DG penetration level of 5 MVA, the head end recloser of the main feeder will operate before the parallel feeder protection for a double line to ground fault. Note that the parallel feeder fault current exceeds 30 kA.

3.4.2.3 Bus 4 DG Connection

In order to assess the level of synchronous machine based DG penetration at bus 4 that the suburban distribution system is able to receive before recloser bi-directionality occurs for a fault on a parallel feeder, the algorithm present in Figure 3.20 is utilized.

Following the steps presented in Figure 3.20, a synchronous machine based DG size of 5.5 MVA is found to cause the recloser to operate for a parallel feeder double line to ground fault before primary protection is able to react. The time response for the main feeder head end recloser following a double line to ground fault on the adjacent feeder with a 5.5 MVA and 8.4 MVA level of DG penetration can be depicted graphically via Figure 3.26.

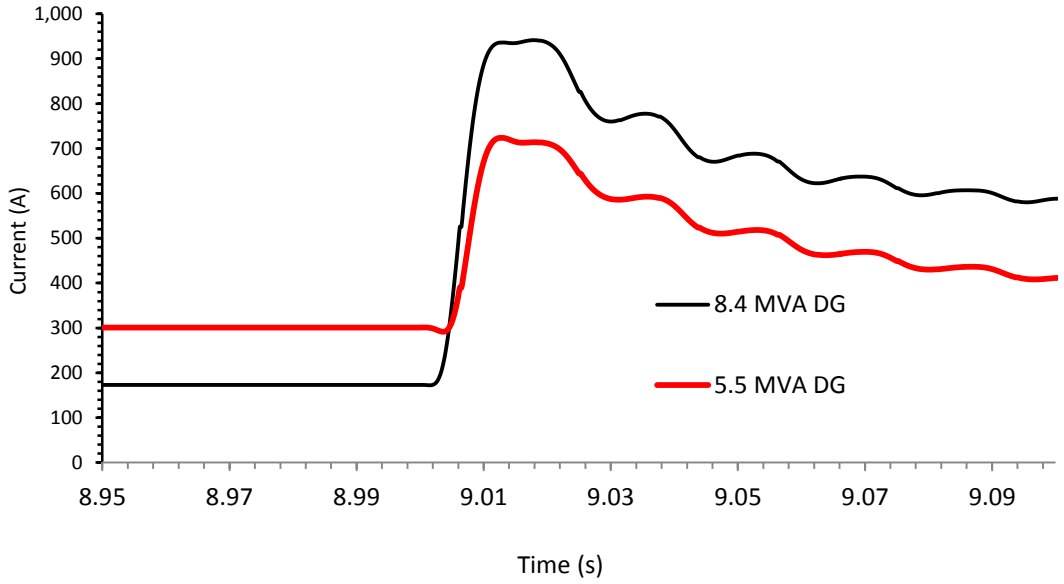

Figure 3.26: Time-domain primary feeder recloser RMS current simulation for a line to line to ground fault applied at the parallel feeder with main feeder synchronous machine based DG source integration at bus 4.

Through observation of Figure 3.26 in conjunction with the recloser ground settings, it is apparent that for a synchronous machine based DG penetration level of 5.5 MVA, the head end recloser of the main feeder will operate before the parallel feeder protection for a double line to ground fault. Note that the parallel feeder fault current exceeds 30 kA.

3.4.2.4 Bus 5 DG Connection

In order to assess the level of synchronous machine based DG penetration at bus 5 that the suburban distribution system is able to receive before recloser bi-directionality occurs for a fault on a parallel feeder, the algorithm present in Figure 3.20 is utilized.

Following the steps presented in Figure 3.20, a synchronous machine based DG size of 5.8 MVA is found to cause the recloser to operate for a parallel feeder double line to ground fault before primary protection is able to react. The time response for the main feeder head end recloser following a double line to ground fault on the adjacent feeder with a 5.8 MVA and 8.4 MVA level of DG penetration can be depicted graphically via Figure 3.27.

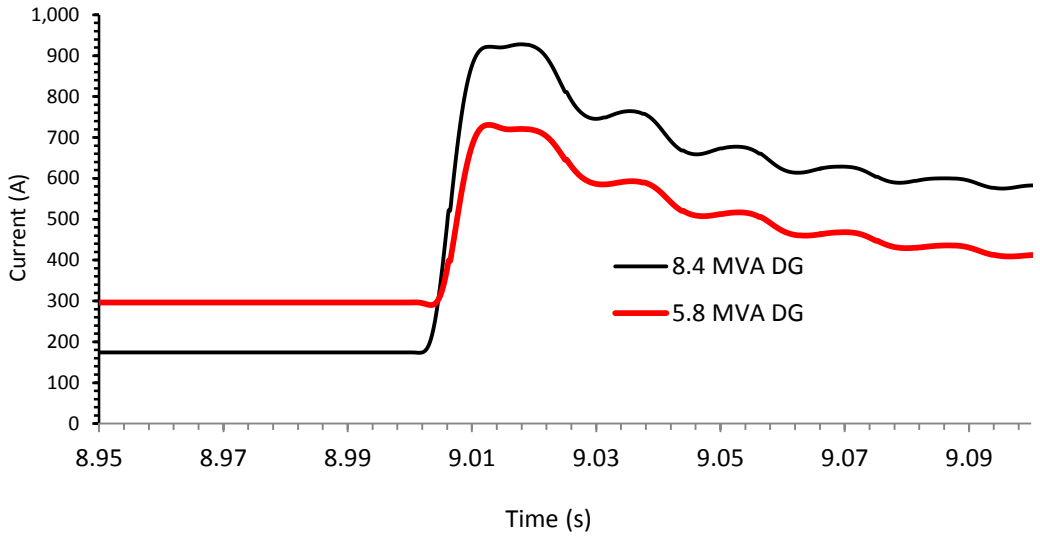

Figure 3.27: Time-domain primary feeder recloser RMS current simulation for a line to line to ground fault applied at the parallel feeder with main feeder synchronous machine based DG source integration at bus 5.

Through observation of Figure 3.27 in conjunction with the recloser ground settings, it is apparent that for a synchronous machine based DG penetration level of 5.8 MVA, the head end recloser of the main feeder will operate before the parallel feeder protection for a double line to ground fault. Note that the parallel feeder fault current exceeds 30 kA.

3.4.2.5 DG Connection Summary

The results for Sections 3.4.2.1 to 3.4.2.4 can be summarized as per Figure 3.28.

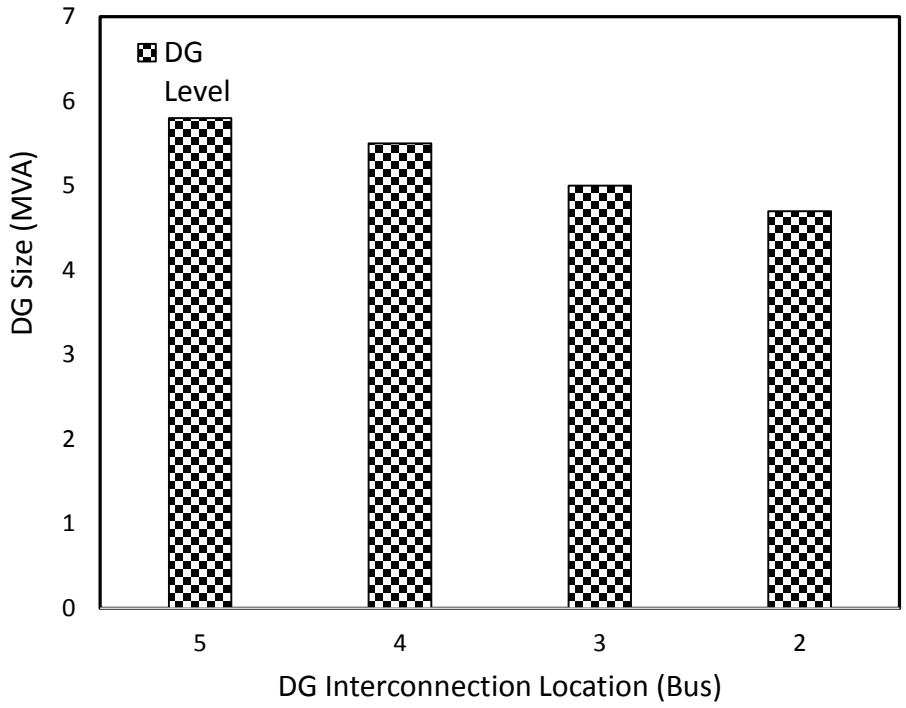

Figure 3.28: Synchronous machine based DG penetration levels for differing interconnection points in the suburban distribution system before bi-directionality occurs for an adjacent feeder.

Observation of Figure 3.28 in conjunction with Figure 2.1 makes it apparent that bi-directionality of recloser operation can occur for the suburban distribution system for low penetration levels of synchronous machine based DG (as low as 29% of the load demand) of interconnection types specified in APPENDIX A. At these levels of penetration, the DG source is able to supply short circuit current to a fault in an adjacent feeder in addition to the utility. Consequently, the DG source causes bi-directional power flow, meaning the main feeder recloser in Figure 2.1 is able to detect the fault condition of the adjacent feeder. This bi-directional behavior of the main head end recloser causes unnecessary interruption of the supply to the healthy feeder compromising system power quality and reliability of supply.

Additionally, comparison of varying DG source levels in Figures 3.24, 3.25, 3.26 and 3.27 makes it apparent that increasing levels of synchronous machine based DG penetration yield more severe bi-directional behavior of the head end recloser of the main feeder.

3.5 Summary

Chapter 3 has provided methods for the assessment of loss of fuse-recloser coordination, loss of head end recloser sensitivity and recloser bi-directionality behavior for adjacent feeder faults that have been applied to the suburban distribution network. Detailed digital time-domain simulations and explanations into the effects of synchronous machine based DG integration into the suburban distribution system for varying connection points are presented. Results obtained demonstrate that low levels of synchronous machine based DG penetration can yield loss of fuse-recloser coordination as well as recloser bi-directionality behavior for adjacent feeder faults, while high penetration is required for recloser sensitivity loss.

4. THE UTILIZATION OF FCLS IN THE MITIGATION OF SYNCHRONOUS MACHINE BASED DG INFLUENCES ON FUSE-RECLOSER PROTECTION INFRASTRUCTURE

4.1 Introduction

This chapter examines the use of superconducting fault current limiters as a solution to mitigation of the detrimental effects that synchronous machine based DG integration has on system short circuit currents during faulted conditions. The proposed approach utilizes FCLs at the DG side of the interconnection transformer as per Figure 4.1. This is in conjunction with the algorithms presented in Figures 3.1, 3.13 and 3.20 and the case study in Section 2.4; the purpose to determine FCL (each type presented in Section 2.3.7) effectiveness for mitigation of subsequent effects on fuse-recloser protection infrastructure in the suburban distribution network presented in Chapter 3.

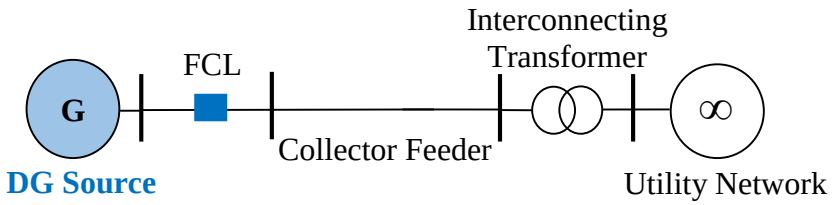

Figure 4.1: A DG interconnecting scheme with the presence of FCLs.

4.2 Fault Current Contribution from Synchronous Machine Based DG Integration in the Presence of FCLs

The case study presented in Section 2.4 demonstrates the effect of synchronous machine based DG integration on short-circuit levels of the suburban distribution network. In order to

determine the effectiveness of each FCL type presented in Section 2.3.7 in the use of mitigation of these increased short circuit currents, the method presented in Section 2.4 is utilized.

As per Figure 4.2, an 8.4 MVA synchronous machine based DG source is integrated into the suburban distribution system at bus 1 with an FCL placed as per Figure 4.1.

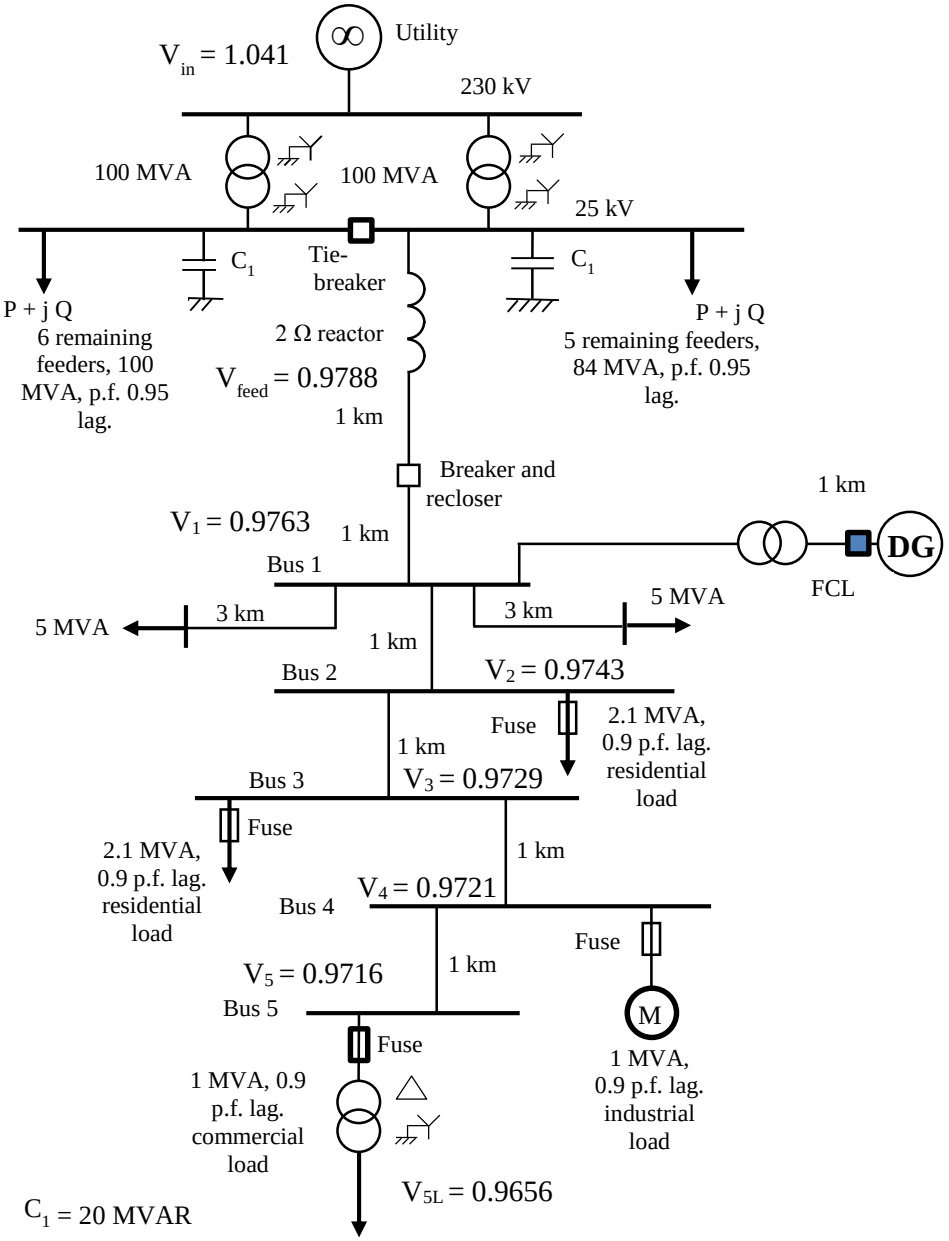

Figure 4.2: Suburban distribution system bus voltages with DG integration at bus 1 with FCL presence.

A three phase fault is applied to the bus 4 load. The time-domain short circuit currents experienced by the bus 4 fuse and head end-recloser for each FCL type is presented in Figures 4.3, 4.4 and 4.5 with a summary presented in Figure 4.6

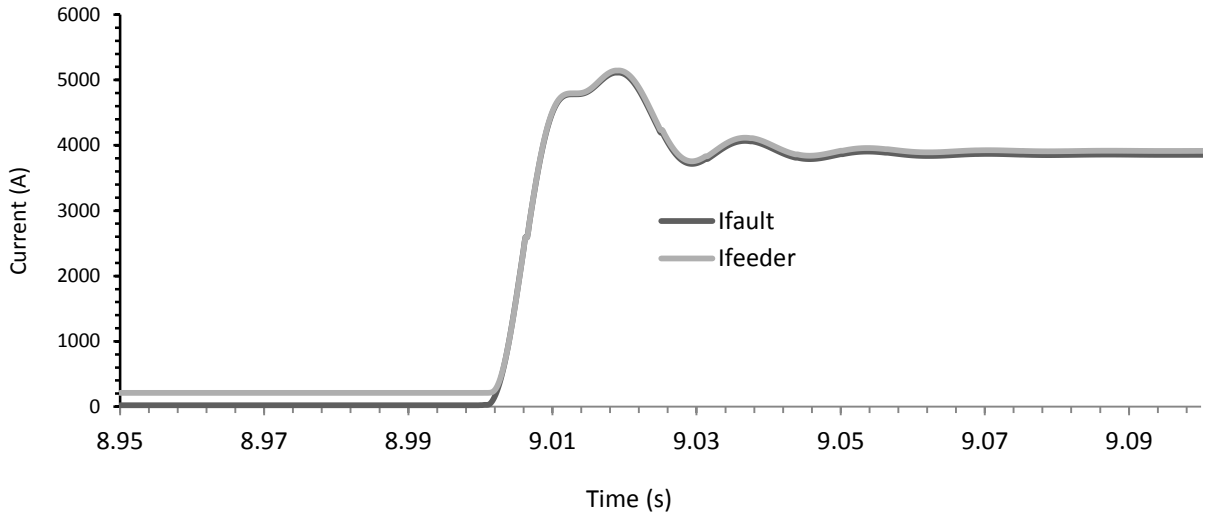

Figure 4.3: Time-domain RMS current simulation for a three phase fault applied at bus 4 with 8.4 MVA DG integration at bus1 in the presence of a 60 Ω R type FCL.

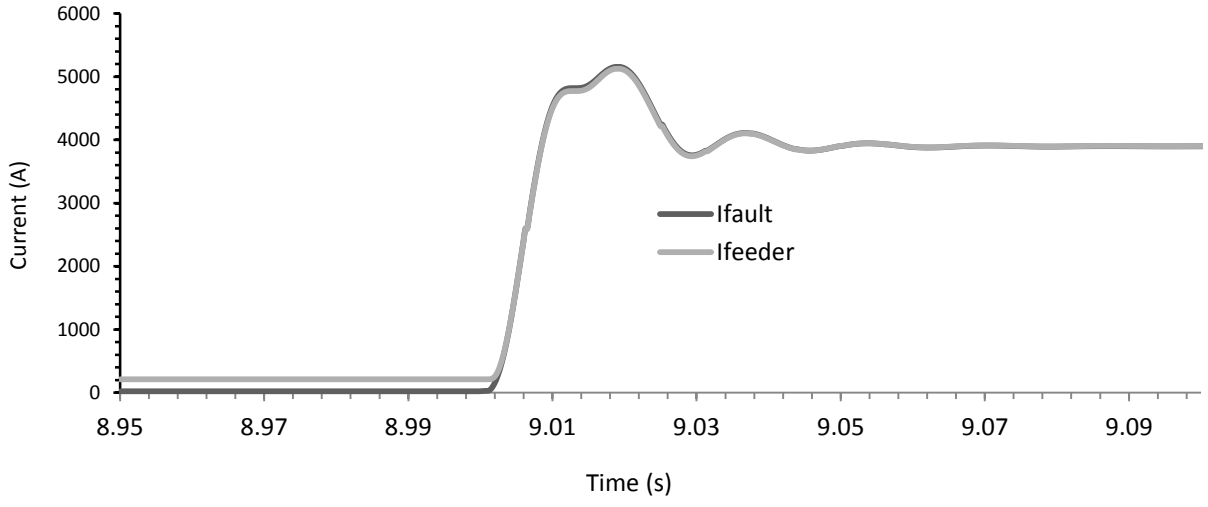

Figure 4.4: Time-domain RMS current simulation for a three phase fault applied at bus 4 with 8.4 MVA DG integration at bus1 in the presence of a 0.16 H L type FCL.

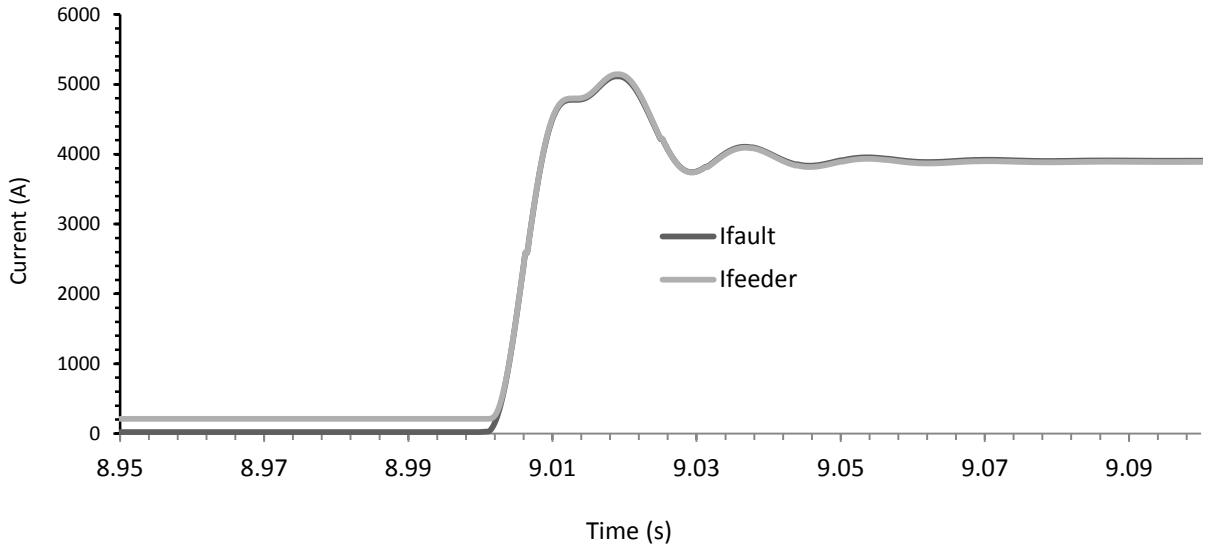

Figure 4.5: Time-domain RMS current simulation for a three phase fault applied at bus 4 with 8.4 MVA DG integration at bus1 in the presence of a resonant type FCL.

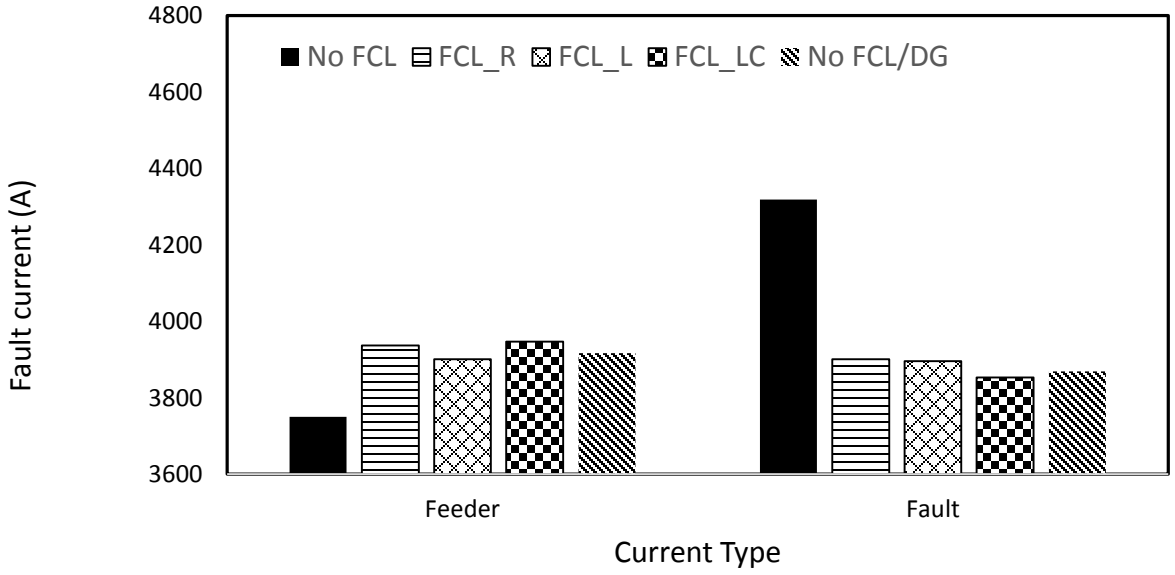

Figure 4.6: Summary of short circuit currents with an 8.4 MVA synchronous machined based DG source integrated at bus 1 in the suburban distribution system with a three phase fault applied at bus 4.

Analysis of Figure 4.6 demonstrates that the introduction of the R, L and resonant type FCL's into the system presented in Figure 4.1 yields 0.8%, 0.7% and 0.1% differences in fault current when compared to that of the original short circuit characteristic presented in Figure 2.19, an improvement from the 12% difference experienced without the presence of FCL's. Observation of Figure 4.6 makes it apparent that the utilization of FCLs on the DG side of the interconnection infrastructure's transformer yields mitigation of synchronous machine based DG source effects on system short circuit current.

In commercial applications there are a wide variety of resistive and inductive type FCLs of varying magnitudes of resistances and inductances. In order to reflect results consistent with varying resistive values, the resistive and inductive type FCLs in the system presented in Figure 4.2 are varied in magnitude. Figures 4.7, 4.8, 4.9 and 4.10 show the time domain simulations and Figures 4.11 and 4.12 shows a summary for each FCL type for a three phase fault at bus 4 for the 8.4 MVA synchronous machine based DG integrated suburban distribution system with the R and L type FCL's values being varied between 20 Ω - 50 Ω and 0.05 H - 0.13 H respectively.

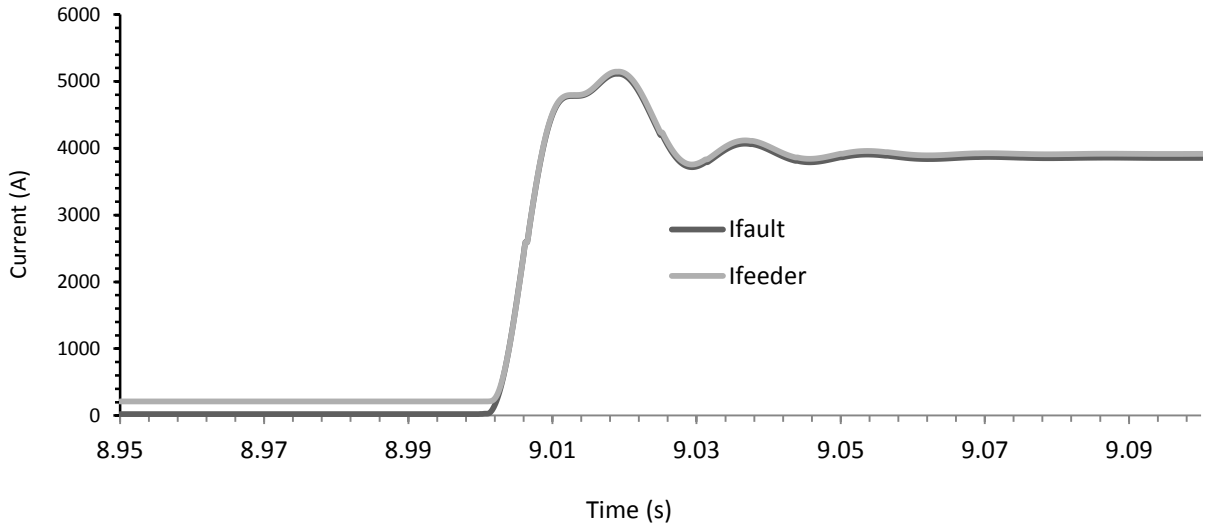

Figure 4.7: Time-domain RMS current simulation for a three phase fault applied at bus 4 with 8.4 MVA DG integration at bus1 in the presence of a 50 Ω R type FCL.

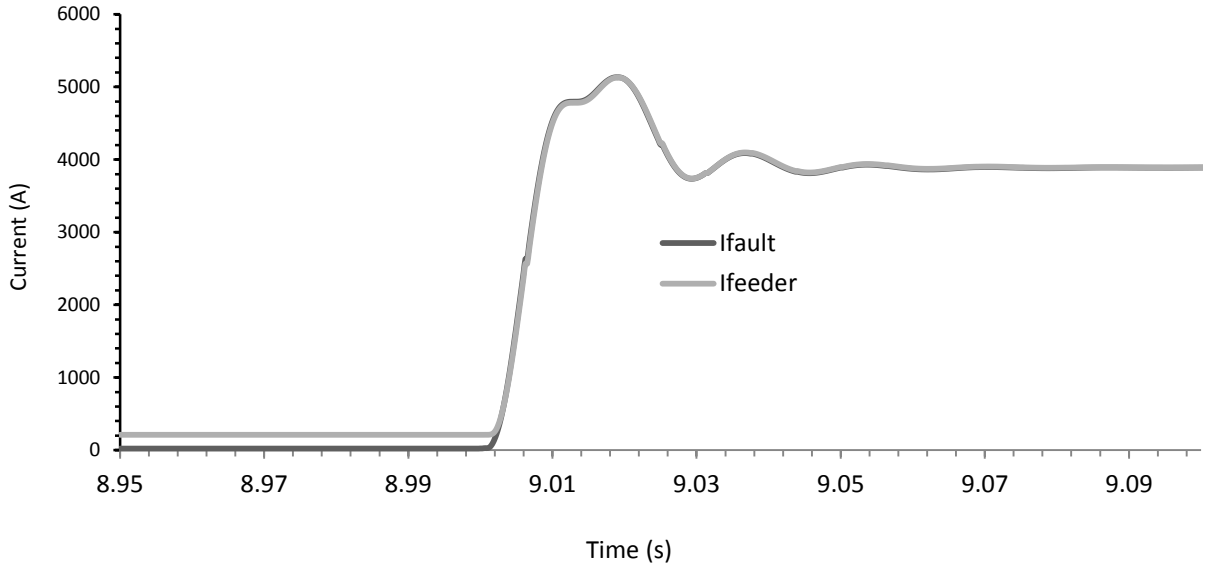

Figure 4.8: Time-domain RMS current simulation for a three phase fault applied at bus 4 with 8.4 MVA DG integration at bus1 in the presence of a 20 Ω R type FCL.

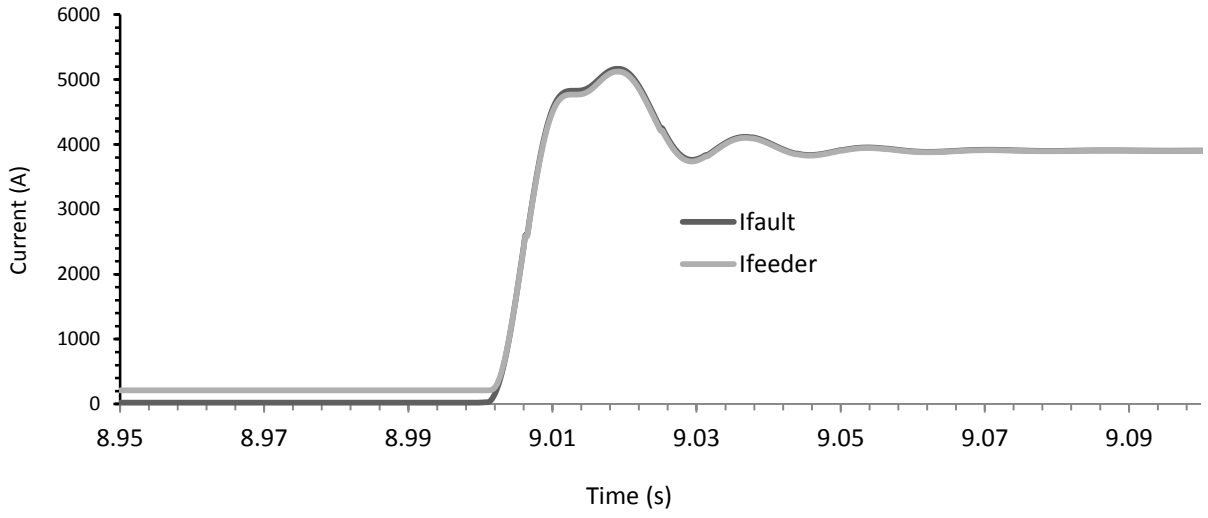

Figure 4.9: Time-domain RMS current simulation for a three phase fault applied at bus 4 with 8.4 MVADG integration at bus1 in the presence of a 0.13 H L type FCL.

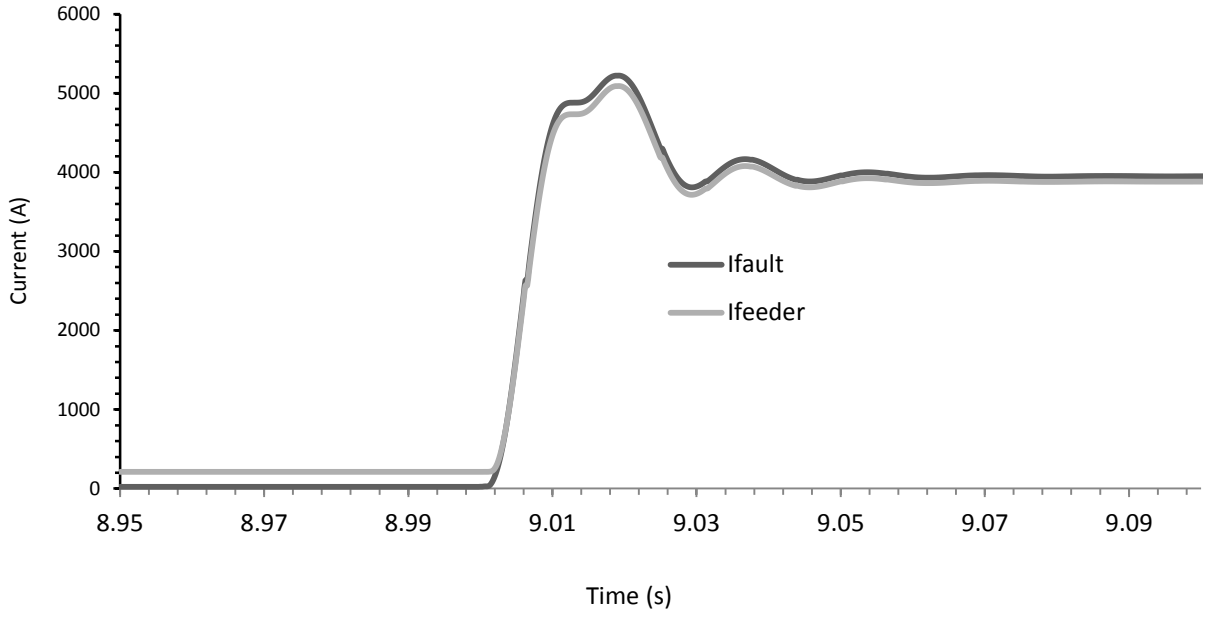

Figure 4.10: Time-domain RMS current simulation for a three phase fault applied at bus 4 with 8.4 MVA DG integration at bus1 in the presence of a 0.05 H L type FCL.

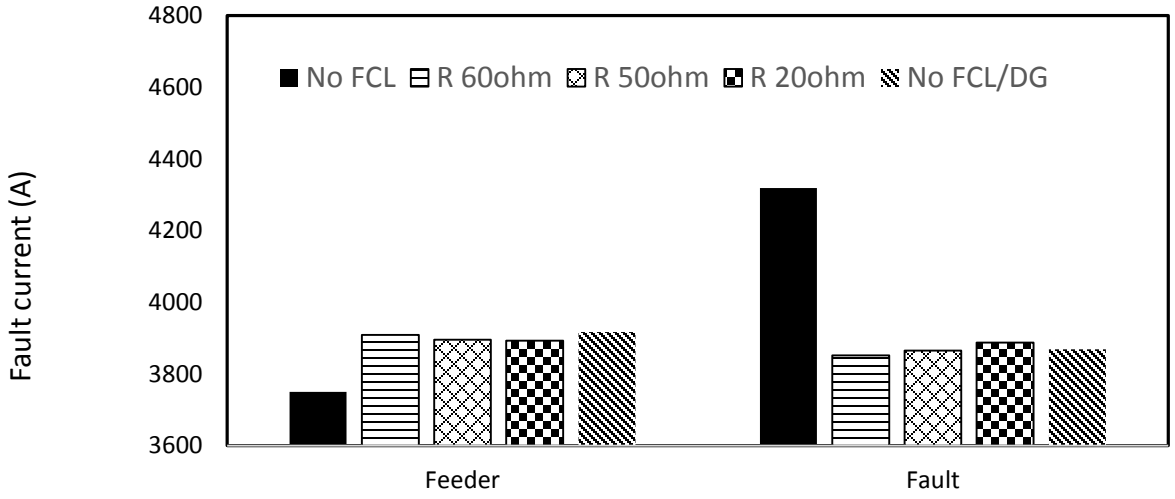

Figure 4.11: Summary of short circuit currents for varying resistive FCL magnitudes with an 8.4 MVA synchronous machine based DG source integrated at bus 1 in the suburban distribution system with a three phase fault applied at bus 4.

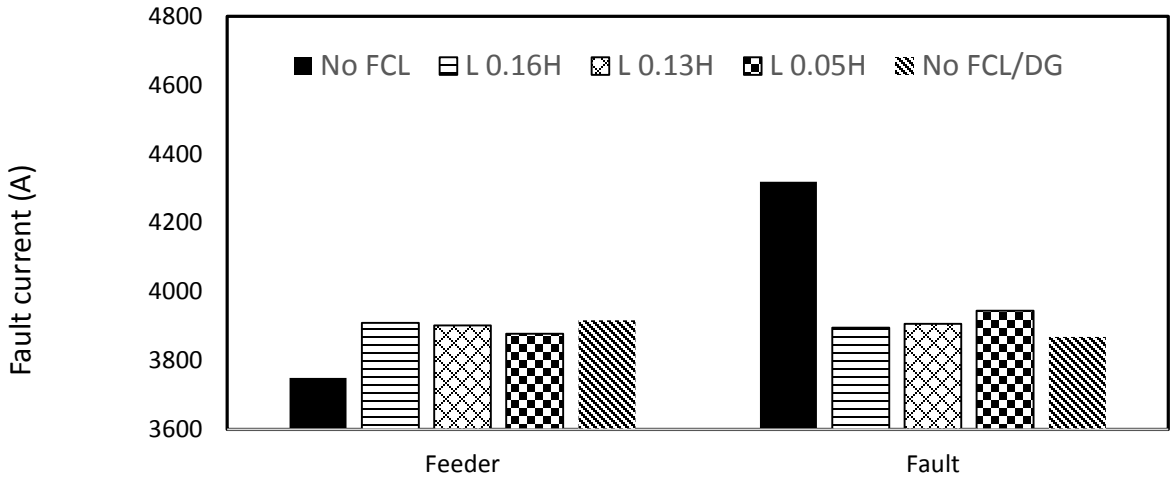

Figure 4.12: Summary of short circuit currents for varying inductive FCL magnitudes with an 8.4 MVA synchronous machine based DG source integrated at bus 1 in the suburban distribution system with a three phase fault applied at bus 4.

Observation of Figures 4.11 and 4.12 makes it apparent that increasing the impedance of a superconducting FCL yields a higher efficiency mitigation capability of synchronous machine based DG integration influences on radial system short circuit characteristics.

In the case of both the resistive and inductive type FCL's, it is apparent that increasing the resistive state impedance yields stronger similarity in short circuit levels when compared to the original non DG integrated systems.

From results obtained it is apparent that the introduction of FCL's on the DG side of the interconnecting transformer of a synchronous machine based DG source can drastically change the effect that DG integration can impose on existing system short circuit characteristics.

4.3 The Use of FCLs for the Mitigation of Synchronous Machine Based DG Influences on Fuse-Recloser Coordination

In order to determine the effectiveness of each type of FCL in mitigating the effect of synchronous machine based DG sources on existing system fuse-recloser coordination, the algorithm presented in Figure 3.1 is utilized.

4.3.1 Bus 1 DG Connection

In order to illustrate the effect of FCL (each type) utilization in the mitigation of synchronous machine based DG influences on fuse-recloser coordination in fuse-saving schemes, consider the case study presented in Section 4.2. As depicted in Figures 4.3, 4.4, 4.5 and 4.6, the short circuit current experienced by the lateral load fuse at bus 4 with synchronous machine based DG source integration with FCL installation decreases to 3901 A, 3896 A, and 3853 A for the resistive (60 Ω), inductive (0.16 H) and resonant type FCLs respectively, when compared to the 4319 A experienced without FCL connection. As shown in APPENDIX B, for the base suburban distribution system (no DG), the short circuit current experienced by the lateral fuse at bus 4 for a three phase fault condition is 3869 A. Comparison highlights that FCL integration reduces the discrepancy between initial non DG integrated short circuit characteristics from 12% to less than 1% for each FCL type.

In contrast, the short circuit current experienced by the head end recloser increases to 3937 A, 3901 A, and 3947 A for the resistive (60 Ω), inductive (0.16 H) and resonant type FCLs respectively when compared to 3750 A experienced without FCL connection. As shown in APPENDIX B, for the base suburban distribution system (no DG), the short circuit current experienced by the head end recloser for a three phase fault condition at bus 4 is 3917 A. Comparison highlights that FCL integration reduces the discrepancy between initial non DG integrated short circuit characteristics from 5% to less than 1% for each FCL type.

Consequently, through the utilization of the coordination chart presented in Figure 2.8, it is apparent that the synchronous machine based DG integrated suburban distribution system with FCL connection, yields a recloser operating time (fast curve) of 0.029 seconds for each of the FCL types. In contrast, the lateral fuse protecting the bus 4 load will operate in 0.0314, 0.0315, and 0.0318 seconds respectively, hence the head end recloser will operate before the fuse resulting in the revalidation of the fuse-saving scheme initially employed. Comparison to the original suburban distribution system bus 4 coordination path demonstrates that for initial short circuit characteristics for a three phase fault at bus 4, the fuse operates in 0.0316 seconds and the head end recloser in 0.029 seconds. Observations show that the discrepancy between the original coordination and FCL installed synchronous machine based DG integrated system is less than 1% and original fuse-saving schemes are still valid. Considering that the three phase fault is the most severe [10], it is

apparent that FCL utilization is effective at mitigation of DG influences on fuse-recloser coordination.

Similarly, Observation of Figures 4.11 and 4.12 makes it apparent that lowering the overall impedance of the FCL during its fault current limiting phase, lowers the mitigation capacity for influences on short circuit current by synchronous machine based DG. This is particularly apparent in the inductive type FCL, where lowering the impedance during the fault current limiting stage, the FCL integrated DG system short circuit current increases from 0.7% to 2% discrepancy when compared to those experienced by the original system.

4.3.2 Bus 2 DG Connection

The case study presented in Section 3.2.2.2 demonstrates the effect of synchronous machine based DG integration at bus 2 on fuse-recloser coordination for the suburban distribution system. The most severe effects of synchronous machine based DG integration on fuse-recloser coordination in the system occurs for three phase faults at bus 4. An 8.4 MVA synchronous machine based DG source was connected at bus 2 with each of the FCL types as depicted in Figure 4.13.

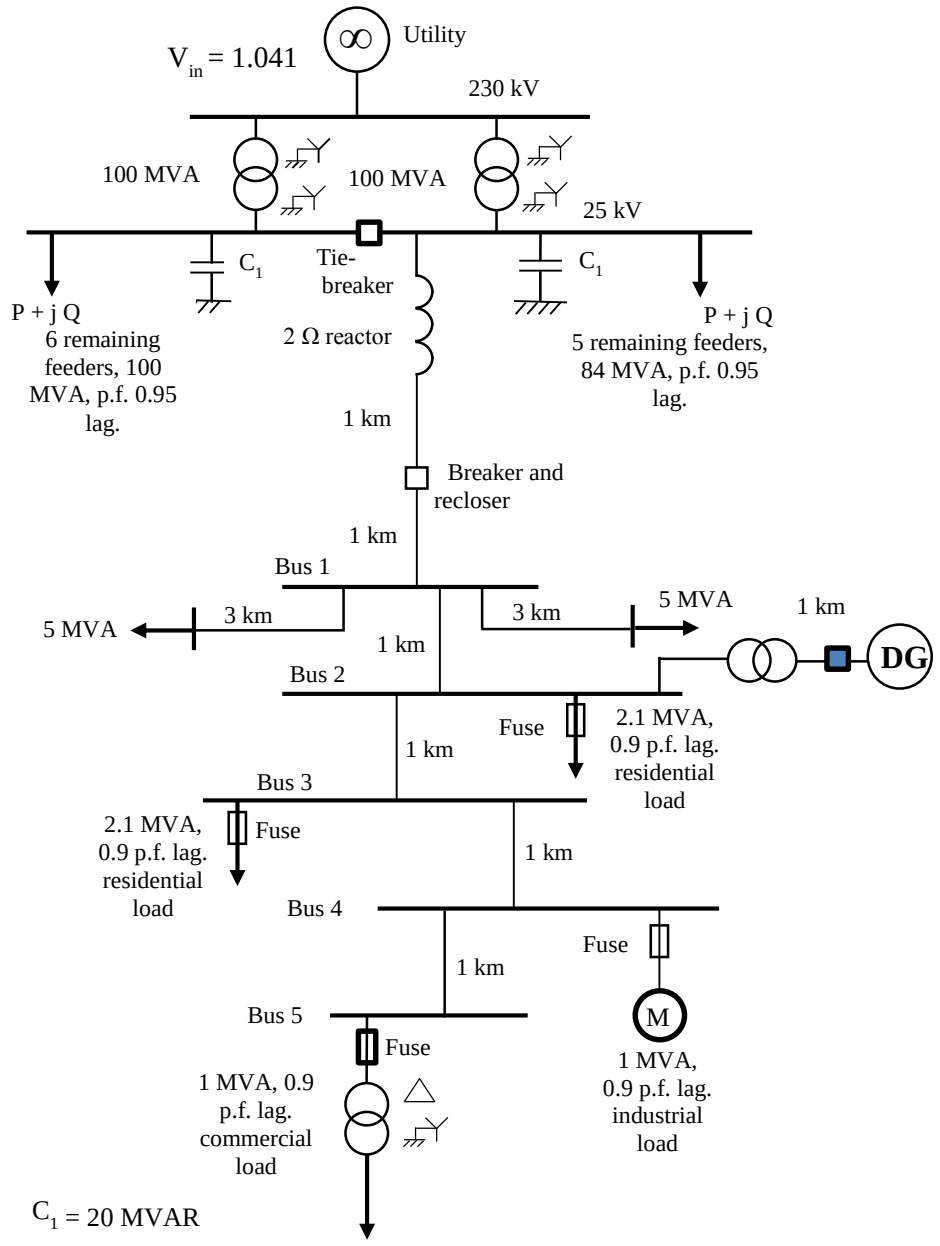

Figure 4.13: Suburban distribution system with DG integration at bus 2 with FCL presence.

A three phase fault is applied to the bus 4 load. The time-domain short circuit currents experienced by the bus 4 fuse and head end-recloser for each FCL type is presented in Figures 4.14 and 4.15 with a summary presented in Figure 4.16.

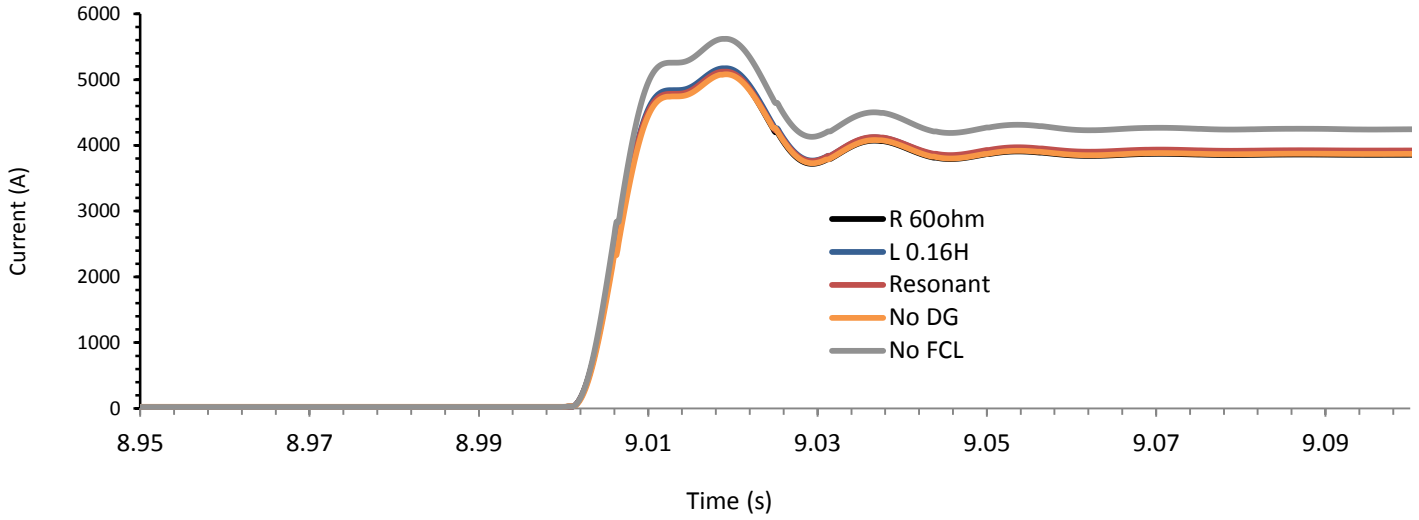

Figure 4.14: Time-domain RMS fault current simulation for a three phase fault applied at bus 4 with 8.4 MVA DG integration at bus 2 in the presence of a varying FCL types.

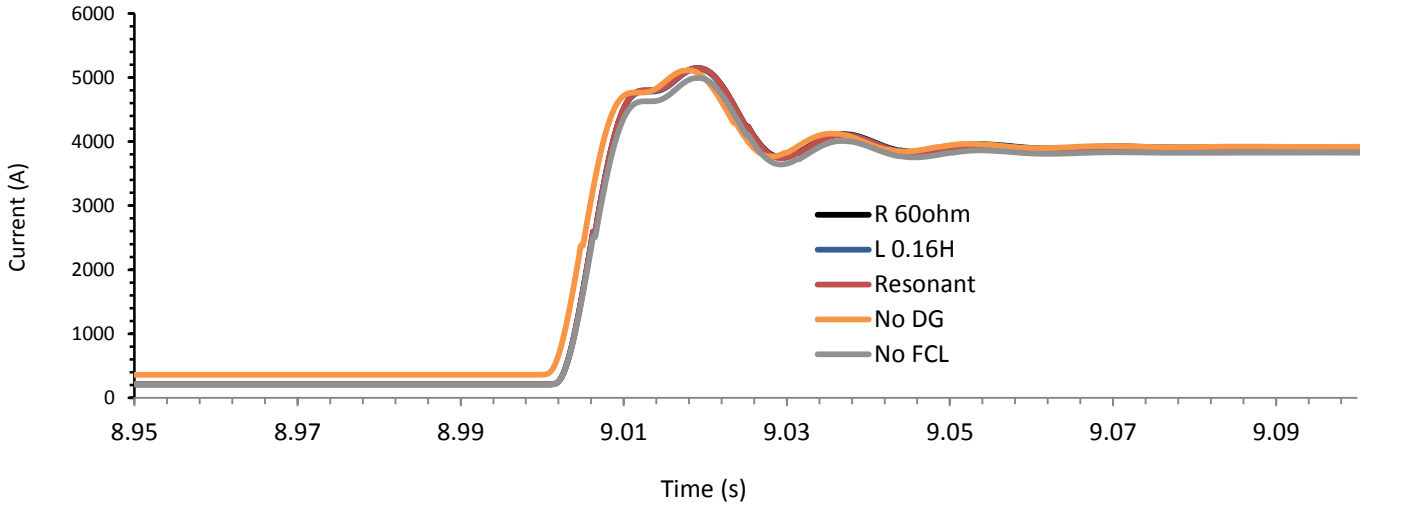

Figure 4.15: Time-domain RMS recloser current simulation for a three phase fault applied at bus 4 with 8.4 MVA DG integration at bus 2 in the presence of varying FCL types.

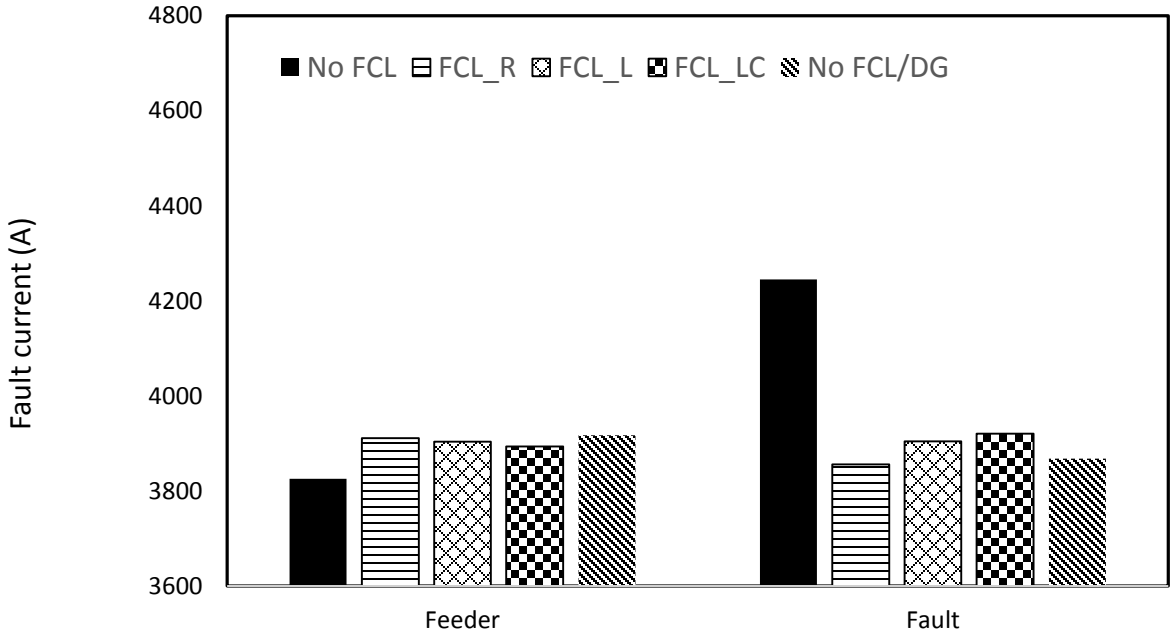

Figure 4.16: Summary of short circuit currents with an 8.4 MVA synchronous machine based DG source integrated at bus 2 in the suburban distribution system with a three phase fault applied at bus 4.

Similar to Section 4.3.1, Analysis of Figure 4.16 demonstrates that the introduction of the R, L and resonant type FCL's into the system presented in Figure 4.13 yields 0.4%, 0.9% and 1.4% differences in fault current when compared to that of the original short circuit characteristic, an improvement from the 10% difference experienced without the presence of FCL's. As depicted in Figure 4.16, the short circuit current experienced by the lateral load fuse at bus 4 with synchronous machine based DG source integration with FCL installation decreases to 3857 A, 3904 A, and 3921 A for the resistive (60 Ω), inductive (0.16 H) and resonant type FCLs respectively, when compared to the 4245 A experienced without FCL connection. As shown in APPENDIX B, for the base suburban distribution system (no DG), the short circuit current experienced by the lateral fuse at bus 4 for a three phase fault condition is 3869 A. Comparison highlights that FCL integration reduces the discrepancy between initial non DG integrated short circuit characteristics from 10% to less than 1% for the inductive and resistive FCL types and 1.4% for the resonant.

In contrast, the short circuit current experienced by the head end recloser changes to 3911 A, 3904 A, and 3894 A for the resistive (60 Ω), inductive (0.16 H) and resonant type FCLs respectively when compared to 3826 A experienced without FCL connection. As shown in APPENDIX B, for the base suburban distribution system (no DG), the short circuit current experienced by the head end recloser for a three phase fault condition at bus 4 is 3917 A.

Consequently, through the utilization of the coordination chart presented in Figure 2.8, it is apparent that the synchronous machine based DG integrated suburban distribution system with FCL connection, yields a recloser operating time (fast curve) of 0.029 seconds for each of the FCL types. In contrast, the lateral fuse protecting the bus 4 load will operate in 0.0318, 0.0314, and 0.0313 seconds respectively, hence the head end recloser will operate before the fuse, resulting in the revalidation of the fuse-saving scheme initially employed. Comparison to the original suburban distribution system bus 4 coordination path demonstrates that for initial short circuit characteristics for a three phase fault at bus 4, the fuse operates in 0.0316 seconds and head end recloser in 0.029 seconds. Observations show that the discrepancy between the original coordination and FCL installed synchronous machine based DG integrated system is less than 1% and original fuse-saving schemes are still valid. Considering that the three phase fault is the most severe [10], it is apparent that FCL utilization is effective at mitigation of DG influences on fuse-recloser coordination. It should also be noted that no synchronous machine based DG penetration level was found that caused loss of fuse-recloser coordination.

4.3.3 Bus 4 DG Connection

The case study presented in Section 3.2.2.3 demonstrates the effect of synchronous machine based DG integration at bus 4 on fuse-recloser coordination for the suburban distribution system. The most severe effects of synchronous machine based DG integration on fuse-recloser coordination in the system occurs for three phase faults at bus 4. An 8.4 MVA synchronous machine based DG source was connected at bus 4 with each of the FCL types, as depicted in Figure 4.17.

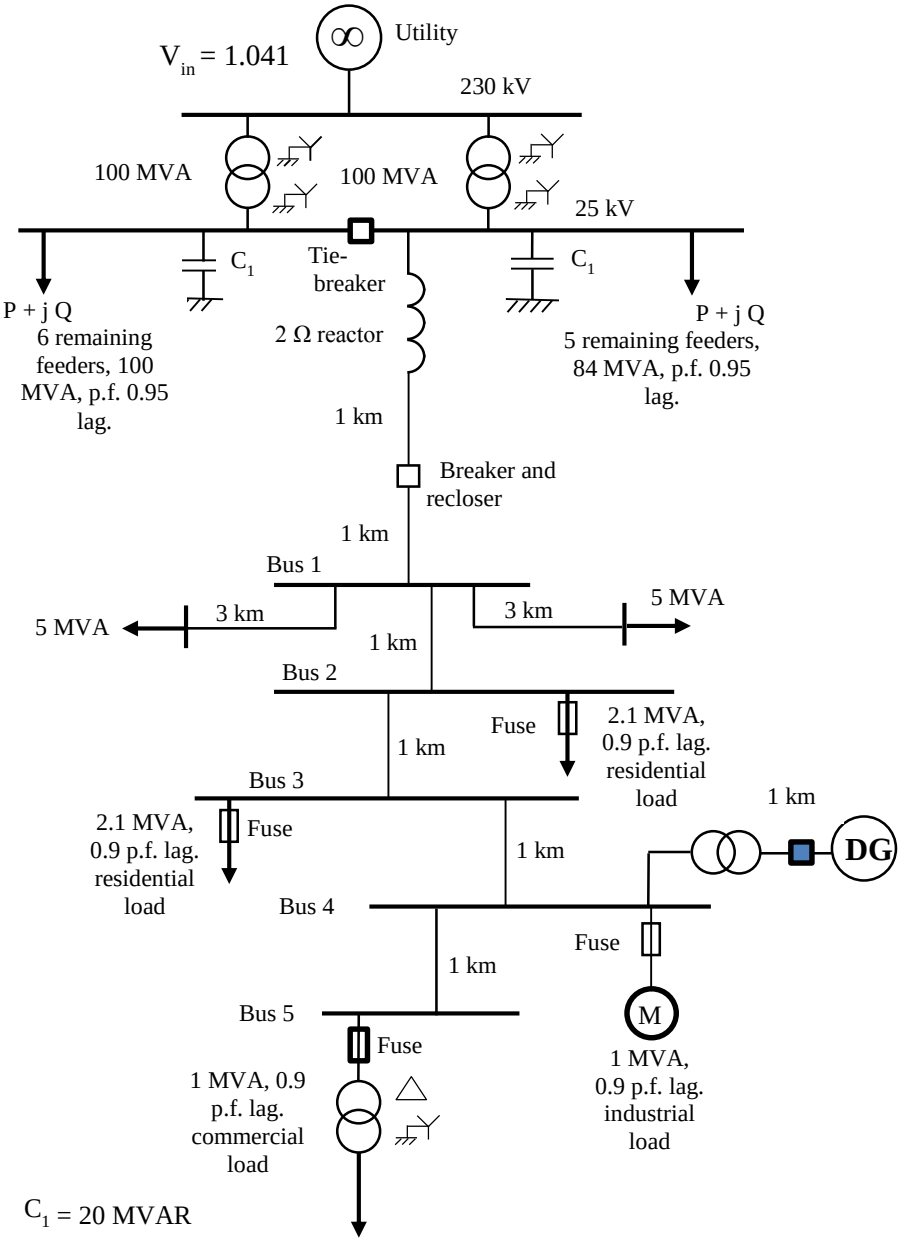

Figure 4.17: Suburban distribution system with DG integration at bus 4 with FCL presence.

A three phase fault is applied to the bus 4 load. The time-domain short circuit currents experienced by the bus 4 fuse and head end-recloser for each FCL type is presented in Figures 4.18 and 4.19 with a summary presented in Figure 4.20.

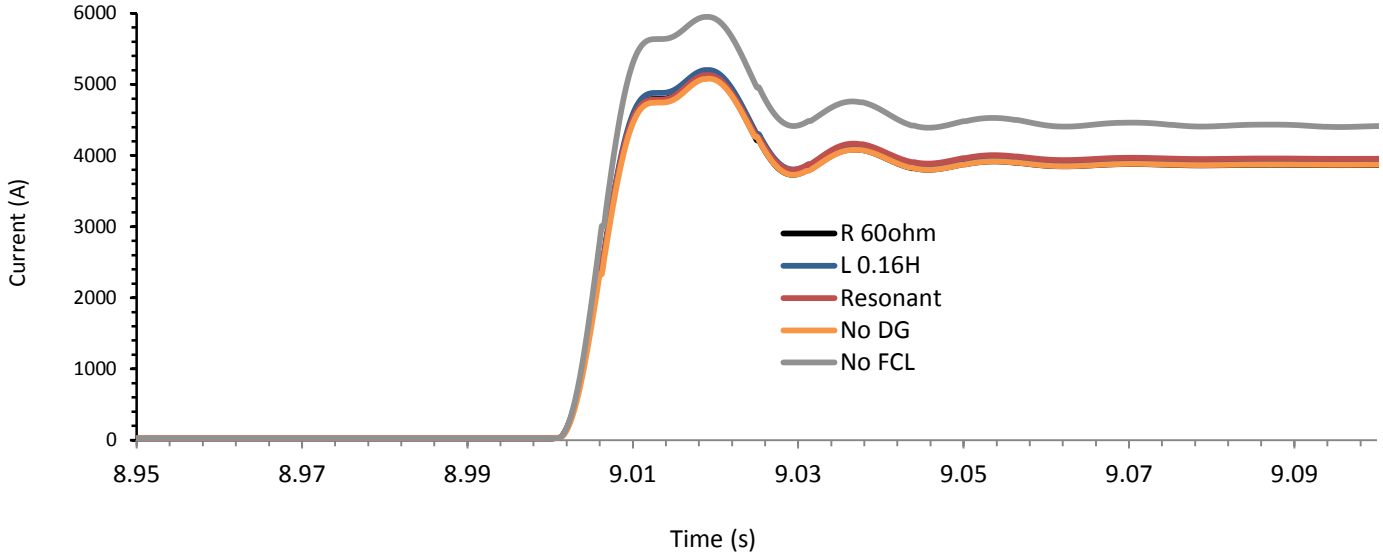

Figure 4.18: Time-domain RMS fault current simulation for a three phase fault applied at bus 4 with 8.4 MVA DG integration at bus 4 in the presence of a varying FCL types.

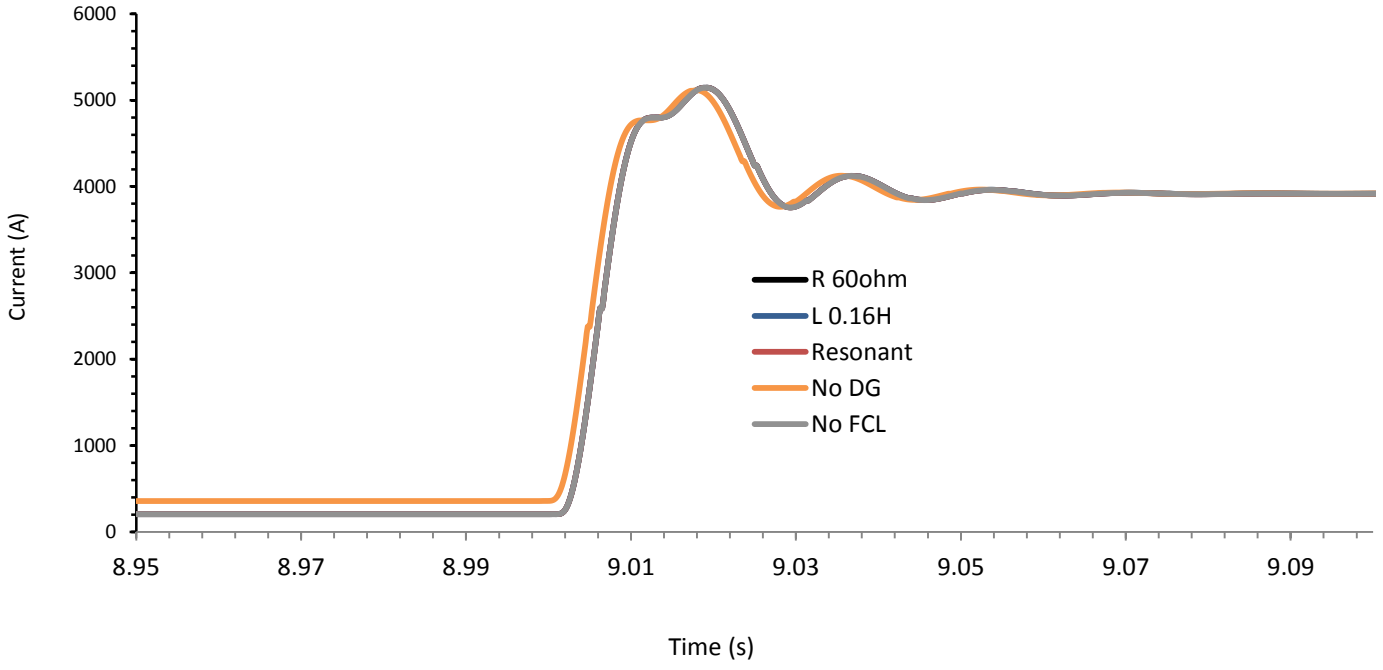

Figure 4.19: Time-domain RMS recloser current simulation for a three phase fault applied at bus 4 with 8.4 MVA DG integration at bus 4 in the presence of varying FCL types.

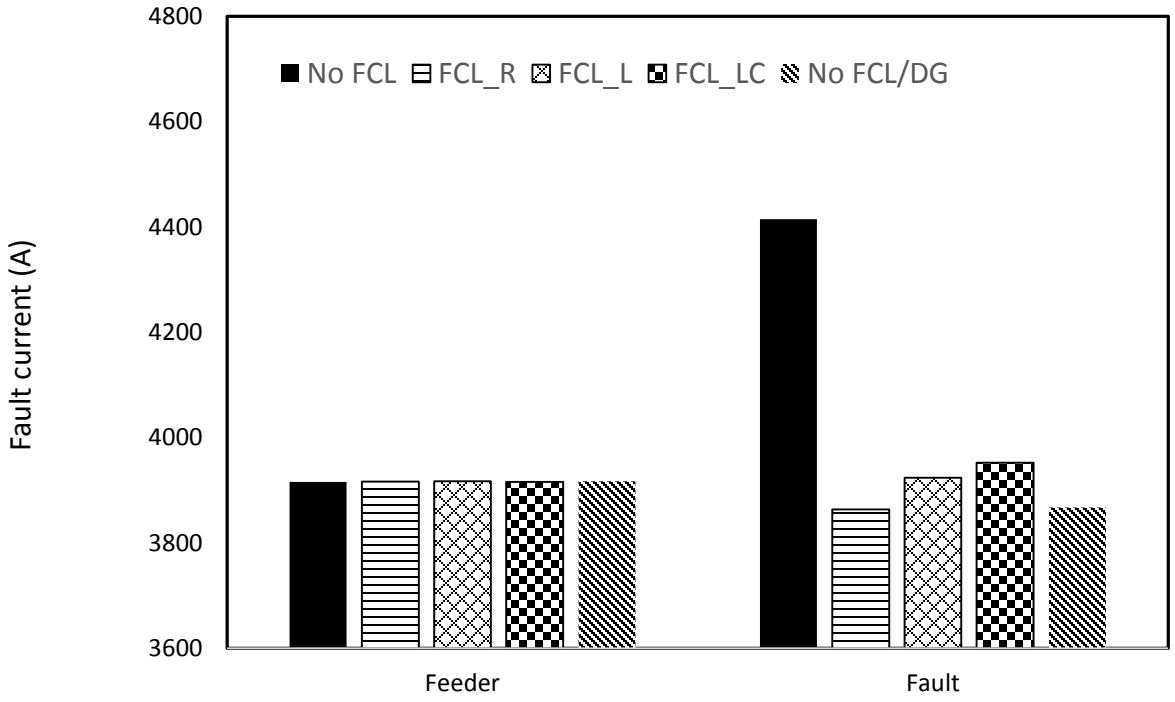

Figure 4.20: Summary of short circuit currents with an 8.4 MVA synchronous machine based DG source integrated at bus 4 in the suburban distribution system with a three phase fault applied at bus 4.

Similar to Section 4.3.2, analysis of Figure 4.20 demonstrates that the introduction of the R, L and resonant type FCL's into the system presented in Figure 4.17 yields 0.1%, 1.5% and 2.2% difference in fault current when compared to that of the original short circuit characteristic, an improvement from the 14% difference experienced without the presence of FCL's. As depicted in Figure 4.20, the short circuit current experienced by the lateral load fuse at bus 4 with synchronous machine based DG source integration with FCL installation decreases to 3864 A, 3924 A, and 3953 A for the resistive (60 Ω), inductive (0.16 H) and resonant type FCLs respectively, when compared to the 4415 A experienced without FCL connection. As shown in APPENDIX B, for the base suburban distribution system (no DG), the short circuit current experienced by the lateral fuse at bus 4 for a three phase fault condition is 3869 A.

In contrast, the short circuit current experienced by the head end recloser remains unchanged, consistent with findings presented in Section 3.3.2. As shown in APPENDIX B, for the base suburban distribution system (no DG), the short circuit current experienced by the head end recloser for a three phase fault condition at bus 4 is 3917 A.

Consequently, through the utilization of the coordination chart presented in Figure 2.8, it is apparent that the synchronous machine based DG integrated suburban distribution system with FCL connection, yields a recloser operating time (fast curve) of 0.029 seconds for each of the FCL types. In contrast, the lateral fuse protecting the bus 4 load will operate in 0.0318, 0.0313, and 0.0308 seconds respectively, hence the head end recloser will operate before the fuse resulting in the fuse-saving scheme initially employed being revalidated. Comparison to the original suburban distribution system bus 4 coordination path demonstrates that for initial short circuit characteristics for a three phase fault at bus 4, the fuse operates in 0.0316 seconds and head end recloser in 0.029 seconds. Observations shows that the discrepancy between the original coordination and FCL installed synchronous machine based DG integrated system is less than 1% for the resistive and inductive types and 3.5% for the resonant type. Considering that the three phase fault is the most severe [10], it is apparent that FCL utilization is effective at mitigation of DG influences on fuse-recloser coordination. It should also be noted that no synchronous machine based DG penetration level was found that caused loss of fuse-recloser coordination.

4.3.4 Bus 5 DG Connection

The case study presented in Section 3.2.2.4 demonstrates the effect of synchronous machine based DG integration at bus 5 on fuse-recloser coordination for the suburban distribution system. The most severe effects of synchronous machine based DG integration on fuse-recloser coordination in the system occurs for three phase faults at bus 4. An 8.4 MVA synchronous machine based DG source was connected at bus 4 with each of the FCL types as depicted in Figure 4.21.

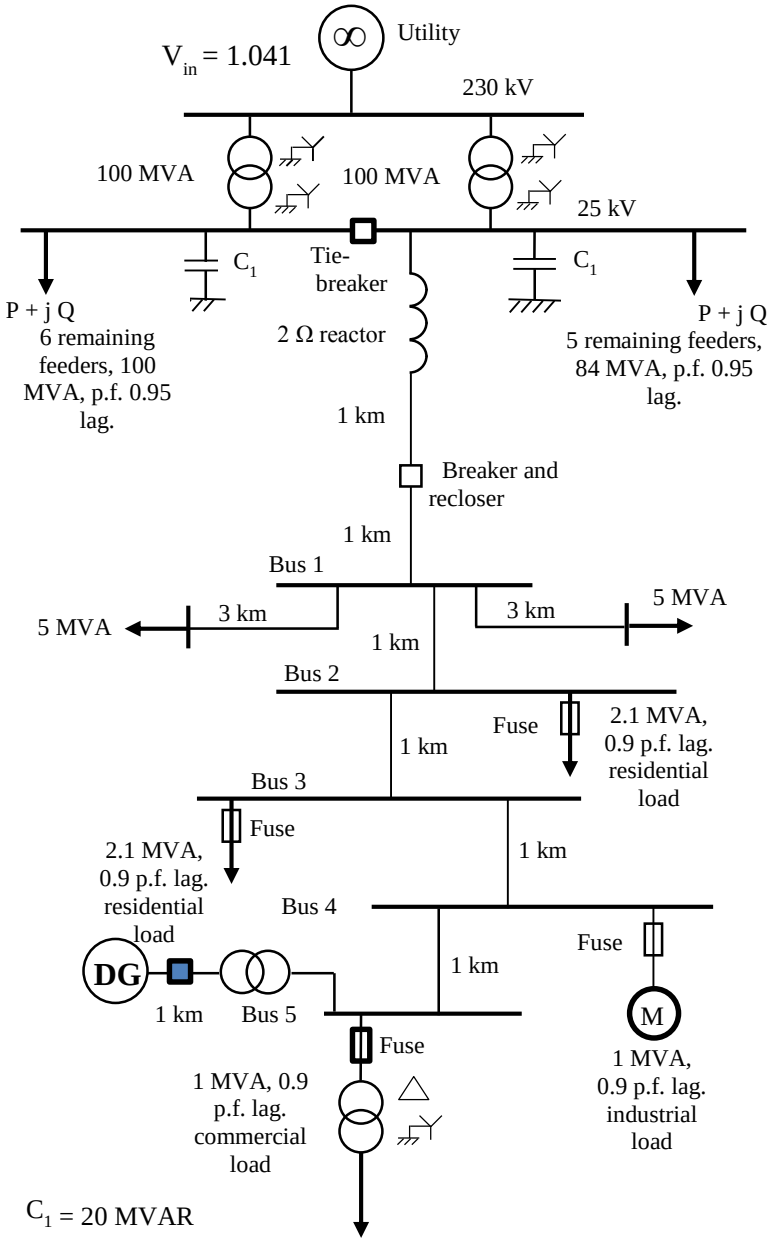

Figure 4.21: Suburban distribution system with DG integration at bus 5 with FCL presence.

A three phase fault is applied to the bus 4 load. The time-domain short circuit currents experienced by the bus 4 fuse and head end-recloser for each FCL type is presented in Figures 4.22 and 4.23 with a summary presented in Figure 4.24.

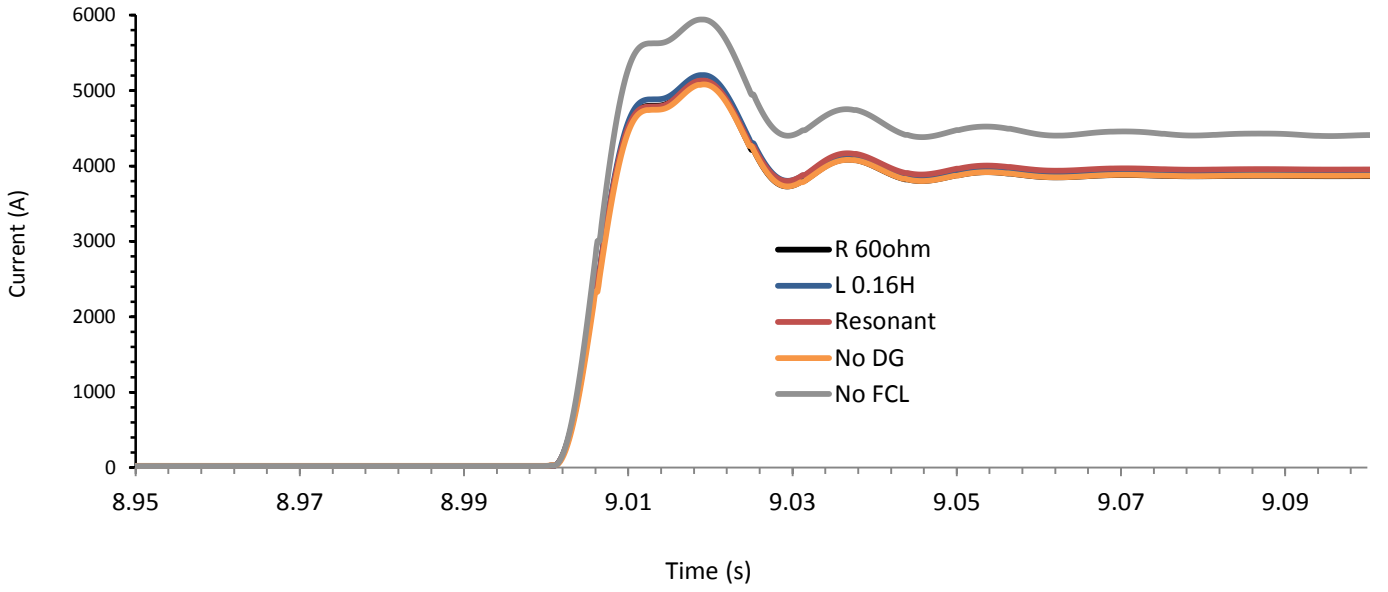

Figure 4.22: Time-domain RMS fault current simulation for a three phase fault applied at bus 4 with 8.4 MVA DG integration at bus 5 in the presence of a varying FCL types.

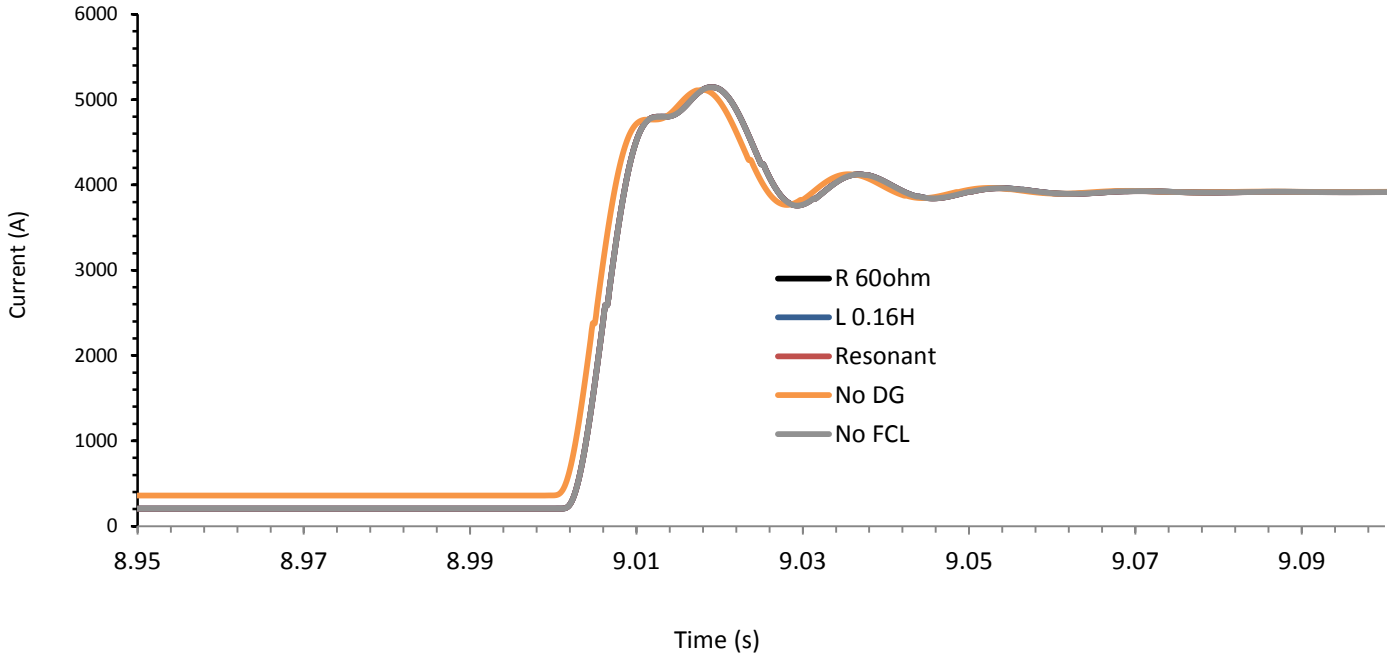

Figure 4.23: Time-domain RMS recloser current simulation for a three phase fault applied at bus 4 with 8.4 MVA DG integration at bus 5 in the presence of varying FCL types.

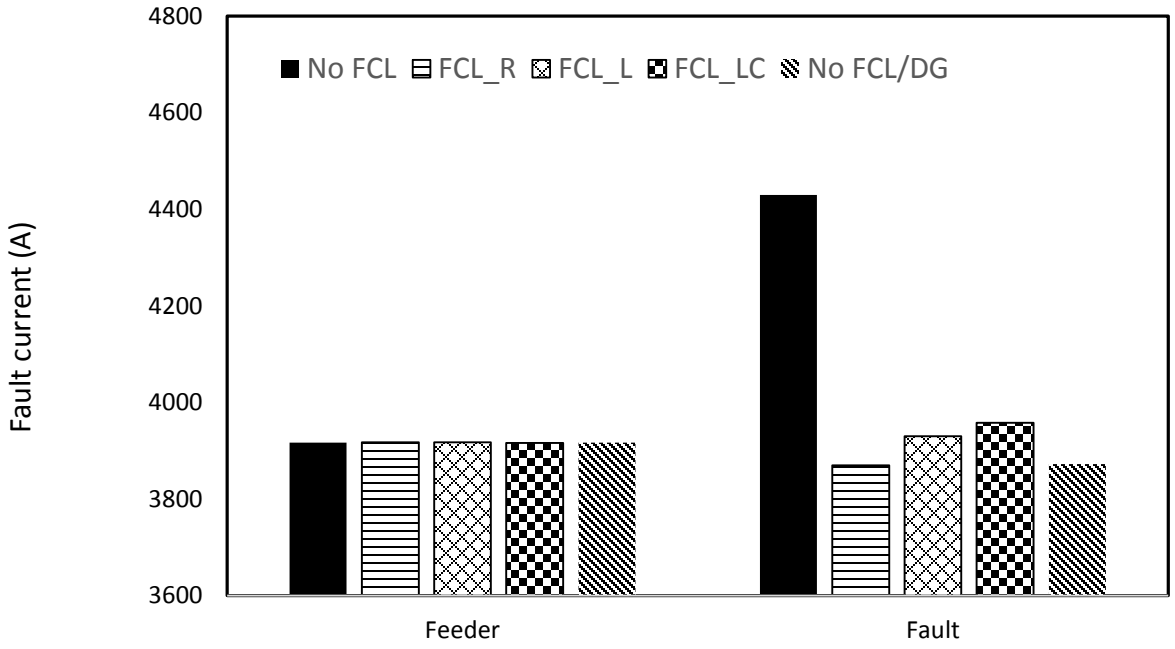

Figure 4.24: Summary of short circuit currents with an 8.4 MVA synchronous machine based DG source integrated at bus 5 in the suburban distribution system with a three phase fault applied at bus 4.

Similar to Section 4.3.3, analysis of Figure 4.24 demonstrates that the introduction of the R, L and resonant type FCL's into the system presented in Figure 4.21 yields 0.1%, 1.5% and 2.2% differences in fault current when compared to that of the original short circuit characteristic, an improvement from the 14% difference experienced without the presence of FCL's. As depicted in Figure 4.24, the short circuit current experienced by the lateral load fuse at bus 4 with synchronous machine based DG source integration with FCL installation decreases to 3871 A, 3931 A, and 3958 A for the resistive (60 Ω), inductive (0.16H) and resonant type FCLs respectively when compared to the 4430 A experienced without FCL connection. As shown in APPENDIX B, for the base suburban distribution system (no DG), the short circuit current experienced by the lateral fuse at bus 4 for a three phase fault condition is 3873 A.

In contrast, the short circuit current experienced by the head end recloser remains unchanged, consistent with findings presented in Section 3.3.2. As shown in APPENDIX B, for

the base suburban distribution system (no DG), the short circuit current experienced by the head end recloser for a three phase fault condition at bus 4 is 3917 A.

Consequently, through the utilization of the coordination chart presented in Figure 2.8, it is apparent that the synchronous machine based DG integrated suburban distribution system with FCL connection, yields a recloser operating time (fast curve) of 0.029 seconds for each of the FCL types. In contrast, the lateral fuse protecting the bus 4 load will operate in 0.0316, 0.0312, and 0.0307 seconds respectively, hence the head end recloser will operate before the fuse resulting in revalidation of the fuse-saving scheme initially employed. Comparison to the original suburban distribution system bus 4 coordination path demonstrates that for initial short circuit characteristics for a three phase fault at bus 4, the fuse operates in 0.0316 seconds and head end recloser in 0.029 seconds. Considering that the three phase fault is the most severe [10], it is apparent that FCL utilization is effective at mitigation of DG influences on fuse-recloser coordination. It should also be noted that no synchronous machine based DG penetration level was found that caused loss of fuse-recloser coordination.

4.3.5 DG Connection Summary

Comparison of results from Section 4.3 makes it apparent that the utilization of superconducting FCLs of resistive, inductive and resonant types are effective at mitigation of synchronous machine based DG influences on existing system fuse-recloser protection coordination. Increasing the impedance of the resistive and inductive type FCLs yields more efficient mitigation capabilities. Analysis of Figures 4.6, 4.16, 4.20 and 4.24 makes it apparent that the resistive type FCL is consistently effective, with discrepancies between non-DG and FCL DG integrated short circuit characteristics being limited to less than 1% for each connection point. Furthermore, it is apparent that the resonant and inductive type FCLs become less effective for DG connections closer to the fault location, however they are still able to restore original coordination schemes.

4.4 The use of FCLs for the Mitigation of Synchronous Machine Based DG Influences on Recloser Sensitivity

As demonstrated in Section 3.3, for the suburban distribution system given in Figure 2.1, the lowest short circuit current experienced by the network is a line to line fault at the bus 5 load corresponding to the coordination path in Figure 2.6. For this coordination path the recloser pick up current is 560 A. In order to determine the effectiveness of each type of FCL in mitigating the effect of synchronous machine based DG sources on existing system recloser sensitivity, the algorithm presented in Figure 3.13 is utilized.

4.4.1 Bus 1 DG Connection

The case study presented in Section 3.3.2.1 demonstrates the effect of synchronous machine based DG integration at bus 1 on recloser sensitivity for the suburban distribution system. An 8.4 MVA and 55.6 MVA synchronous machine based DG source was connected at bus 1 (each connected for separate tests) with each of the FCL types as depicted in Figure 4.2. A line to line fault is applied to the bus 5 load. The time-domain short circuit currents experienced by the head end-recloser for each DG size and FCL type is presented in Figures 4.25 and 4.26 with a summary presented in Figure 4.27.

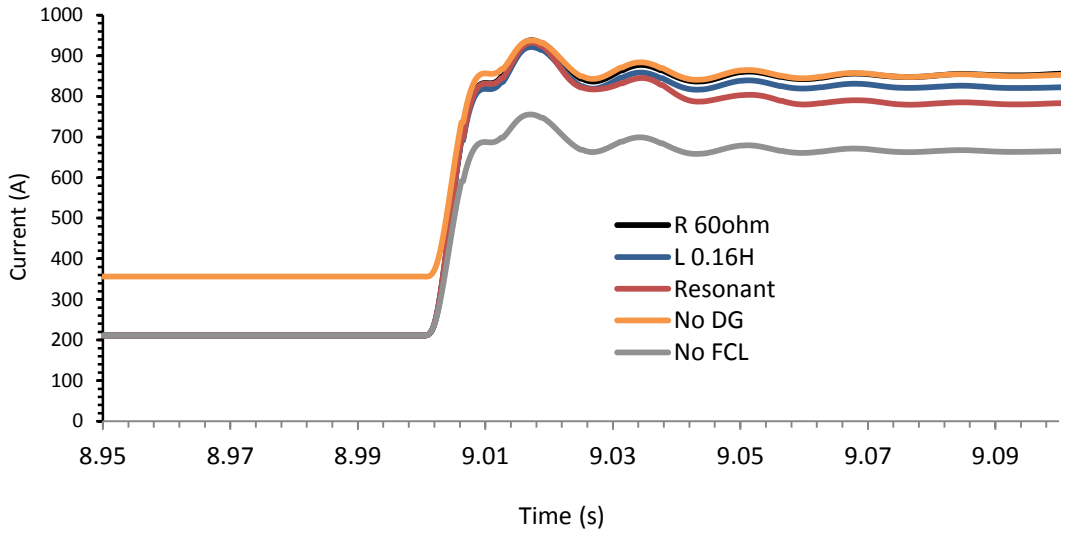

Figure 4.25: Time-domain recloser RMS current simulation for a line to line fault applied at the bus 5 load with an 8.4 MVA synchronous machine based DG source integrated at bus 1 with FCL presence.

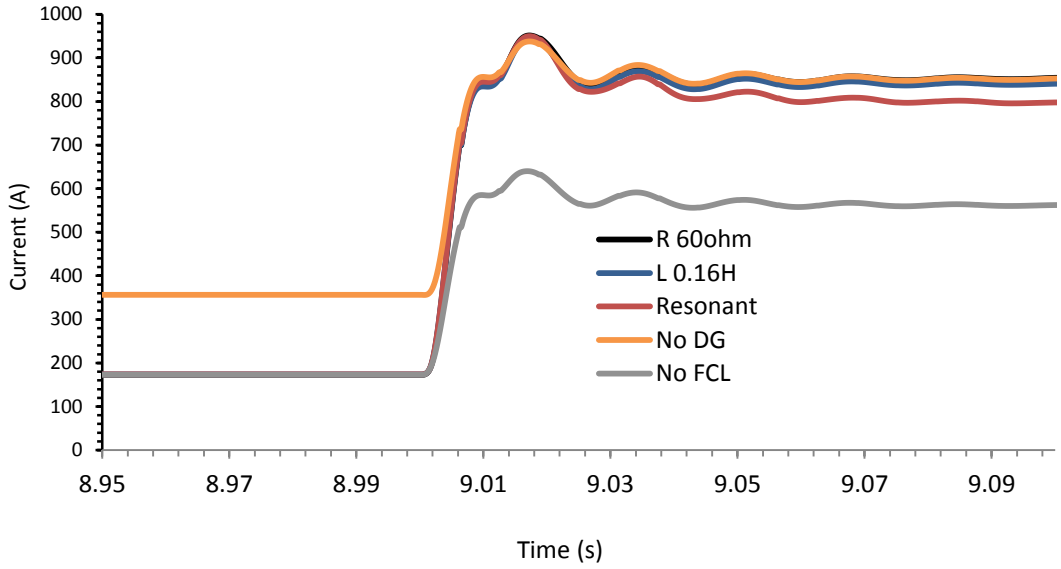

Figure 4.26: Time-domain recloser RMS current simulation for a line to line fault applied at the bus 5 load with a 55.6 MVA synchronous machine based DG source integrated at bus 1 with FCL presence.

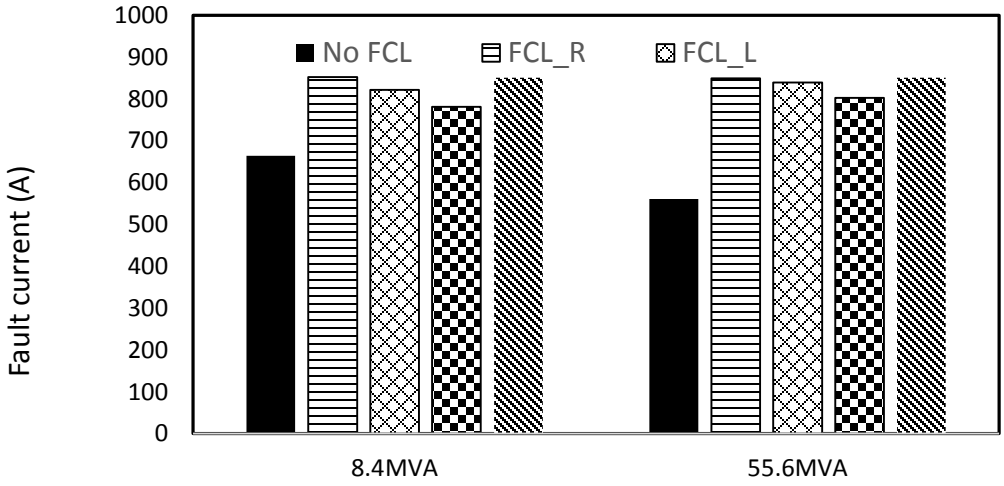

Figure 4.27: Summary of recloser short circuit currents with an 8.4 MVA and 55.6 MVA synchronous machine based DG source integrated at bus 1 in the suburban distribution system with a line to line fault applied at the bus 5 load with FCL presence.

Observation of Figures 4.25 and 4.26 in conjunction with Figure 4.27 makes it apparent that each FCL type is successfully able to mitigate synchronous machine based DG influences for increasing levels of penetration. In the case of the 55.6 MVA DG source, the discrepancy between the original suburban distribution system short circuit behavior and the DG integrated network improves from 34% to 0.2%, 1.3% and 5.7% for the resistive, inductive and resonant FCL type respectively. It should also be noted that no synchronous machine based DG penetration level was found that caused loss of fuse-recloser coordination.

As mentioned in Section 4.3.1, in commercial applications there are a wide variety of resistive and inductive type FCLs of varying magnitude of resistances and inductances. In order to reflect results consistent with varying resistive values, the resistive and inductive type FCLs in the system presented in Figure 4.2 are varied in magnitude. Figures 4.28, 4.29, 4.30 and 4.31 show the time domain simulations. Figures 4.32 and 4.33 show a summary for each FCL type for a line to line fault at the bus 5 load for the 8.4 MVA and 55.6 MVA synchronous machine based DG integrated suburban distribution system with the R and L type FCL's values being varied between 20 Ω - 60 Ω and 0.05 H - 0.16 H respectively.

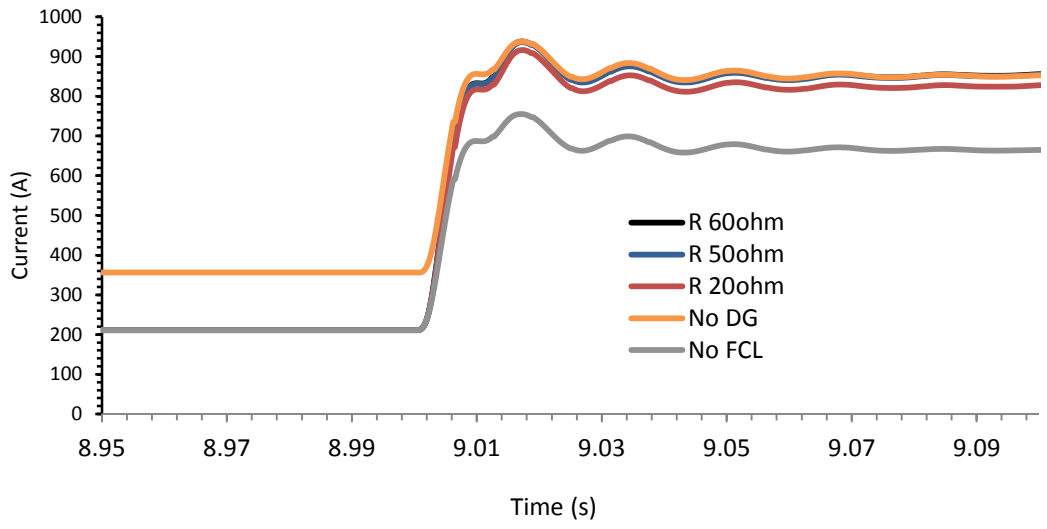

Figure 4.28: Time-domain recloser RMS current simulation for a line to line fault applied at the bus 5 load with an 8.4 MVA synchronous machine based DG source integrated at bus 1 with varying resistive FCL impedance.

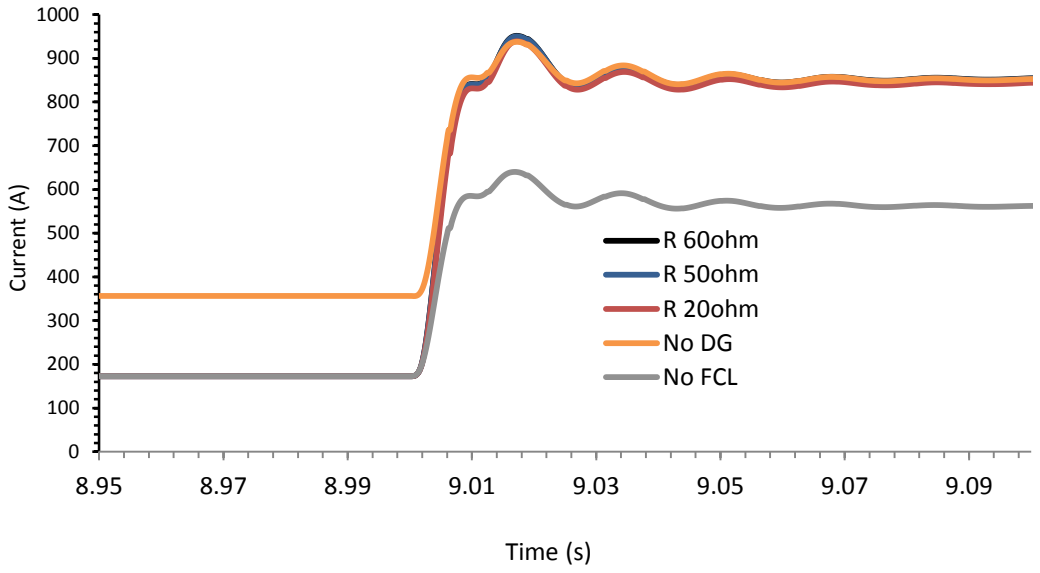

Figure 4.29: Time-domain recloser RMS current simulation for a line to line fault applied at the bus 5 load with a 55.6 MVA synchronous machine based DG source integrated at bus 1 with varying resistive FCL impedance.

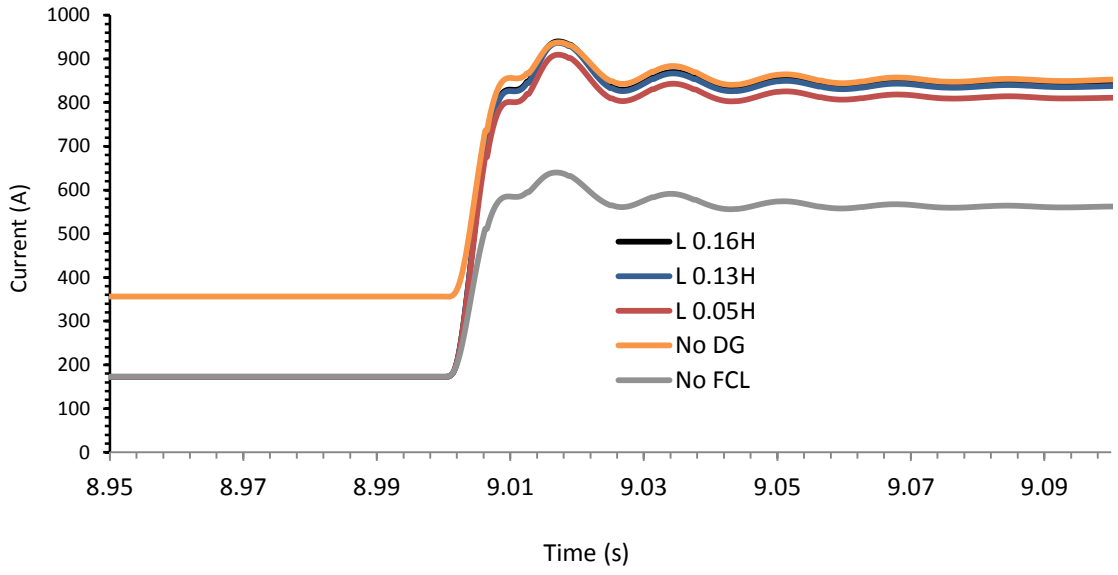

Figure 4.30: Time-domain recloser RMS current simulation for a line to line fault applied at the bus 5 load with an 8.4 MVA synchronous machine based DG source integrated at bus 1 with varying inductive FCL impedance.

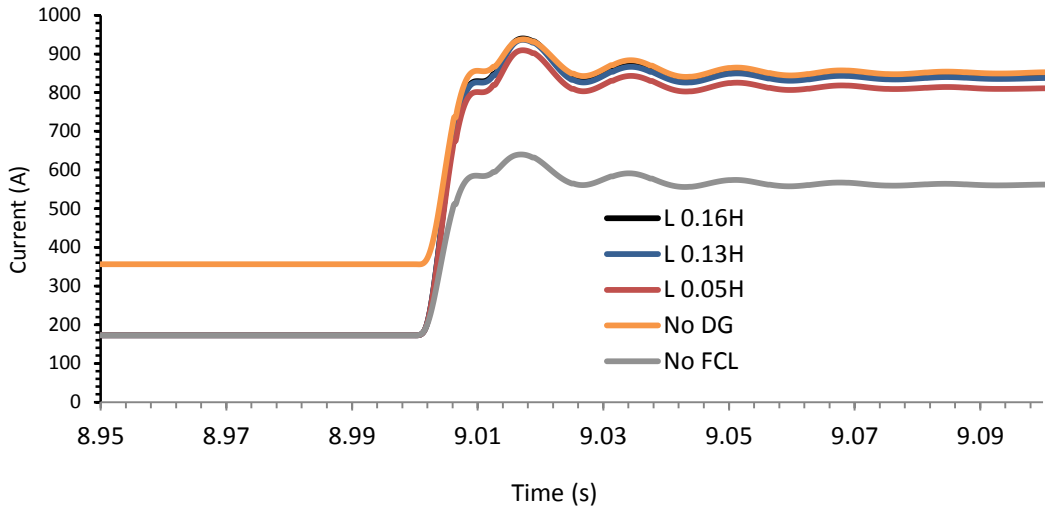

Figure 4.31: Time-domain recloser RMS current simulation for a line to line fault applied at the bus 5 load with a 55.6 MVA synchronous machine based DG source integrated at bus 1 with varying inductive FCL impedance.

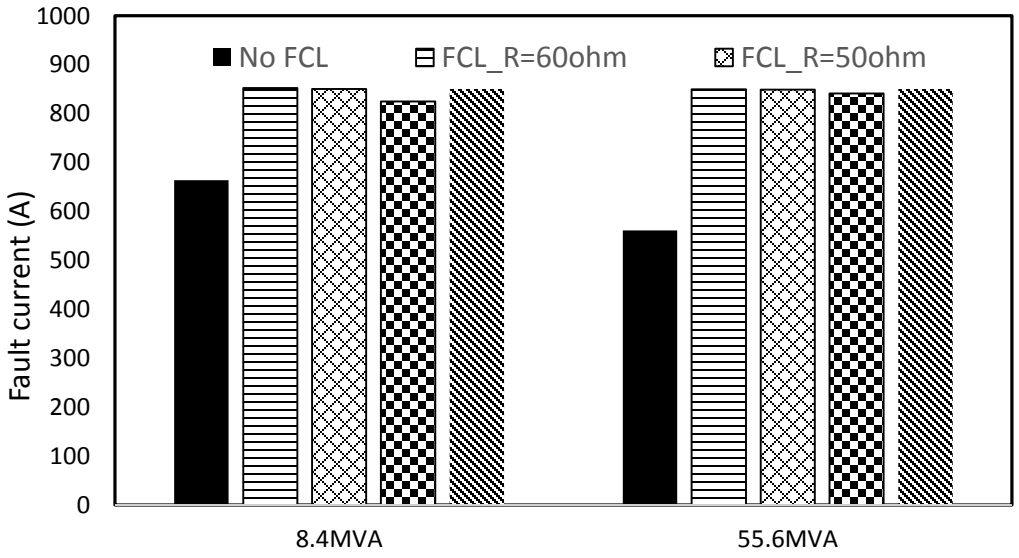

Figure 4.32: Summary of recloser short circuit currents with an 8.4 MVA and 55.6 MVA synchronous machine based DG source integrated at bus 1 in the suburban distribution system with a line to line fault applied at the bus 5 load with varying resistive FCL impedance.

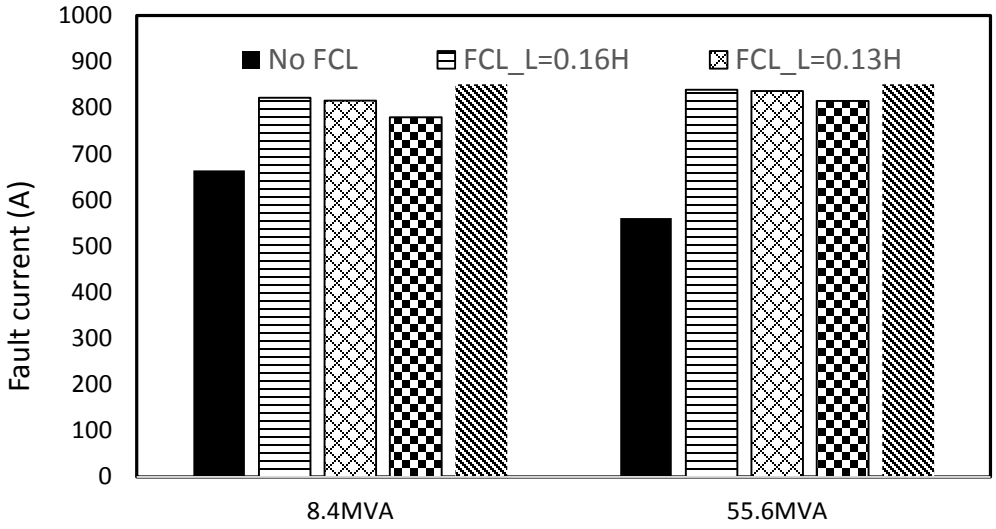

Figure 4.33: Summary of recloser short circuit currents with an 8.4 MVA and 55.6 MVA synchronous machine based DG source integrated at bus 1 in the suburban distribution system with a line to line fault applied at the bus 5 load with varying inductive FCL impedance.

Observation of Figure 4.32 in conjunction with Figure 4.33 confirms the hypothesis presented in Section 4.3.1, as it is apparent that lowering the impedance of the resistive and inductive FCL is detrimental to the effectiveness of the FCL in mitigation of synchronous machine based DG influences on recloser sensitivity. In both cases, for the 55.6 MVA DG the discrepancy between original system short circuit characteristics and the DG integrated decreases from 0.2% to 1.1% and 1.3% to 4.9% for the resistive and inductive type FCL respectively.

4.4.2 Bus 2 DG Connection

The case study presented in Section 3.3.2.2 demonstrates the effect of synchronous machine based DG integration at bus 2 on recloser sensitivity for the suburban distribution system. An 8.4 MVA and 55.5 MVA synchronous machine based DG source is connected at bus 2 (each connected for separate tests) with each of the FCL types as depicted in Figure 4.13. A line to line fault is applied to the bus 5 load. The time-domain short circuit currents experienced by the head end-recloser for each DG size and FCL type are presented in Figures 4.34 and 4.35 with a summary presented in Figure 4.36.

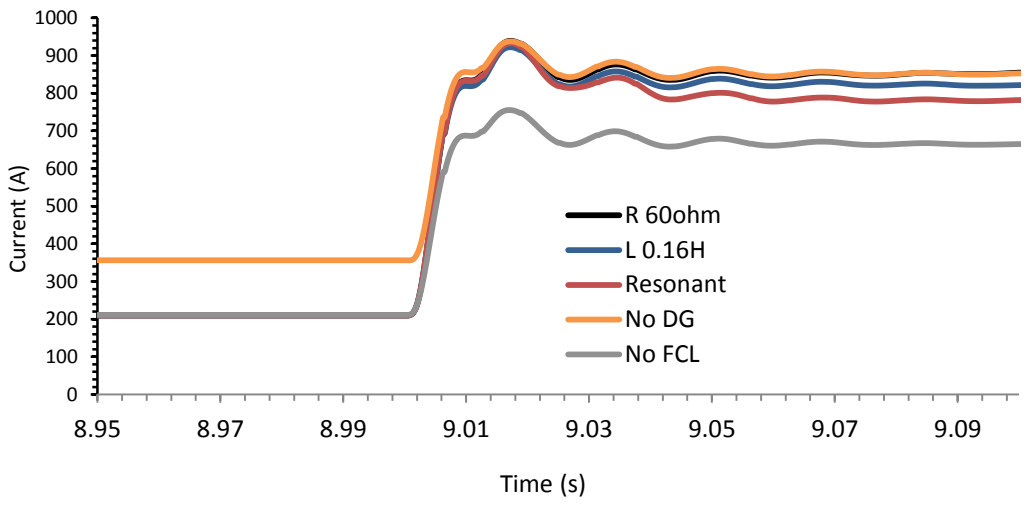

Figure 4.34: Time-domain recloser RMS current simulation for a line to line fault applied at the bus 5 load with an 8.4 MVA synchronous machine based DG source integrated at bus 2 with FCL presence.

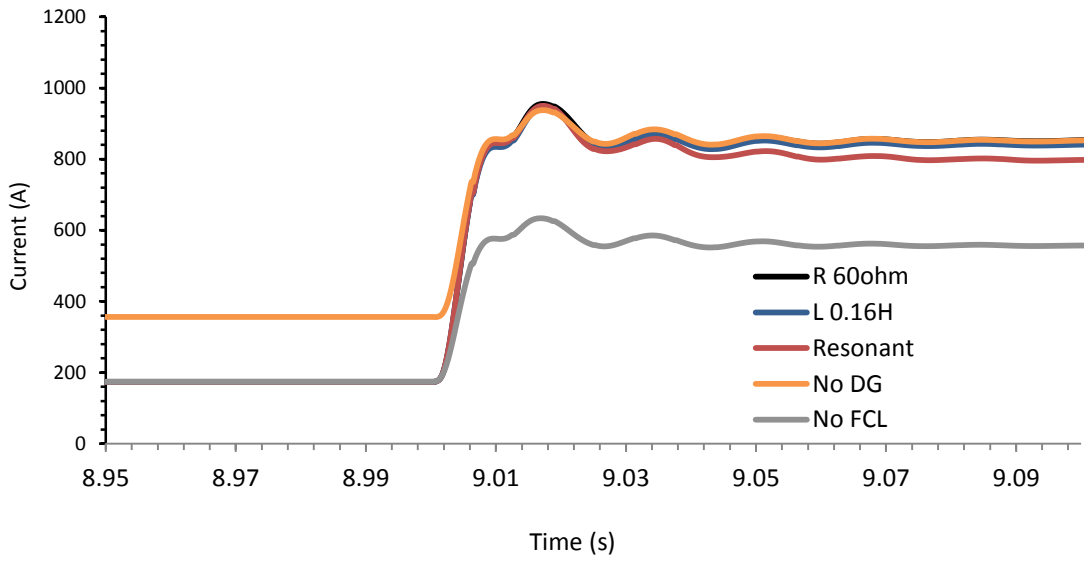

Figure 4.35: Time-domain recloser RMS current simulation for a line to line fault applied at the bus 5 load with a 55.5 MVA synchronous machine based DG source integrated at bus 2 with FCL presence.

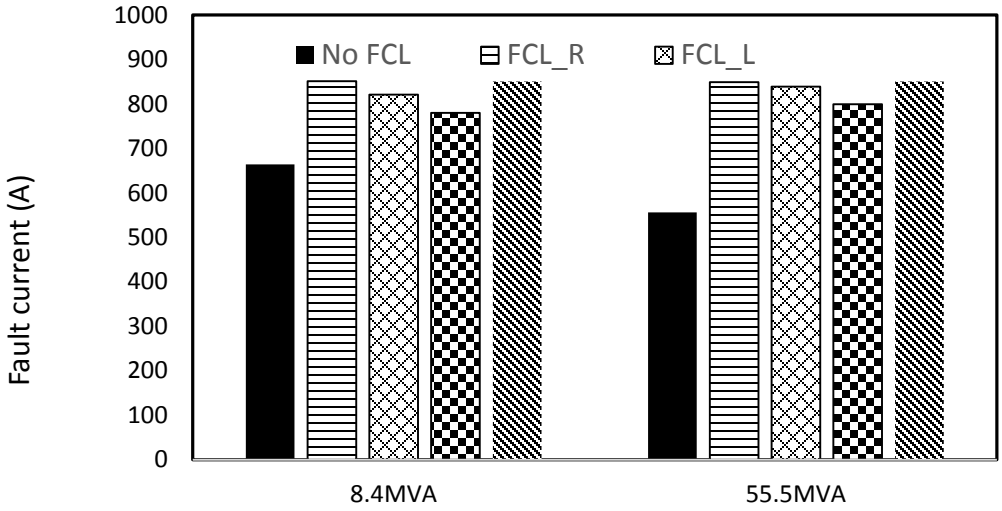

Figure 4.36: Summary of recloser short circuit currents with an 8.4 MVA and 55.5 MVA synchronous machine based DG source integrated at bus 2 in the suburban distribution system with a line to line fault applied at the bus 5 load with FCL presence.

Observation of Figures 4.34 and 4.35 in conjunction with Figure 4.36 makes it apparent that each FCL type is successfully able to mitigate synchronous machine based DG influences for increasing levels of penetration. In the case of the 55.5 MVA DG source, the discrepancy between the original suburban distribution system short circuit behavior and the DG integrated network improves from 34% to 0.2%, 1.4% and 6.1% for the resistive, inductive and resonant FCL type respectively. It should also be noted that no synchronous machine based DG penetration level was found that caused loss of fuse-recloser coordination.

4.4.3 Bus 4 DG Connection

The case study presented in Section 3.3.2.3 demonstrates the effect of synchronous machine based DG integration at bus 4 on recloser sensitivity for the suburban distribution system. An 8.4 MVA and 50.5 MVA synchronous machine based DG source is connected at bus 4 (each connected for separate tests) with each of the FCL types, as depicted in Figure 4.17. A line to line fault is applied to the bus 5 load. The time-domain short circuit currents experienced by the head end-recloser for each DG size and FCL type is presented in Figures 4.37 and 4.38 with a summary presented in Figure 4.39.

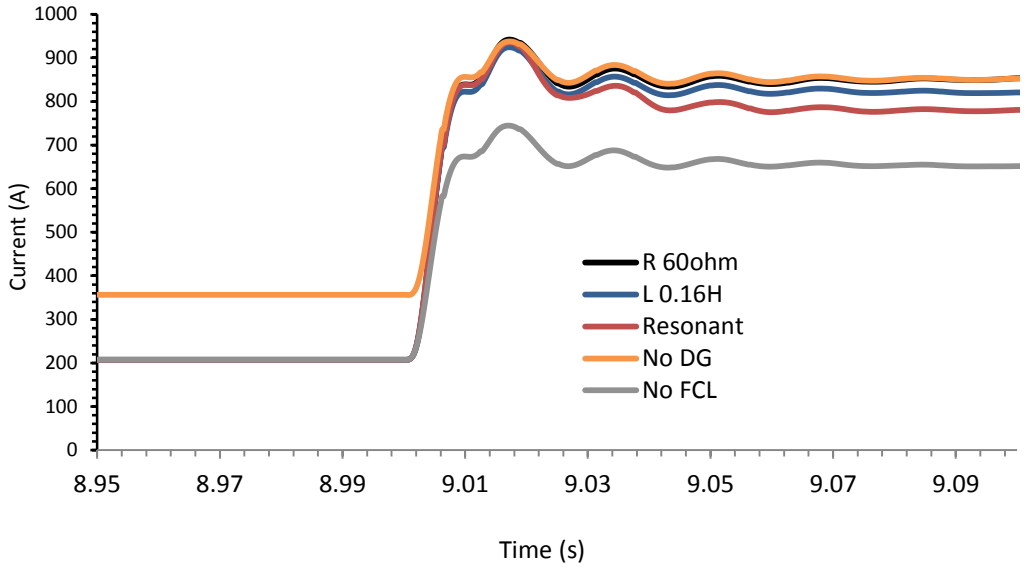

Figure 4.37: Time-domain recloser RMS current simulation for a line to line fault applied at the bus 5 load with an 8.4 MVA synchronous machine based DG source integrated at bus 4 with FCL presence.

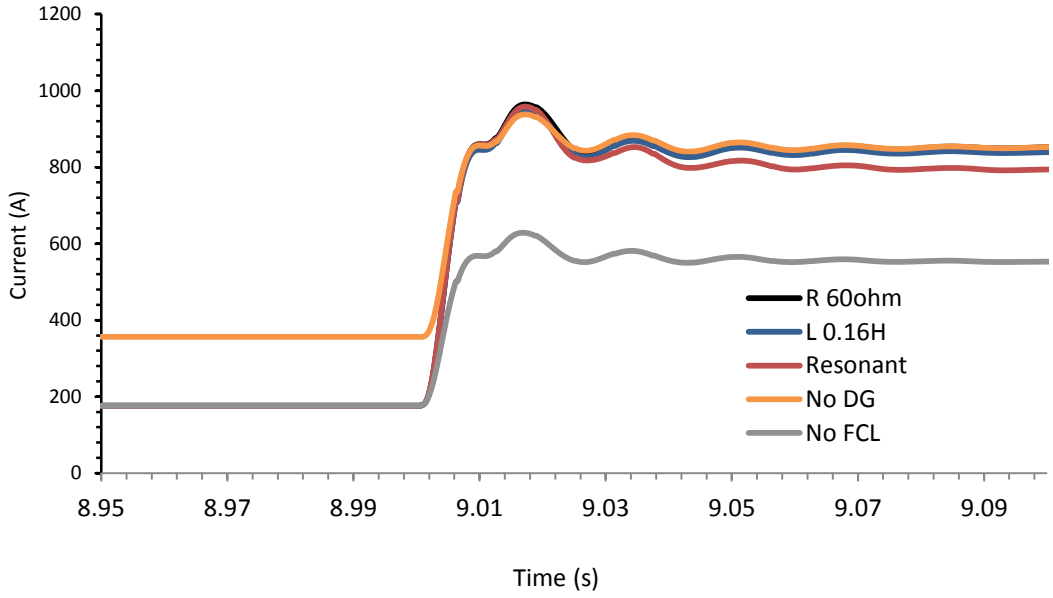

Figure 4.38: Time-domain recloser RMS current simulation for a line to line fault applied at the bus 5 load with a 50.5 MVA synchronous machine based DG source integrated at bus 4 with FCL presence.

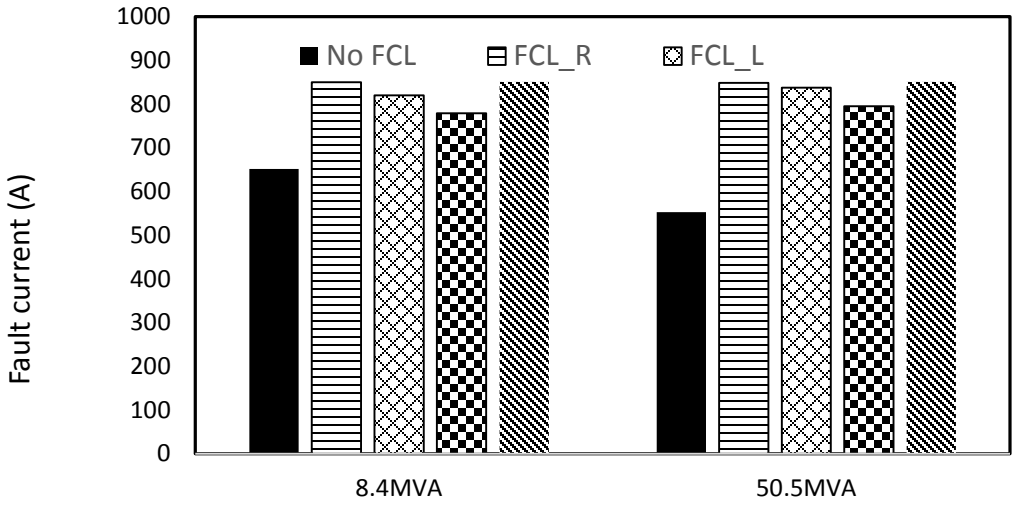

Figure 4.39: Summary of recloser short circuit currents with an 8.4 MVA and 50.5 MVA synchronous machine based DG source integrated at bus 1 in the suburban distribution system with a line to line fault applied at the bus 5 load with FCL presence.

Observation of Figures 4.37 and 4.38 in conjunction with Figure 4.39 makes it apparent that each FCL type is successfully able to mitigate synchronous machine based DG influences for increasing levels of penetration. In the case of the 50.5 MVA DG source, the discrepancy between the original suburban distribution system short circuit behavior and the DG integrated network improves from 35% to 0.3%, 1.5% and 6.5% for the resistive, inductive and resonant FCL types respectively. It should also be noted that no synchronous machine based DG penetration level was found that caused loss of fuse-recloser coordination.

4.4.4 Bus 5 DG Connection

The case study presented in Section 3.3.2.4 demonstrates the effect of synchronous machine based DG integration at bus 5 on recloser sensitivity for the suburban distribution system. An 8.4 MVA and 48.8 MVA synchronous machine based DG source is connected at bus 5 (each connected for separate tests) with each of the FCL types as depicted in Figure 4.21. A line to line fault is applied to the bus 5 load. The time-domain short circuit currents experienced by the head end-recloser for each DG size and FCL type is presented in Figures 4.40 and 4.41, with a summary presented in Figure 4.42.

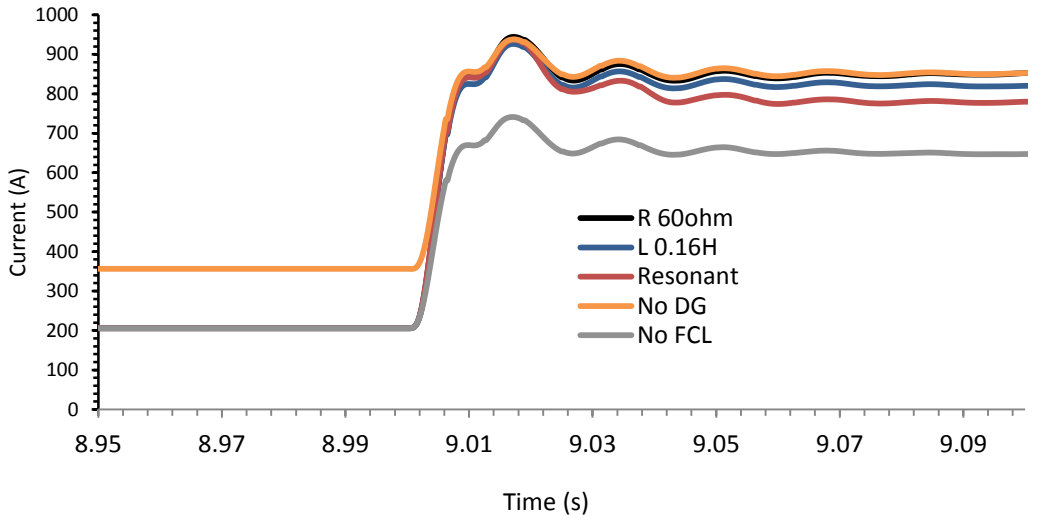

Figure 4.40: Time-domain recloser RMS current simulation for a line to line fault applied at the bus 5 load with an 8.4 MVA synchronous machine based DG source integrated at bus 5 with FCL presence.

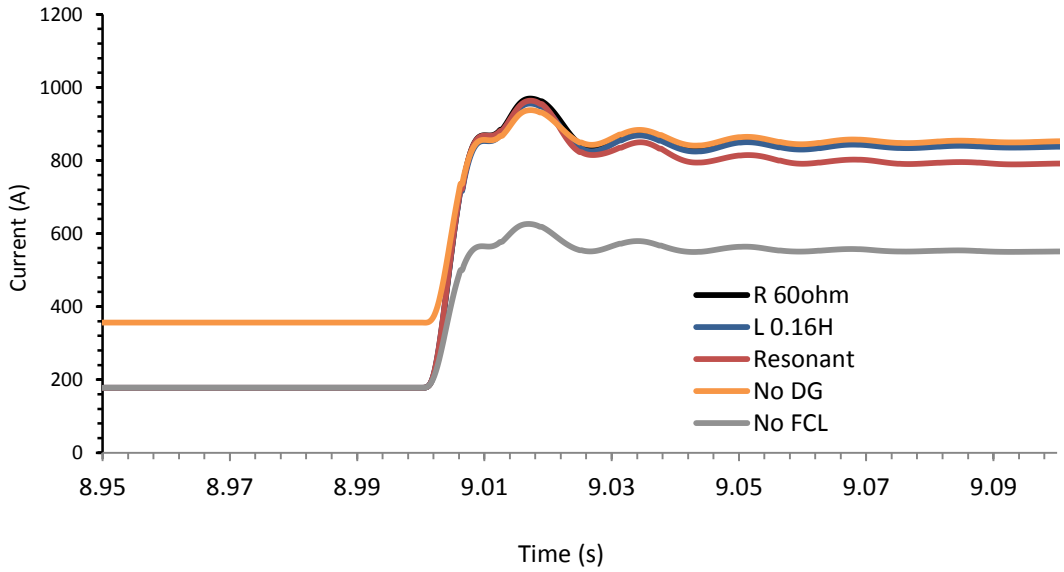

Figure 4.41: Time-domain recloser RMS current simulation for a line to line fault applied at the bus 5 load with a 48.8 MVA synchronous machine based DG source integrated at bus 5 with FCL presence.

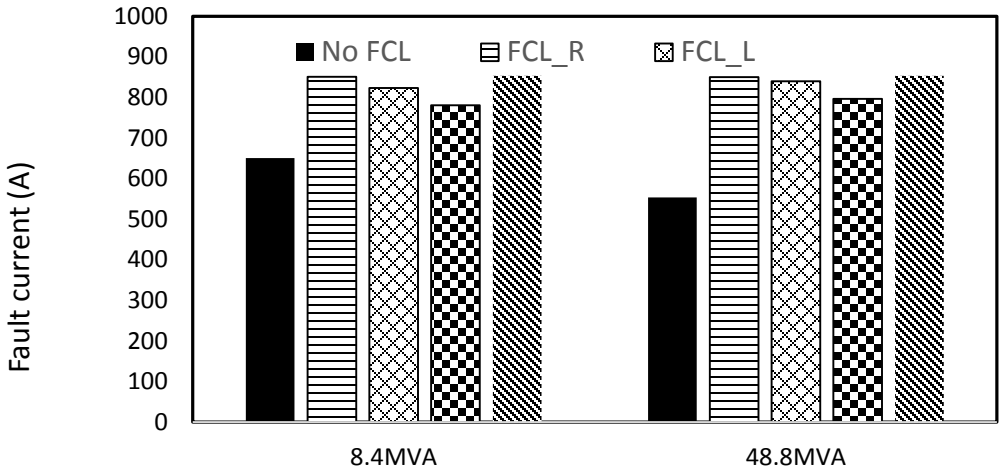

Figure 4.42: Summary of recloser short circuit currents with an 8.4 MVA and 48.8 MVA synchronous machine based DG source integrated at bus 5 in the suburban distribution system with a line to line fault applied at the bus 5 load with FCL presence.

Observation of Figures 4.40 and 4.41 in conjunction with Figure 4.42 makes it apparent that each FCL type is successfully able to mitigate synchronous machine based DG influences for increasing levels of penetration. In the case of the 48.8 MVA DG source, the discrepancy between the original suburban distribution system short circuit behavior and the DG integrated network improves from 35% to 0.4%, 1.6% and 6.6% for the resistive, inductive and resonant FCL type respectively. It should also be noted that no synchronous machine based DG penetration level was found that caused loss of fuse-recloser coordination.

4.4.5 DG Connection Summary

Observation of results obtained in Section 4.4 makes it apparent that the utilization of superconducting FCLs of resistive, inductive and resonant types are effective at mitigation of synchronous machine based DG influences on existing system recloser protection sensitivity, even at DG penetration levels as high as 300% load demand. Resistive type FCL's are consistently effective with discrepancies between non-DG and FCL DG integrated short circuit characteristics being limited to less than 1% for each connection point. Furthermore, it is apparent that the resonant and inductive type FCLs become less effective for DG connections closer to the fault location, however, they are still able to restore recloser sensitivity at high penetration levels.

4.5 The use of FCLs for the Mitigation of Synchronous Machine Based DG Influences on Recloser Bi-Directionality

As demonstrated in Section 3.4, for the suburban distribution system given in Figure 2.1, the lowest level of synchronous machine based DG penetration required for bi-directional recloser behavior occurs for a line to line to ground fault on an adjacent feeder. For bi-directional current to cause main feeder recloser nuisance tripping, the short circuit level experienced by the recloser needs to exceed 624 A for the grounded fault condition. In order to determine the effectiveness of each type of FCL in mitigating the effect of synchronous machine based DG sources on existing system recloser bi-directionality, the algorithm presented in Figure 3.20 is utilized.

4.5.1 Bus 1 DG Connection

The case study presented in Section 3.4.2.1 demonstrates the effect of synchronous machine based DG integration at bus 1 on recloser bi-directionality for the suburban distribution system. 4.7 MVA and 8.4 MVA synchronous machine based DG sources are connected at bus 1 (each connected for separate tests) with each of the FCL types as depicted in Figure 4.2. A line to line to ground fault is applied to the double load feeder specified in Section 3.4.2.1. The time-domain short circuit currents experienced by the head end-recloser for each DG size and FCL type is presented in Figures 4.43 and 4.44 with a summary presented in Figure 4.45.

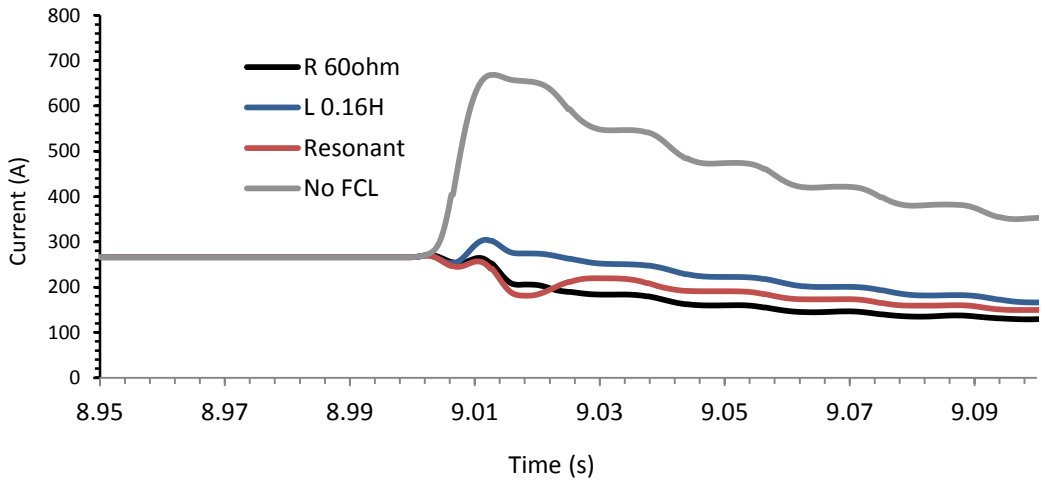

Figure 4.43: Time-domain recloser RMS current simulation for a line to line to ground fault applied at the double load adjacent feeder with a 4.7 MVA synchronous machine based DG source integrated at bus 1 with FCL presence.

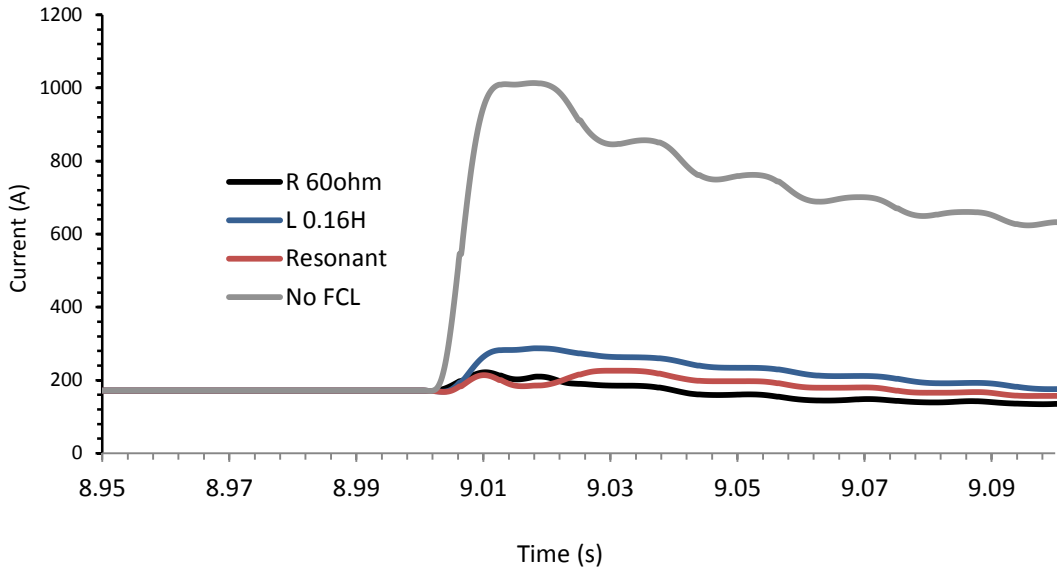

Figure 4.44: Time-domain recloser RMS current simulation for a line to line to ground fault applied at the double load adjacent feeder with a 8.4 MVA synchronous machine based DG source integrated at bus 1 with FCL presence.

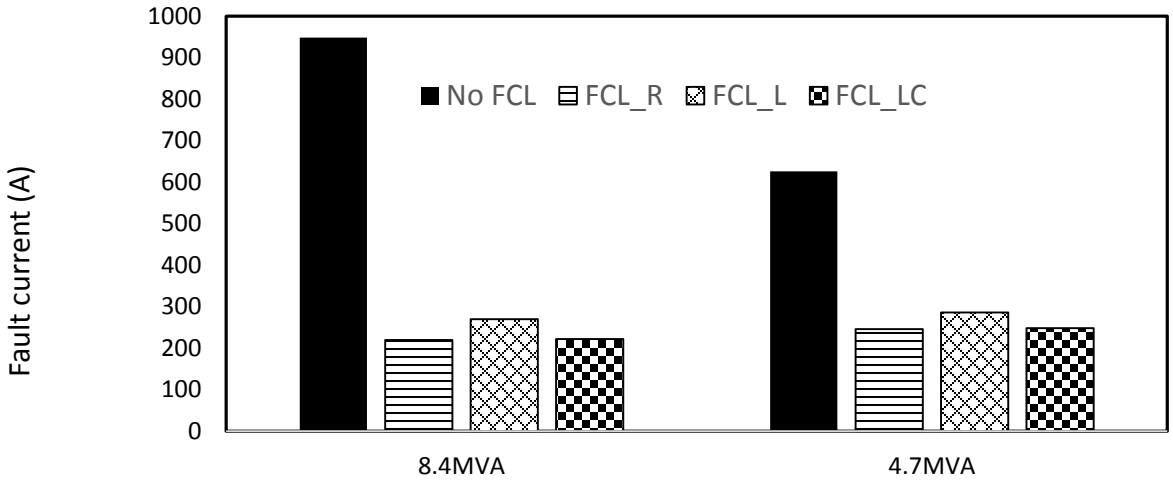

Figure 4.45: Summary of recloser short circuit currents with a 4.7 MVA and 8.4 MVA synchronous machine based DG source integrated at bus 1 in the suburban distribution system with a line to line to ground fault applied at double load adjacent feeder with FCL presence.

Observation of Figures 4.43 and 4.44 in conjunction with Figure 4.45 makes it apparent that each FCL type is successfully able to mitigate synchronous machine based DG influences for increasing levels of penetration. In the case of the 8.4 MVA DG source, for a line to line to ground fault (in this case the most severe type of ground fault), each FCL type reduces the short circuit current experienced by the main feeder head end recloser to below the 624 A nuisance trip criteria and below the ground pick up setting. Subsequently, it will not operate for a parallel feeder fault. Furthermore, it is apparent that the resistive type FCL is the most effective at limiting the short circuit contribution of a synchronous machine based DG source to a parallel feeder fault. It should also be noted that no synchronous machine based DG penetration level was found that caused loss of fuse-recloser coordination. Note that the parallel feeder fault current exceeded 30 kA.

As mentioned in Section 4.4.1, in commercial applications there are a wide variety of resistive and inductive type FCLs of varying magnitude of resistances and inductances. In order to reflect results consistent with varying resistive values, the resistive and inductive type FCLs in the system presented in Figure 4.2 are varied in magnitude. Figures 4.46, 4.47 and 4.48 show the time domain simulations and Figures 4.49 and 4.50 show a summary for each FCL type for a line to line to ground fault at the double load adjacent feeder for the 4.7 MVA and 8.4 MVA synchronous machine based DG integrated distribution system with the R and L type FCL's values being varied between 20 Ω - 60 Ω and 0.05 H - 0.16 H respectively.

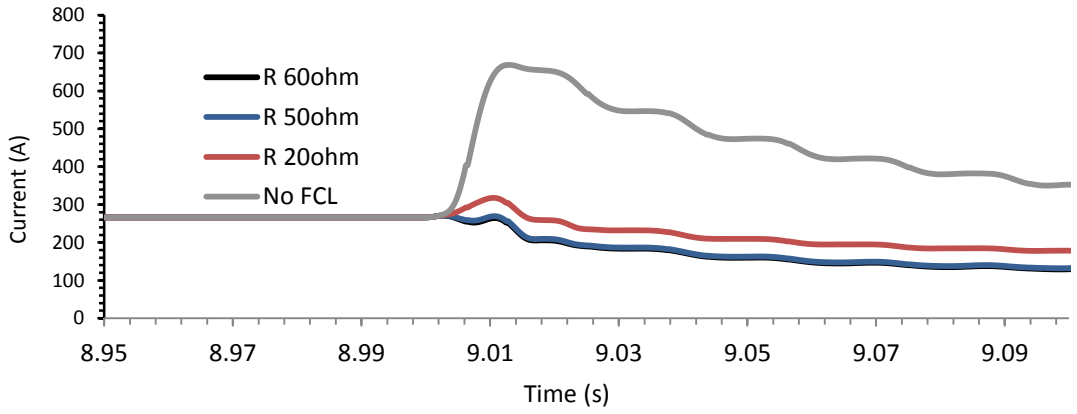

Figure 4.46: Time-domain recloser RMS current simulation for a line to line to ground fault applied at the double load adjacent feeder with a 4.7 MVA synchronous machine based DG source integrated at bus 1 with varying resistive FCL impedance.

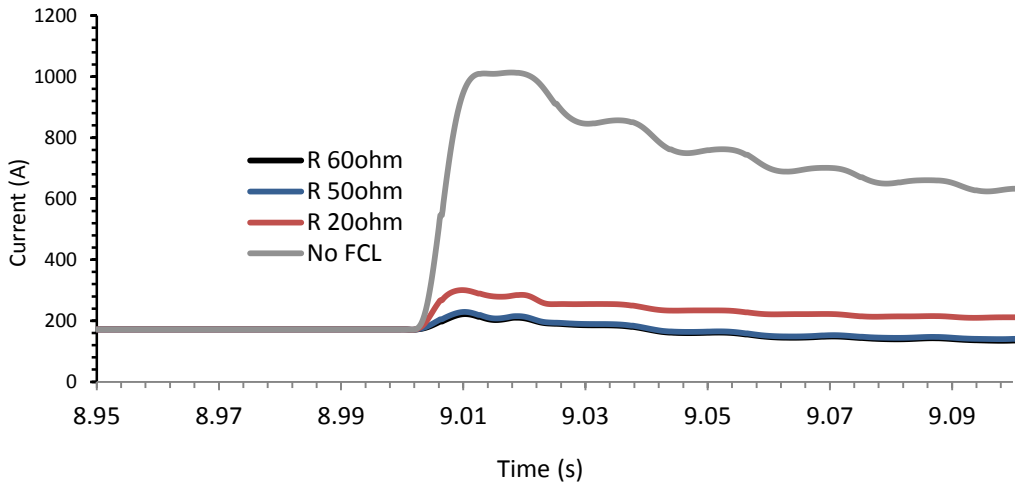

Figure 4.47: Time-domain recloser RMS current simulation for a line to line to ground fault applied at the double load adjacent feeder with a 8.4 MVA synchronous machine based DG source integrated at bus 1 with varying resistive FCL impedance.

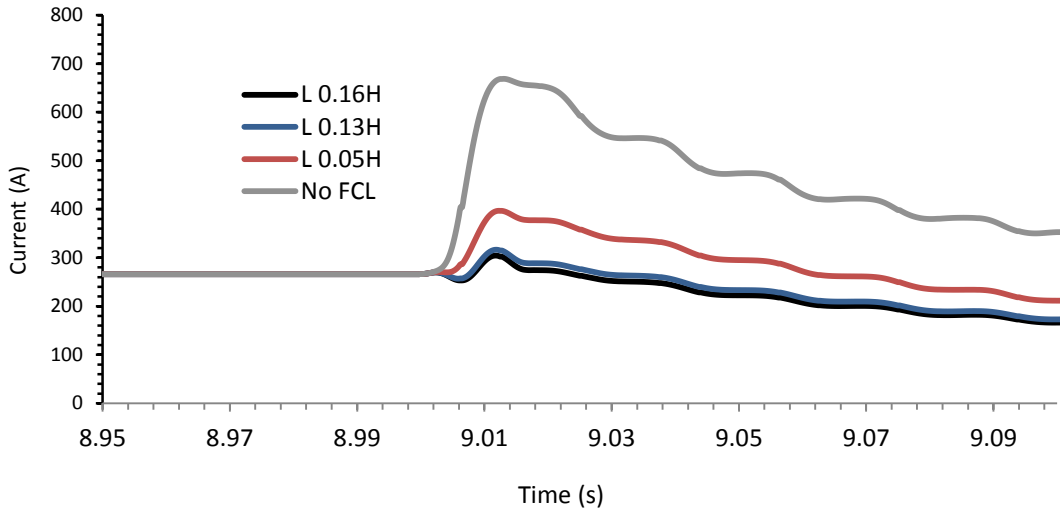

Figure 4.48: Time-domain recloser RMS current simulation for a line to line to ground fault applied at the double load adjacent feeder with a 4.7 MVA synchronous machine based DG source integrated at bus 1 with varying inductive FCL impedance.

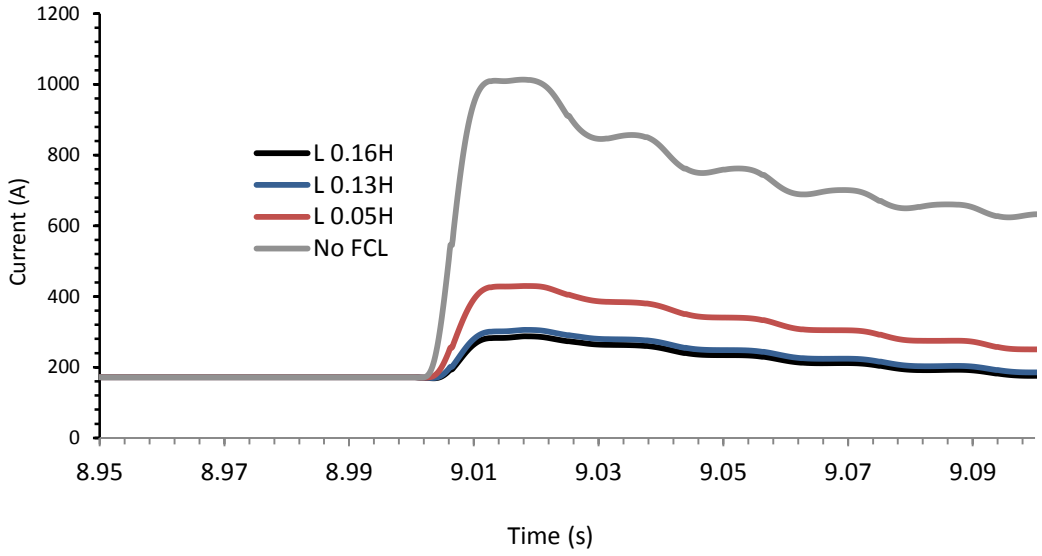

Figure 4.49: Time-domain recloser RMS current simulation for a line to line to ground fault applied at the double load adjacent feeder with a 8.4 MVA synchronous machine based DG source integrated at bus 1 with varying inductive FCL impedance.

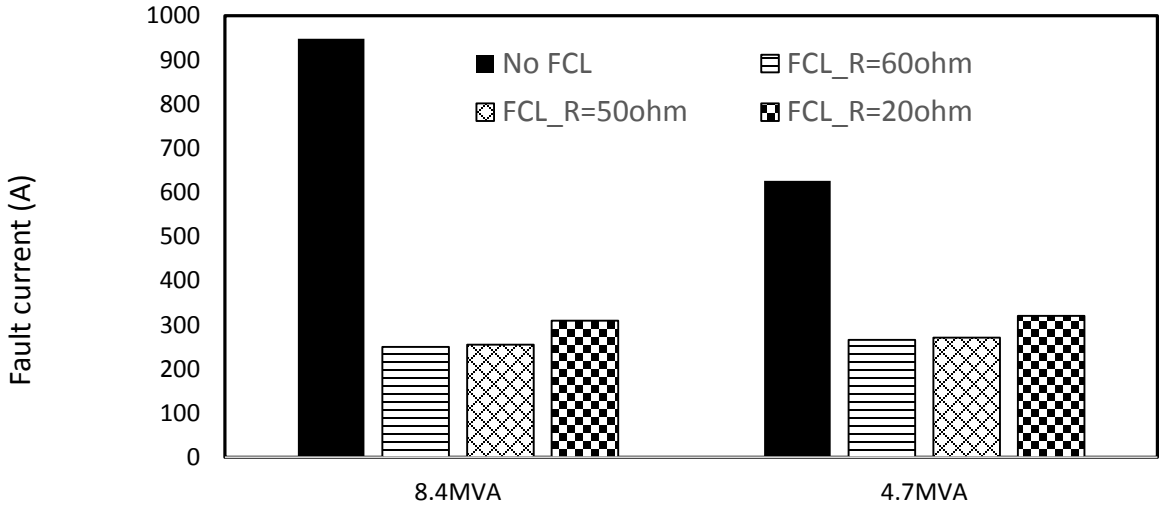

Figure 4.50: Summary of recloser short circuit currents with a 4.7 MVA and 8.4 MVA synchronous machine based DG source integrated at bus 1 in the suburban distribution system with a line to line to ground fault applied at double load adjacent feeder with varying resistive FCL impedance.

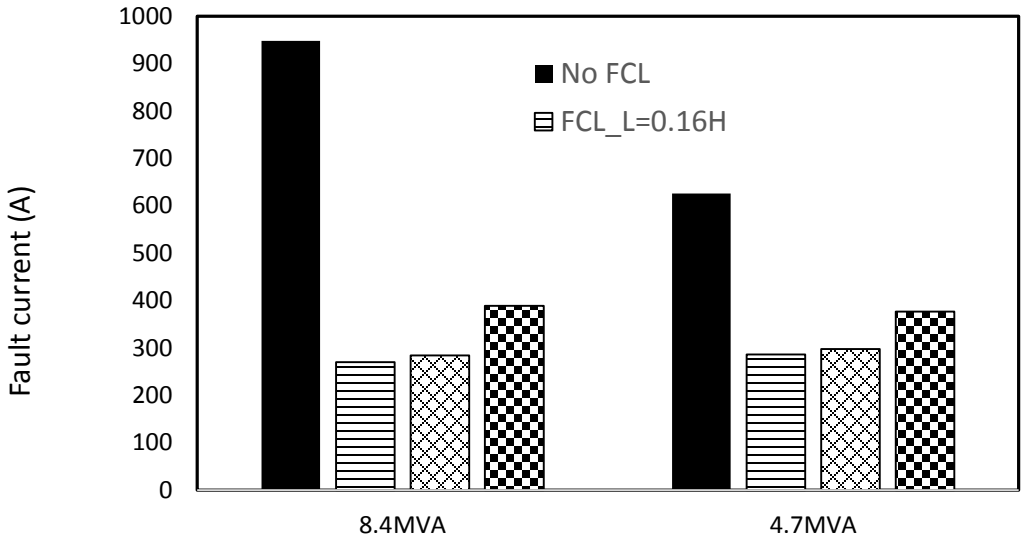

Figure 4.51: Summary of recloser short circuit currents with a 4.7 MVA and 8.4 MVA synchronous machine based DG source integrated at bus 1 in the suburban distribution system with a line to line to ground fault applied at double load adjacent feeder with varying inductive FCL impedance.

Observation of Figure 4.50 in conjunction with Figure 4.51 confirms the hypothesis presented in Section 4.4.1 as it is apparent that lowering the impedance of the resistive and inductive FCL is detrimental in the effectiveness of the FCL in mitigation of synchronous machine based DG influences on recloser bi-directionality. In both cases, for lower impedance values the short circuit current contribution from the synchronous machine based DG source increased to levels where the recloser was able to detect the fault condition.

4.5.2 Bus 2 DG Connection

The case study presented in Section 3.4.2.2 demonstrates the effect of synchronous machine based DG integration at bus 2 on recloser bi-directionality for the suburban distribution system. A 5 MVA and 8.4 MVA synchronous machine based DG source is connected at bus 2 (each connected for separate tests) with each of the FCL types as depicted in Figure 4.13. A line to line to ground fault is applied to the double load feeder specified in Section 3.4.2.2. The time-domain short circuit currents experienced by the head end-recloser for each DG size and FCL type is presented in Figures 4.53 and 4.54 with a summary presented in Figure 4.55.

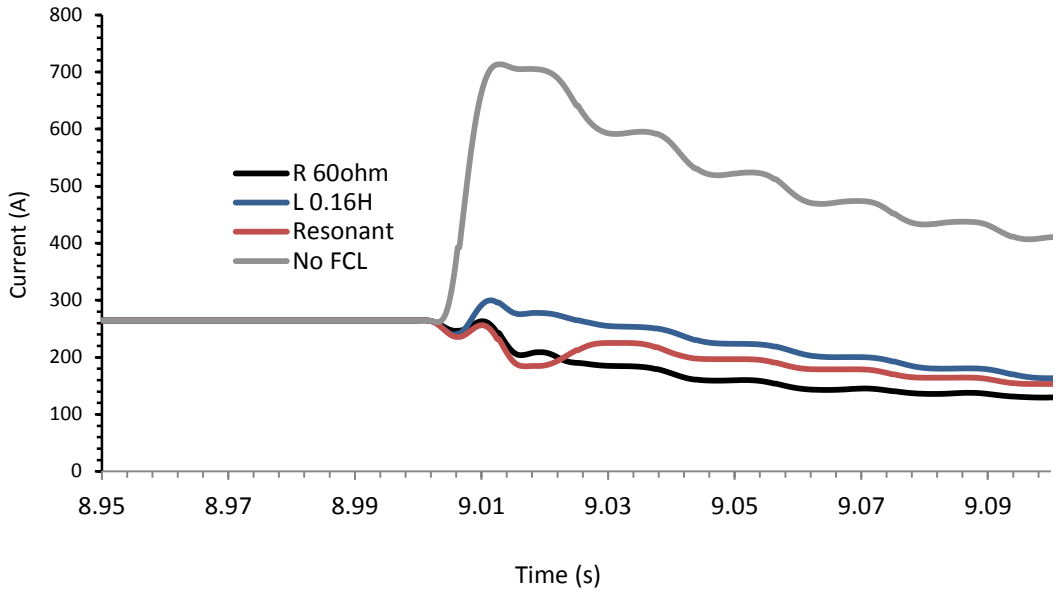

Figure 4.52: Time-domain recloser RMS current simulation for a line to line to ground fault applied at the double load adjacent feeder with a 5 MVA synchronous machine based DG source integrated at bus 2 with FCL presence.

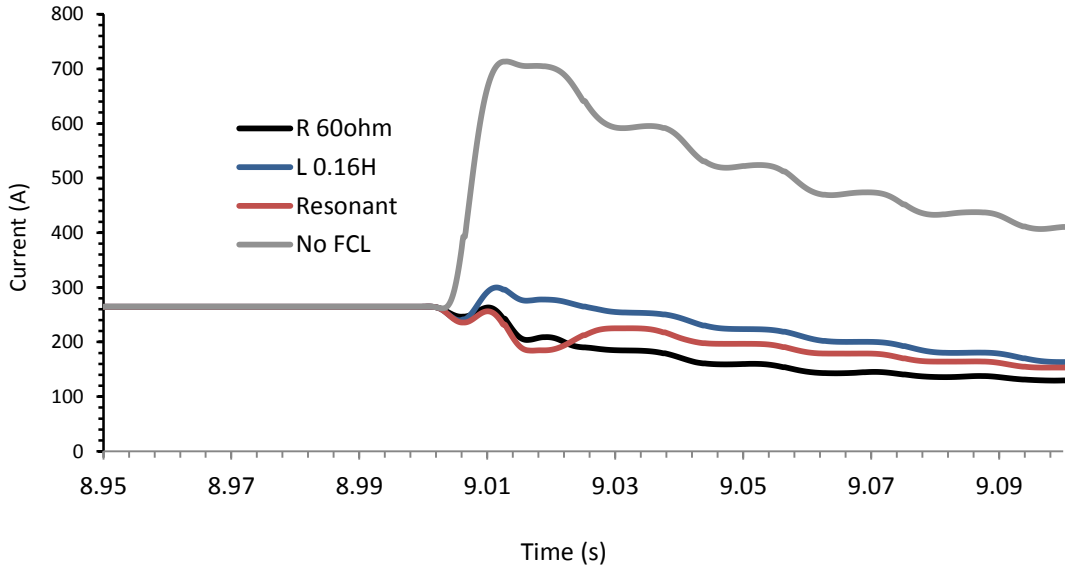

Figure 4.53: Time-domain recloser RMS current simulation for a line to line to ground fault applied at the double load adjacent feeder with a 5 MVA synchronous machine based DG source integrated at bus 2 with FCL presence.

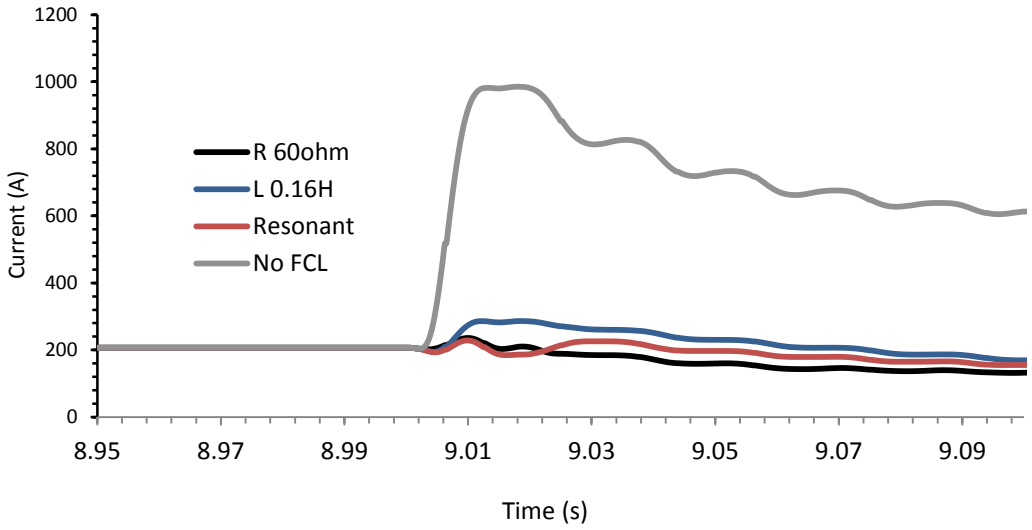

Figure 4.54: Time-domain recloser RMS current simulation for a line to line to ground fault applied at the double load adjacent feeder with a 8.4 MVA synchronous machine based DG source integrated at bus 2 with FCL presence.

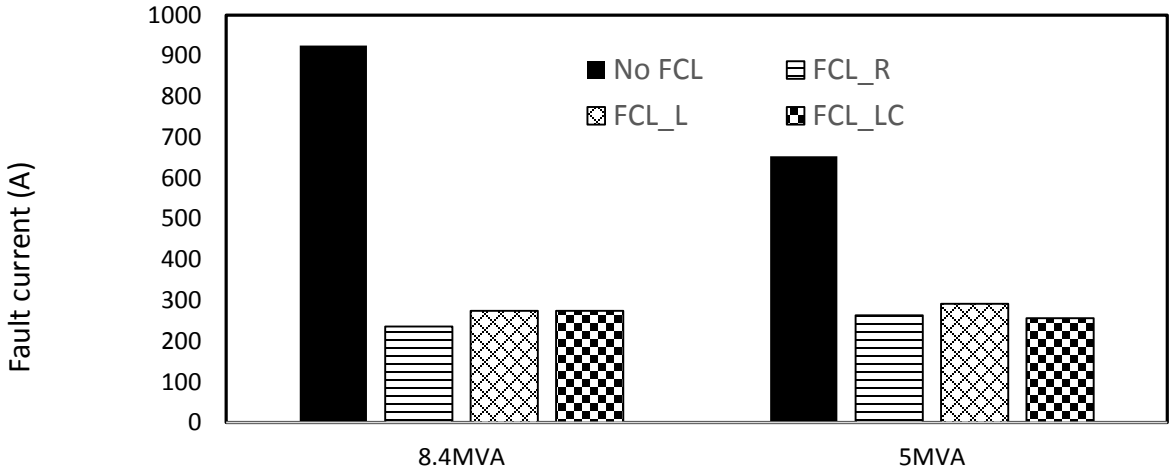

Figure 4.55: Summary of recloser short circuit currents with a 5 MVA and 8.4 MVA synchronous machine based DG source integrated at bus 2 in the suburban distribution system with a line to line to ground fault applied at double load adjacent feeder with FCL presence.

Observation of Figures 4.53 and 4.54 in conjunction with Figure 4.55 makes it apparent that each FCL type is successfully able to mitigate synchronous machine based DG influences for increasing levels of penetration. In the case of the 8.4 MVA DG source, for a line to line to ground fault (in this case the most severe type of ground fault), each FCL type reduces the short circuit current experienced by the main feeder head end recloser to below the 624 A nuisance trip criteria and below the ground pick up setting. Subsequently, it will not operate for a parallel feeder fault. Furthermore, it is apparent that the resistive type FCL is the most effective at limiting the short circuit contribution of a synchronous machine based DG source to a parallel feeder fault. It should also be noted that no synchronous machine based DG penetration level was found that caused loss of fuse-recloser coordination. Note that the parallel feeder fault current exceeded 30 kA.

4.5.3 Bus 4 DG Connection

The case study presented in Section 3.4.2.3 demonstrates the effect of synchronous machine based DG integration at bus 4 on recloser bi-directionality for the suburban distribution system. A 5.5 MVA and 8.4 MVA synchronous machine based DG source was connected at bus 4 (each connected for separate tests) with each of the FCL types as depicted in Figure 4.17. A line to line to ground fault is applied to the double load feeder specified in Section 3.4.2.3. The time-domain short circuit currents experienced by the head end-recloser for each DG size and FCL type is presented in Figures 4.56 and 4.57 with a summary presented in Figure 4.58.

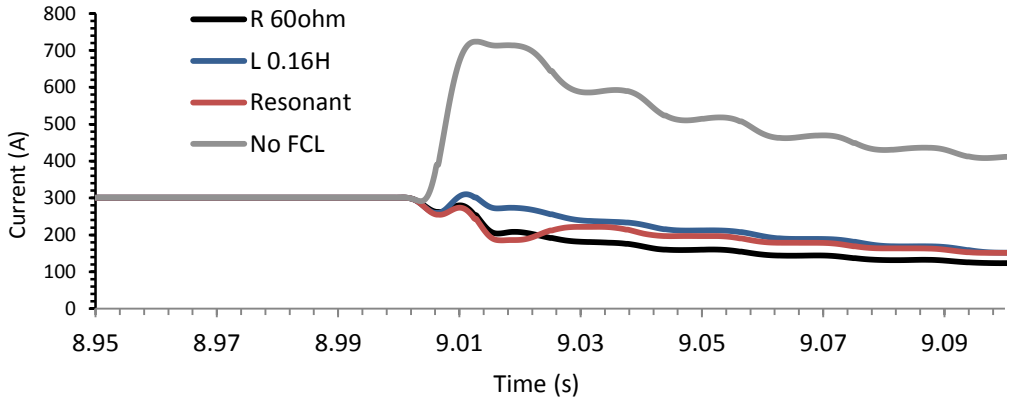

Figure 4.56: Time-domain recloser RMS current simulation for a line to line to ground fault applied at the double load adjacent feeder with a 5.5 MVA synchronous machine based DG source integrated at bus 4 with FCL presence.

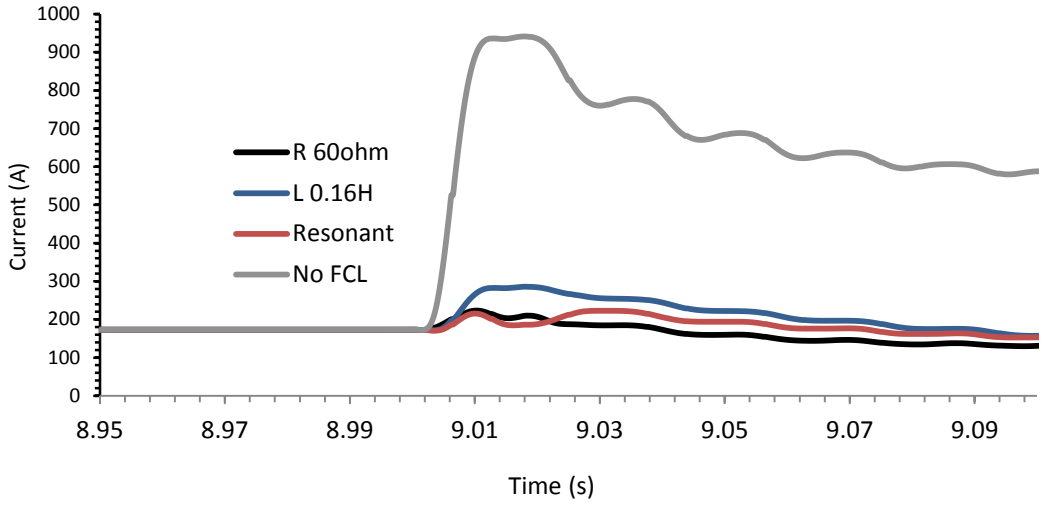

Figure 4.57: Time-domain recloser RMS current simulation for a line to line to ground fault applied at the double load adjacent feeder with a 8.4 MVA synchronous machine based DG source integrated at bus 4 with FCL presence.

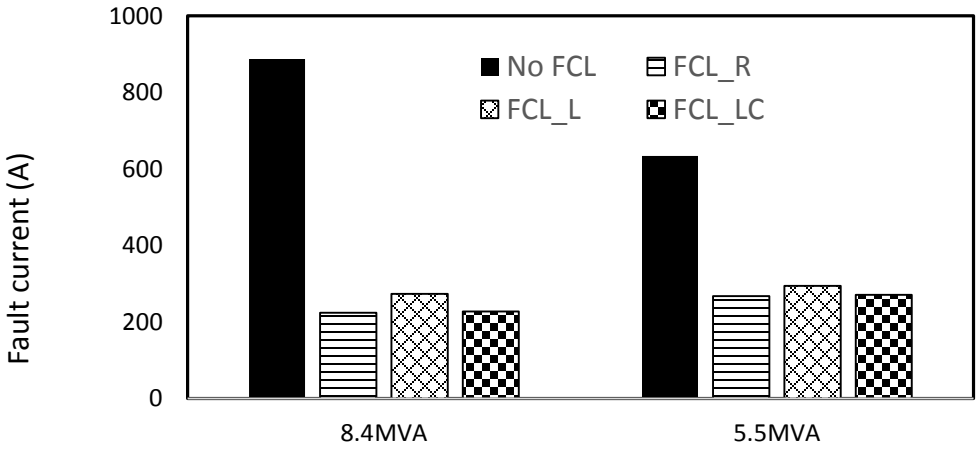

Figure 4.58: Summary of recloser short circuit currents with a 5.5 MVA and 8.4 MVA synchronous machine based DG source integrated at bus 4 in the suburban distribution system with a line to line to ground fault applied at double load adjacent feeder with FCL presence.

Observation of Figures 4.56 and 4.57 in conjunction with Figure 4.58 makes it apparent that each FCL type is successfully able to mitigate synchronous machine based DG influences for increasing levels of penetration. In the case of the 8.4 MVA DG source, for a line to line to ground fault (in this case the most severe type of ground fault), each FCL type reduces the short circuit

current experienced by the main feeder head end recloser to below the 624 A nuisance trip criteria and below the ground pick up setting. Subsequently, it will not operate for a parallel feeder fault. Furthermore, it is apparent that the resistive type FCL is the most effective at limiting the short circuit contribution of a synchronous machine based DG source to a parallel feeder fault. It should also be noted that no synchronous machine based DG penetration level was found that caused loss of fuse-recloser coordination. Note that the parallel feeder fault current exceeded 30 kA.

4.5.4 Bus 5 DG Connection

The case study presented in Section 3.4.2.4 demonstrates the effect of synchronous machine based DG integration at bus 5 on recloser bi-directionality for the suburban distribution system. A 5.8 MVA and 8.4 MVA synchronous machine based DG source is connected at bus 5 (each connected for separate tests) with each of the FCL types as depicted in Figure 4.21. A line to line to ground fault is applied to the double load feeder specified in Section 3.4.2.4. The time-domain short circuit currents experienced by the head end-recloser for each DG size and FCL type is presented in Figures 4.59 and 4.60 with a summary presented in Figure 4.61.

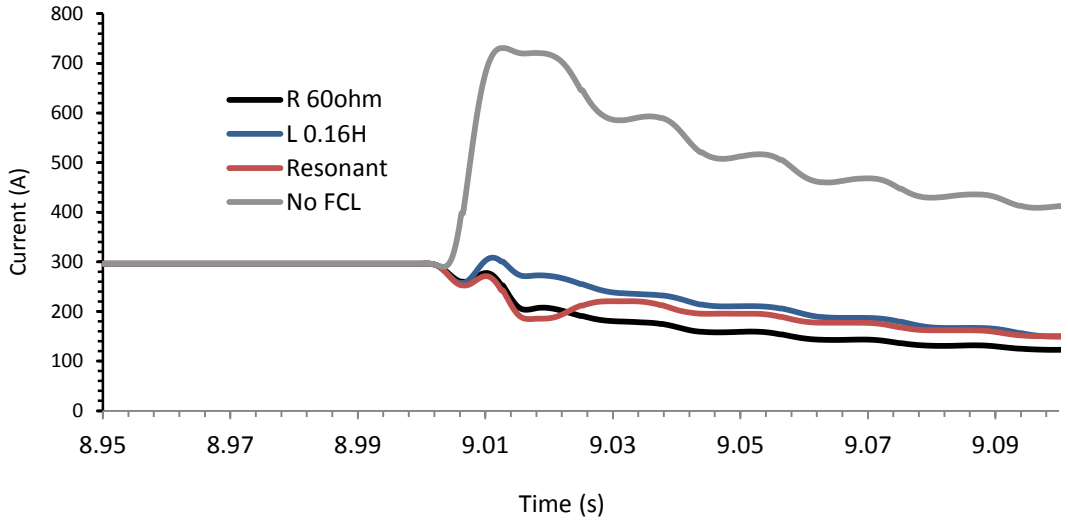

Figure 4.59: Time-domain recloser RMS current simulation for a line to line to ground fault applied at the double load adjacent feeder with a 5.8 MVA synchronous machine based DG source integrated at bus 5 with FCL presence.

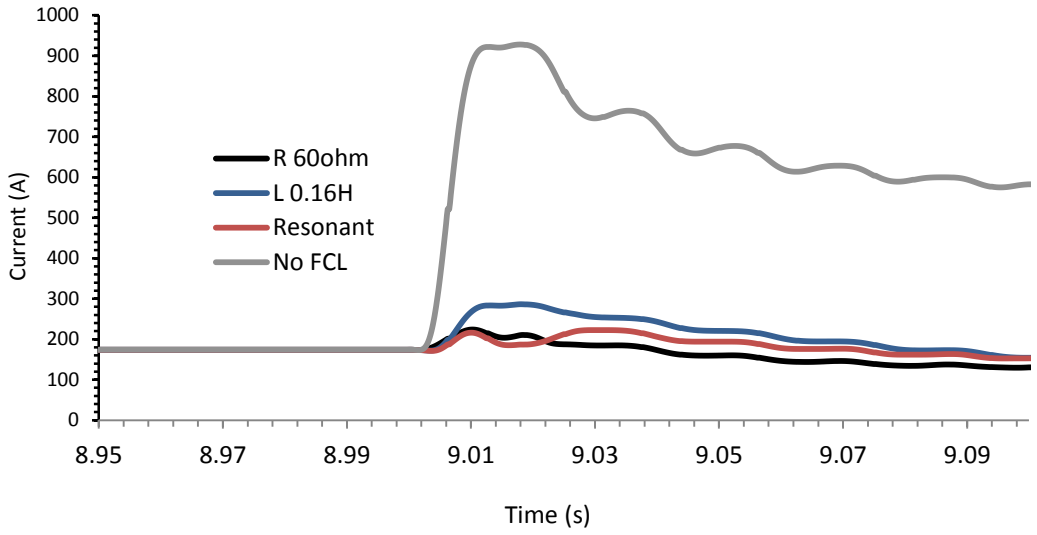

Figure 4.60: Time-domain recloser RMS current simulation for a line to line to ground fault applied at the double load adjacent feeder with a 8.4 MVA synchronous machine based DG source integrated at bus 5 with FCL presence.

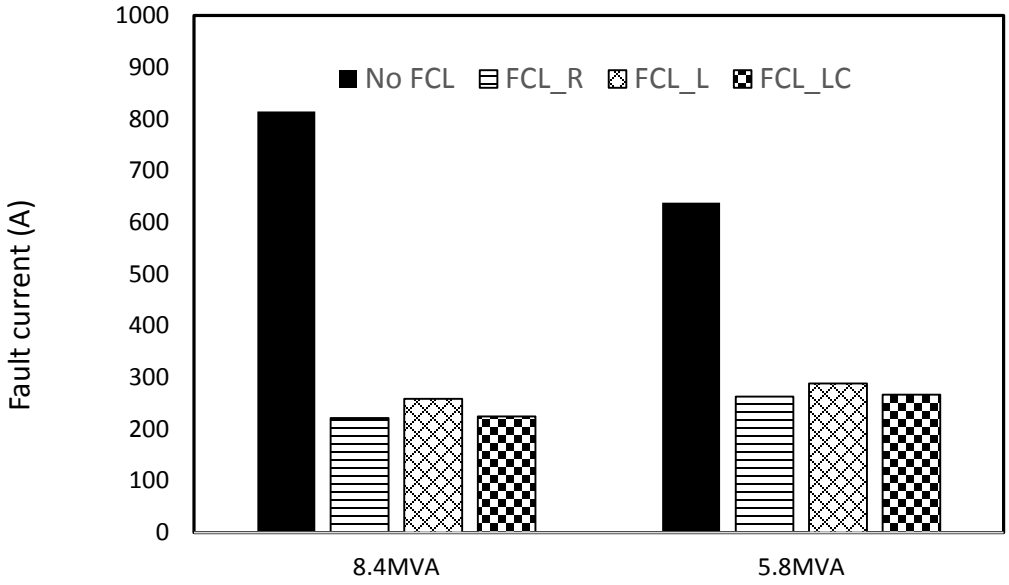

Figure 4.61: Summary of recloser short circuit currents with a 5.8 MVA and 8.4 MVA synchronous machine based DG source integrated at bus 5 in the suburban distribution system with a line to line to ground fault applied at double load adjacent feeder with FCL presence.

Observation of Figures 4.59 and 4.60 in conjunction with Figure 4.61 makes it apparent that each FCL type is successfully able to mitigate synchronous machine based DG influences for increasing levels of penetration. In the case of the 8.4 MVA DG source, for a line to line to ground fault (in this case the most severe type of ground fault), each FCL type reduces the short circuit current experienced by the main feeder head end recloser to below the 624 A nuisance trip criteria and below the ground pick up setting. Subsequently, it will not operate for a parallel feeder fault. Furthermore, it is apparent that the resistive type FCL is the most effective at limiting the short circuit contribution of a synchronous machine based DG source to a parallel feeder fault. It should also be noted that no synchronous machine based DG penetration level was found that caused loss of fuse-recloser coordination. Note that the parallel feeder fault current exceeded 30 kA.

4.5.5 DG Connection Summary

Observation of results obtained in Section 4.5 makes it apparent that the utilization of superconducting FCLs of resistive, inductive and resonant types are effective at mitigation of synchronous machine based DG influences on existing system recloser bi-directionality for faults on adjacent feeders. The resistive type FCL is consistently more effective with the recloser short circuit current consistently being further below the pickup setting than the inductive and resonant type FCL. Furthermore, it is apparent that the resonant type FCL is more efficient than the inductive type in the context of bi-directionality.

4.6 Summary

Chapter 4 has demonstrated the effectiveness of the use of resistive, inductive and resonant type FCLs in the mitigation of synchronous machine based DG source influences on fuse-recloser protection. Detailed digital time-domain simulations and explanations into the effects FCL use in synchronous machine based DG integration in the suburban distribution system for varying connection points are presented. Results obtained demonstrate that FCLs are useful in the context of mitigation of DG influences on protection, with the resistive type being consistently most effective.

5. SUMMARY AND CONCLUSIONS

5.1 Critical Analysis of Results

Comparison of results obtained in Chapter 4 makes it apparent that the proposed use of FCLs in mitigating synchronous machine based DG effects during fault conditions is plausible. As demonstrated in Sections 3.2 and 3.4, when no FCL is integrated at the DG connection point, there is a low synchronous machine based DG source penetration requirement before adverse effects on the suburban distribution system's short circuit characteristics results in violation of existing protection infrastructure settings. This level of penetration is mainly related to the loading demands of the main feeders in distribution networks whereby a higher load draws a higher current. The higher the load the more DG penetration is able to be introduced without adversely affecting the protection settings [34]. Further analysis of results obtained in Chapter 3 demonstrate that adverse effects are first observable in fuse-recloser coordination for synchronous machine based DG penetration levels as low as 24% of the load demand.

Observation of results obtained in Sections 4.2 to 4.5 makes it apparent that FCL use at the connection point of synchronous machine based DG sources is effective in mitigation of DG influences on system short circuit characteristics and consequently existing protective infrastructure schemes and settings. As demonstrated in Section 4.2, the introduction of FCL technology into the 52% load demand synchronous machine based DG penetrated suburban distribution system can improve the DG influence on short circuit characteristics from 1% to less than 1% in each FCL case. Furthermore it can be seen that the mitigation capability in the case of the inductive and resonant type FCL reduces relative to distance between DG interconnection and fault location.

Analysis of results obtained in Section 4.3 in conjunction with those in Section 4.2 makes it apparent that resistive, inductive and resonant type FCLs can reduce synchronous machine based DG influences on fuse-recloser coordination. In the case of the resistive type FCL, the short circuit and fuse-recloser operating characteristic of the DG integrated suburban distribution system returns to within 1% of the non-DG connected network. For other FCL types, the short circuit and fuse-recloser operating characteristic returns to within 1.5% and 2.2% of the non-DG connected network for the inductive and resonant type respectively, although coordination is still restored.

As demonstrated in Section 4.4, the introduction of synchronous machine based DG sources can results in recloser inability to detect faulted conditions. The introduction of resistive, inductive and resonant type FCLs for penetration levels of above 300% can result in the mitigation of DG effects from 35% to less than 1%, 1.6% and 6.6% for each type respectively, when compared to original short circuit currents experienced by the suburban distribution system head end recloser.

Examination of results presented in Section 4.5 highlight the efficient use of resistive, inductive and resonant FCL types in the mitigation of synchronous machine based DG source influences on short circuit characteristics following parallel feeder faults in radial distribution networks. As discussed, in regular radial distribution networks, when a fault occurs on an adjacent feeder, the short circuit current experienced by the main feeder head end recloser is zero. The introduction of synchronous machine based DG infrastructure results in short circuit current contribution to adjacent feeder faults consequently allowing possible nuisance tripping of the main feeder recloser. Although the introduction of the resistive, inductive and resonant type FCLs does not reduce the short circuit contribution by the DG source to zero, it does mitigate the influences. Results obtained in Section 4.5 highlight that for a line to line to ground fault, the parallel feeder experiences a short circuit current in excess of 30 kA. In the worst case scenario, the head end recloser of the main feeder experiences 300 A, 52% below the required 624 A nuisance trip requirement. Additionally, the influence on the adjacent feeder fault characteristic is less than 1% for each FCL type. Consequently the influence of the main feeder synchronous machine based DG source on a parallel feeder's short circuit characteristic is negligible, ensuring existing protection infrastructure characteristic adequacy.

Comparison of results obtained in Sections 4.2.1, 4.3.1, 4.4.1 and 4.5.1 makes it apparent that increasing the impedance of a superconducting FCL yields a higher efficiency mitigation capability of synchronous machine based DG integration influences on radial system short circuit characteristics. In the case of both the resistive and inductive type FCL's, comparison demonstrates that increasing the resistive state impedance yields stronger similarities in short circuit levels when compared to the original non DG integrated systems.

Furthermore comparison and analysis of results obtained in Chapter 3 and 4 demonstrate that the introduction of FCL's on the DG side of the interconnecting transformer of a synchronous

machine based DG source can drastically change the effect that DG integration can impose on existing system short circuit characteristics. The use of the algorithms presented in Chapter 3 are also useful in the determination of synchronous machine base DG penetration level requirements before mitigation effects of FCL technology is required.

Pricing and economic concerns are key factors affecting the practicality of introducing the proposed approach into the market. Engineers should consider the comparative cost of re-evaluating the existing protection settings or the cost of purchasing, maintaining, and installing FCLs.

Practical applications of the proposed approach are in regions that have an expanding population size which requires network expansion to meet increases in power demand from an expanding consumer base, increasing the strain on generating units. This increased demand is likely to lead to faster fatigue of existing generation sources, decreasing system supply security and highlighting the need for DG sources.

Given the results obtained it is apparent that implementation of the proposed methods in Chapter 3 and 4 will be dependent on economic considerations and forward network planning.

5.2 Summary

Due to the growing complexity of modern utility grids and increasing consumer energy demand, power utilities worldwide are seeking methods of increasing generation capacities. One low capital outlay method of increasing this capacity is presented in this research through the inclusion of small synchronous machine based generators on the distribution side of the grid to meet local power demands. The resultant increased capacity yields improvement in distribution system voltage profile, reliability and generation capability however, it also has detrimental effects on existing operational characteristics and network design.

The main objective of this research is to determine the efficiency in the use of resistive, inductive and resonant superconducting FCLs for mitigation of synchronous machine based DG source influences on radial distribution system short circuit characteristics and its consequential effect on fuse-recloser coordination, recloser sensitivity, and recloser bi-directionality during fault

conditions. In this context, the effectiveness of the proposed FCL approach at the DG side of the interconnection transformer is scrutinized and investigated through comprehensive time-domain studies on the suburban distribution system so as to prevent DG source disconnection requirements as per IEEE Std. 1547 or redesign of coordination schemes to restore protective design adequacy.

In Chapter 2, the system under study is introduced along with the details associated with the modelling of individual components. A sample case study is also presented in this chapter.

Chapter 3 outlines the approach taken for DG impact assessment on fuse-recloser loss of coordination, recloser loss of sensitivity and recloser bi-directionality. Case studies are also presented for each problem.

Chapter 4 presents results in the validation of the use of FCLs in mitigating the effects of synchronous machine based DG integration on distribution networks during fault conditions. A critical analysis of results is also presented in this chapter.

5.3 Conclusions

Studies in this thesis yield the following conclusions for the suburban distribution system:

1. Synchronous machine based DG sources have the capacity to adversely affect existing radial power system short circuit characteristics based on both size relative to load demand and location.
2. The consequential effects on short circuit characteristic yield deterioration of existing fuse-recloser coordination often resulting in invalidation of fuse-saving schemes.
3. Malfunction and inability of head end reclosers in detection of downstream faults with upstream synchronous machine based DG source connection is yielded consequentially to increasing levels of DG penetration.
4. Increased synchronous machine based DG source penetration has detrimental effects on unidirectional power flow characteristics which can consequentially result in recloser nuisance tripping for adjacent feeder faults in the same system.
5. Algorithms are presented for the assessment of synchronous machine based DG influences on radial distribution networks on fuse-recloser coordination, recloser sensitivity and recloser bi-directionality.

6. The introduction of resistive, inductive and resonant type FCLs is effective in the mitigation of synchronous machine based DG influences on system short circuit characteristics.
7. Consequentially, utilization of each FCL results in restoration of existing protection infrastructure adequacy.
8. Reduction in resistive and inductive FCL impedances yields lower efficiencies in mitigation characteristics.
9. The resistive type FCL consistently mitigates the effect of synchronous machine based DG influences on short circuit and consequentially protection infrastructure characteristics to within 1% of original system designs outperforming other FCL types at penetration levels ranging from 23% to 343% of load demands.
10. The inductive type FCL consistently mitigates the effect of synchronous machine based DG influences on short circuit and consequentially protection infrastructure characteristics to within 2% of original system designs at penetration levels ranging from 23% to 343% of load demands.
11. The resonant type FCL consistently mitigates the effect of synchronous machine based DG influences on short circuit and consequentially protection infrastructure characteristics to within 3% of original system designs for penetration levels at 23%. Inefficiencies become apparent at higher penetration levels particularly in the context of recloser sensitivity.
12. The proposed DG integration assessment method in conjunction with the use of FCLs offers significant practical value in the domain of network expansion planning and reinforcement options in power distribution networks, as well as demonstrating the effect of synchronous machine based DG penetration on existing protection infrastructure in power systems.

This thesis is a stepping-stone in the direction of more research on DG influence mitigation on existing distribution system short circuit characteristics and fuse-recloser protection infrastructure. It is hoped that the research work documented in this thesis will provide useful guidance for conducting more studies and analyzing other technical issues that might be impacted by DG source integration.

REFERENCES

[1] G. Pepermans, J. Driesen, D. Haeseldonckx, R. Belmans and W. D'Haeseleer, "Distributed generation: Definition, benefits and issues," *Energy Policy - Elsevier*, vol. 33, no. 6, pp. 787-798, April 2005.

[2] T. K. Abdel-Galil, A. E. B. Abu-Elanin, E. F. El-Saadany, A. Girgis, A. R. I. Mohamed, M. M. A. Salama and H. H. M. Zeineldin, "Protection Coordination Planning with Distributed Generation," Qualsys Engco Inc, 2007.

[3] G. M. Masters, Renewable and Efficient Electric Power Systems, Hoboken: John Wiley & Sons, 2004.

[4] "Renewable Energy," United Nations High-Level Group on Sustainable Energy for all, 2012. [Online]. Available: http://www.se4all.org/our-vision/our-objectives/renewable-energy/. [Accessed 4 November 2014].

[5] L. Fried, S. Sawyer, S. Shukla and L. Qiao, "Global Wind Report Annual Market Update 2013," Global Wind Energy Council, Brussels, 2014.

[6] U. Karaagac, S. O. Faried, J. Mahseredjian and A.A. Edris, "Coordinated Control of Wind Energy Conversion Systems for Mitigating Subsynchronous Interaction in DFIG-Based Wind Farms," *IEEE Transactions on Smart Grid*, vol. 5, no. 5, pp. 2440-2449, September 2014.

[7] O. Anaya-Lara, N. Jenkins, J. Ekanayake, P. Cartwright and M. Hughes, Wind Energy Generation: Modeling and Control, John Wiley and Sons, 2006.

[8] C. J. Mozina, "Impact of Green Power Generation on Distribution Systems in a Smart Grid," in *Power Systems Conference and Exposition (PSCE)*, Phoenix, 2011.

[9] A. T. Moore, "Distributed Generation (DG) Protection Overview," 5 May 2008. [Online]. Available: http://www.eng.uwo.ca/people/tsidhu/Documents/DG%20Protection%20V4.pdf. [Accessed 20 June 2014].

[10] D. J. Glover, M. S. Sarma and T. J. Overbye, Power System Analysis and Design, 4th ed., Stamford: Cengage Learning, 2008.

[11] P. M. Anderson, Power System Protection, Hoboken: John Wiley & Sons, 1999.

[12] N. Rajaei, M. H. Ahmed, M. M. A. Salama and R. K. Varma, "Fault Current Management Using Inverter-Based Distributed Generators in Smart Grids," *IEEE Transactions on Smart Grid*, vol. 5, no. 5, pp. 2183-2193, September 2014.

[13] F. Sulla, "Fault Behaviour of Wind Turbines," Ph.D. dissertation, Dept. Measurement Tech. Industrial Elect. Eng., Lund University, Lund, 2012.

[14] S. J. Chapman, Electric Machinery Fundamentals, 4th ed., New York: McGraw-Hill, 2005.

[15] T. Gonen, Electric Power Distribution System Engineering, 2nd ed., Boca Raton: Taylor & Francis Group, 2008.

[16] Cooper Power Systems, "Kearney Type T TCC," 2013. [Online]. Available: http://www.cooperindustries.com/content/dam/public/powersystems/resources/library/Kearney/K51000AB.pdf. [Accessed 15 July 2014].

[17] A. S. Rones V and K. P. Vittal, "Modeling of Recloser and Sectionalizer and their Coordination Using PSCAD," in *International Conference on Circuits, Power and Computing Technologies*, Nagercoil, 2013.

[18] IEEE guide for Automatic Reclosing of Line Circuit Breakers for AC Distribution and Transmission Lines, IEEE Standard C37.104, 2002.

[19] Asea Brown Boveri (ABB), "ABB PCD Control Protection Curves," September 2002. [Online]. Available: http://www05.abb.com/global/scot/scot235.nsf/veritydisplay/1bc69ae25de85ac585256c44005e98c4/$file/pcd%20protection%20curves.pdf. [Accessed 15 July 2014].

[20] IEEE Standard Inverse-Time Characteristic Equations for Overcurrent Relays, IEEE Standard C37.112, 1997.

[21] T. A. Short, Electric Power Distribution Handbook, Boca Raton: CRC Press, 2004.

[22] A. Zamani, T. S. Sidhu and A. Yazdani, "A Strategy for Protection Coordination in Radial Distribution Networks with Distributed Generators," in *Power and Energy Society General Meeting*, Minneapolis, 2010.

[23] U.S. Department of Energy, "Fault Current Limiters," 6 November 2009. [Online]. Available: http://energy.gov/sites/prod/files/oeprod/DocumentsandMedia/hts_fcl_110609.pdf. [Accessed 29 May 2014].

[24] M. Elsamahy, S. O. Faried and T. S. Sidhu, "Impact of Superconducting Fault Current Limiters on the Coordination Between Generator Distance Phase Backup Protection and Generator Capability Curves," *IEEE Transactions on Power Delivery*, vol. 26, no. 3, pp. 1854-1863, July 2011.

[25] L. Wang, P. Jiang and D. Wang, "Summary of Superconducting Fault Current Limiter Technology," in *Frontiers in Computer Education*, Berlin, Springer, 2012, pp. 819-825.

[26] H. Arai, M. Inaba, T. Ishigohka, H. Tanaka, K. Arai, M. Furuse and M. Umeda, "Fundamental Characteristics of Superconducting Fault Current Limiter Using LC Resonance Circuit," *IEEE Transactions on Applied Superconductivity*, vol. 16, no. 2, pp. 642-645, June 2006.

[27] S. O. Faried and M. Elsamahy, "Incorporating superconducting fault current limiters in the probabilistic evaluation of transient recovery voltage," *IET Generation, Transmission & Distribution*, vol. 5, no. 1, pp. 101-107, 2011.

[28] M. Dewadasa, Protection of distributed generation interfaced networks, PhD dissertation, Dept. Elect. Eng., Queensland University of Technology, Queensland, 2010.

[29] IEEE Standard for Interconnecting Distributed Resources with Electric Power Systems, IEEE Standard 1547, 2003.

[30] A. Zamani, T. S. Sidhu and A. Yazdani, "A Protection Strategy and Microprocessor-Based Relay for Low-Voltage Microgrids," *IEEE Transactions on Power Delivery*, vol. 26, no. 3, pp. 1873-1883, July 2011.

[31] J. O. Williams, "Narrow-band analyzer," PhD dissertaion," Department of Electrical Engineering, Harvard University, Cambridge, MA, 1993.

[32] S. M. Brahma and A. A. Girgis, "Development of adaptive protection scheme for distribution systems with high penetration of distributed generation," *IEEE Transactions on Power Delivery*, vol. 19, pp. 56-63, 2004.

[33] E. Sortomme, S. S. Venkata and J. Mitra, "Microgrid Protection using Communication-Assisted Digital Relays," *IEEE Transactions on Power Delivery*, vol. 25, no. 4, pp. 2789-2796, October 2010.

[34] W. El-Khattam and T. S. Sidhu, "Restoration of Directional Overcurrent Relay Coordination in Distributed Generation Systems Utilizing Fault Current Limiter," *IEEE Transactions on Power Delivery*, vol. 23, no. 2, pp. 576-585, April 2008.

[35] L. Chen, C. Deng, F. Guo, Y. Tang, J. Shi and L. Ren, "Reducing the Fault Current and Overvoltage in a Distribution System with Distributed Generation Units Through and Active Type SFCL," *IEEE Transactions on Applied Superconductivity*, vol. 24, no. 3, June 2014.

[36] Manitoba HVDC Research Centre, PSCAD Power System Computer Aided Design, Winnipeg: Manitoba Hydro International Ltd., 2010.

[37] Manitoba HVDC Research Centre, Applications of PSCAD/EMTDC, Winnipeg: Manitoba Hydro International Ltd., 2008.

[38] J. M. Gers and E. J. Holmes, Protection of Electricity Distribution Networks, 2nd ed., London: The Institution of Engineering and Technology, 2004.

[39] H. Joshi, Residential, Commercial and Industrial Electrical Systems, vol. 3, New Delhi: Tata McGraw-Hill, 2008.

[40] P. Kundur, Power System Stability and Control, New York: McGraw-Hill, 1994.

[41] J. C. Das, Power System Analysis Short-Circuit Load Flow and Harmonics, New York: Marcel Dekker, 2002.

[42] L. Pham, "Dynamic Enhancement of the Future SaskPower Interconnected North and South Systems: The HVDC Connection," M.S. Thesis, Dept. Elect. Eng., University of Saskatchewan, Saskatoon, 2014.

APPENDIX A

DATA OF THE SUBURBAN DISTRIBUTION SYSTEM

A.1 Synchronous Generators

Table A.1: Synchronous generator data.

Rating, MVA	8.4
Rated voltage, kV	12.47
Armature resistance, r_a , p.u.	0.0051716
Direct-axis synchronous reactance, x_d , p.u.	1.014
Quadrature-axis synchronous reactance, x_q , p.u.	0.77
Direct-axis transient reactance, x'_d , p.u.	0.314
Direct-axis subtransient reactance, x''_d , p.u.	0.28
Quadrature-axis subtransient reactance, x''_q , p.u.	0.375
Direct-axis transient open-circuit time constant, T'_{do} , s	6.55
Direct-axis subtransient open-circuit time constant, T''_{do} , s	0.039
Quadrature-axis subtransient open-circuit time constant, T''_{qo} ,s	0.071
Inertia constant, s	3.117
Neutral series resistance, p.u.	0.01
Neutral series reactance, p.u.	0.01
Mechanical friction and windage, p.u.	0.01
Iron loss resistance, p.u.	300

A.2 Transformers

Table A.2: Transformer data.

	Interconnecting Transformer		Substation	Bus 5 Load	Motor
Scenario	DG size less than 16 MVA	16 MVA<DG<75 MVA	N/A	N/A	N/A
Rating, MVA	16	75	100	2	2
Rated voltage, kV	12.47/25	12.47/25	240/25	25/0.208	12.47/25
No load losses, p.u.	0.001	0.001	0.005	0.005	0.005
Copper losses, p.u.	0.002	0.002	0.003	0.003	0.003
Leakage reactance, x_T, p.u.	0.1	0.46875	0.1	0.03	0.0614
Configuration	Wye-Gnd/ Wye-Gnd	Wye-Gnd/ Wye-Gnd	Wye-Gnd/ Wye-Gnd	Delta/Wye-Gnd	Wye-Gnd/Delta

A.3 Line and Cable Data

Table A.3: Line and cable data.

	Feeder cables	Underground Cable	Collector Feeder
Positive Sequence Resistance (mΩ/ m)	.166	0.0601	.166
Positive Sequence Reactance (mΩ/ m)	.29	0.07979	.29
Positive Sequence Capacitive Reactance (MΩ×m)	170	4237350	170
Zero Sequence Multiplication Factor	3	0.575	3

A.4 Induction Motor Data

1 MW, 12.47 kV, 60 Hz

Stator/Rotor turns ratio = 1.3, Angular Moment of Inertia = 0.7267 seconds, Mechanical Damping = 0.001 p.u, R_s = 0.005 p.u., Wound Rotor Resistance = 0.008 p.u., Magnetizing Inductance = 4.362 p.u., Stator Leakage Inductance = 0.102 p.u., Wound Rotor Inductance = 0.11 p.u.

A.5 Other Components

Main Feeder Load = 14.58 MW + 7.06 MVAR

Resistive FCL values: R_{FCL} = 60, 50, 20Ω, R_p = 0

Inductive FCL values: I_{FCL} = 0.16, 0.13, 0.05H, L_{TC} = 0

Resonant FCL values: L_f = 0.187, C_f = 37.665μF

APPENDIX B

SHORT CIRCUIT CURRENTS FOR THE NORMAL AND SYNCHRONOUS MACHINE BASED DG INTEGRATED SUBURBAN DISTRIBUTION SYSTEM

Table B.1: Short circuit currents for varying fault types at the bus 5 load.

	Synchronous Machine Based DG Interconnection Point									
	Bus 1		Bus 2		Bus 4		Bus 5		No DG	
Type	Ifeed	Ifault	Ifeed	Ifault	Ifeed	Ifault	Ifeed	Ifault	Ifeed	Ifault
3ø	806	1156	791	1176	790	1212	801	1227	1171	1059
LG	705	735	699	742	688	758	682	766	937	701
LLG	609	704	599	714	582	736	574	749	889	657
LL	653	577	650	584	643	599	640	608	853	545

Table B.2: Short circuit currents for varying fault types at the bus 4.

	Synchronous Machine Based DG Interconnection Point									
	Bus 1		Bus 2		Bus 4		Bus 5		No DG	
Type	Ifeed	Ifault	Ifeed	Ifault	Ifeed	Ifault	Ifeed	Ifault	Ifeed	Ifault
3P	3750	4319	4041	4315	3919	4503	3917	4494	3917	3869
LG	1835	2277	1881	2429	2114	2935	3446	2879	2102	2034
LLG	3323	3863	3359	3947	3447	4146	2101	2878	3516	3402
LL	3371	3808	3403	3887	3472	4056	3473	4053	3534	3342

Table B.3: Short circuit currents for varying fault types at the bus 3.

	Synchronous Machine Based DG Interconnection Point									
	Bus 1		Bus 2		Bus 4		Bus 5		No DG	
Type	Ifeed	Ifault	Ifeed	Ifault	Ifeed	Ifault	Ifeed	Ifault	Ifeed	Ifault
3P	4403	4627	4300	4711	4283	4878	4283	4881	4283	4186
LG	2221	2766	2308	2969	2455	3264	2446	3218	2476	2420
LLG	3700	4311	3747	4346	3801	4519	3805	4513	3868	3781
LL	3712	4233	3750	4262	3793	4413	3793	4409	3854	3649

Table B.4: Short circuit currents for varying fault types at the bus 2.

	Synchronous Machine Based DG Interconnection Point									
	Bus 1		Bus 2		Bus 4		Bus 5		No DG	
Type	Ifeed	Ifault	Ifeed	Ifault	Ifeed	Ifault	Ifeed	Ifault	Ifeed	Ifault
3P	4776	5229	4725	5303	4724	5331	4724	5336	4724	4707
LG	2813	3519	2988	3872	2972	3788	2966	3749	3023	2988
LLG	4184	4878	4255	4980	4252	4987	4253	4981	4313	4256
LL	4128	4709	4172	4792	4174	4799	4178	4797	4240	4098